Contraction and Partial Contraction: a Study of Synchronization in Nonlinear Networks

by

Wei Wang

B.S., Thermal Engineering (1994)
Tsinghua University
M.S., Thermal Engineering (1997)
Tsinghua University

Submitted to the Department of Mechanical Engineering
in partial fulfillment of the requirements for the degree of

Doctor of Philosophy in Mechanical Engineering

at the

MASSACHUSETTS INSTITUTE OF TECHNOLOGY

February 2005

Author .....
Department of Mechanical Engineering
December 16, 2004

Certified by .....
Jean-Jacques E. Slotine
Professor of Mechanical Engineering and Information Sciences;
Professor of Brain and Cognitive Sciences
Thesis Supervisor

Accepted by .....
Lallit Anand
Chairman, Department Committee on Graduate Students

Contraction and Partial Contraction: a Study of Synchronization in Nonlinear Networks

by

Wei Wang

Submitted to the Department of Mechanical Engineering
on December 16, 2004, in partial fulfillment of the
requirements for the degree of
Doctor of Philosophy in Mechanical Engineering

Abstract

This thesis focuses on the study of collective dynamic behaviors, especially the spontaneous synchronization behavior, of nonlinear networked systems. We derives a body of new results, based on contraction and partial contraction analysis. Contraction is a property regarding the convergence between two arbitrary system trajectories. A nonlinear dynamic system is called contracting if initial conditions or temporary disturbances are forgotten exponentially fast. Partial contraction, introduced in this thesis, is a straightforward but more general application of contraction. It extends contraction analysis to include convergence to behaviors or to specific properties (such as equality of state components, or convergence to a manifold). Contraction and partial contraction provide powerful analysis tools to investigate the stability of large-scale complex systems. For diffusively coupled nonlinear systems, for instance, a general synchronization condition can be derived which connects synchronization rate to network structure explicitly. The results are applied to construct flocking or schooling models by extending to coupled networks with switching topology.

We further study the networked systems with different kinds of group leaders, one specifying global orientation (power leader), another holding target dynamics (knowledge leader). In a knowledge-based leader-followers network, the followers obtain dynamics information from the leader through adaptive learning.

We also study distributed networks with non-negligible time-delays by using simplified wave variables and other contraction-oriented analysis. Conditions for contraction to be preserved regardless of the explicit values of the time-delays are derived. Synchronization behavior is shown to be robust if the protocol is linear.

Finally, we study the construction of spike-based neural network models, and the development of simple mechanisms for fast inhibition and de-synchronization.

Thesis Supervisor: Jean-Jacques E. Slotine
Title: Professor of Mechanical Engineering and Information Sciences; Professor of Brain and Cognitive Sciences

Acknowledgments

First, I wish to express my deepest gratitude to my advisor, Professor Jean-Jacques Slotine. Without his consistent support, guidance and patience, none of the results in this thesis could be done.

I would also like to thank other two faculty members in my thesis committee, Professor Michael Triantafyllou and Professor Rodolfo Rosales. I appreciate their professional advice on my thesis work. The discussions with them were very stimulating.

I thank all my friends and labmates, who make my life in MIT enjoyable and easy. Special thanks go to Martin Grepl, who gave me many helps in the beginning of my research, Tu Duc Nguyen, who visited MIT very shortly but will be my friend for ever.

Finally and most importantly, I would like to thank my family. My parents and my sister have supported me with their selfless love since I was born. My wife Minqi, who accompanied me through my whole study in MIT, has shared each piece of my happiness and sadness. This thesis is dedicated to her.

This work was supported in part by grants from the National Institutes of Health and the National Science Foundation.

Contents

List of Figures

Chapter 1

Introduction

The complexity of the world we live is based on accumulation and combination of simple elements. Collective behaviors of dynamic networked systems, such as spontaneous synchronization, pervade nature at every scale. Although the study of these natural phenomena has lasted for a few centuries, it remains a mystery and attracts more and more attention from researchers working across disciplines. In this thesis, a body of new results on nonlinear networked systems is derived based on *contraction* and *partial contraction* analysis.

Contraction is a property regarding the convergence between two arbitrary system trajectories. A nonlinear dynamic system is called contracting if initial conditions or temporary disturbances are forgotten exponentially fast. The basic results of Contraction Theory are briefly reviewed in Chapter 2, followed which we derive a sufficient condition to preserve contraction through an arbitrary feedback combination, and then develop the theory of partial contraction. Partial contraction (or meta-contraction) is a straightforward but more general application of contraction. It extends contraction analysis to include convergence to behaviors or to specific properties (such as equality of state components, or convergence to a manifold). Not surprisingly contraction can be considered as a particular case of partial contraction.

The development of Partial Contraction Theory provides a general analysis tool to investigate the stability of large-scale complex systems. In particular, it is powerful to study synchronization behavior by inheriting the central feature of contraction that, convergence and explicit dynamics are treated separately, leading to significant conceptual simplifications. We illustrate the idea in Chapter 3 by investigating the behaviors of two coupled oscillators. Chapter 4 generalizes the analysis to coupled networks with various structures and arbitrary sizes. For nonlinear systems with positive-definite diffusive couplings, we show that synchronization will always occur if coupling strengths are strong enough, and an explicit upper bound on the corresponding threshold can be computed through eigenvalue analysis. Rather than linearized, the results are exact and global, and can be easily extended to study nonlinear couplings, to unidirectional couplings, and to positive semi-definite couplings as well. We further connect the synchronization rate to a network's geometric properties, such as connectivity, graph diameter or mean distance. A fast inhibition mechanism is also studied.

In fact, synchronization research has a very close connection with group cooperation study. Recently, there is considerable interest in understanding how various animal aggregations, such as bird flocks or fish schools, coordinate their collective motions to perform useful tasks. A great effort has made to achieve similar behaviors of artificial multi-agent systems, such as vehicles or satellites, with distributed cooperative control rules. In Chapter 5 we build corresponding flocking or schooling models by extending the previous analysis to coupled networks with switching topology.

We study the networked systems with different kinds of group leaders in Chapter 6. The leader specifying global orientation is named *power leader*, while that holding target dynamics is *knowledge leader*. In a knowledge-based leader-followers network, the followers obtain dynamics information from the leader through adaptive learning. Such a mechanism may exist in many natural processes, for instance, in evolutionary biology or in disease dynamics. Synchronization conditions for both kinds of networks are derived based on contraction or graph analysis.

In real-world engineering applications, communications between different systems always involve non-negligible time-delays. In Chapter 7, we conduct a contraction analysis on time-delayed feedback communications using simplified wave variables. A condition to preserve contraction regardless of the delay values is derived. The approach is then applied to study the group cooperation problem with time-delayed communications.We show that synchronization is robust to time delays with linear protocol, no matter if the dynamics is continuous or discrete-time, or if the network is leaderless or leader-followers. A different but more general study of time-delayed nonlinear systems will be presented in Chapter 8.

Finally, in Chapter 9 we develop an effective de-synchronization mechanism, based on which a networked system converges to a well-ordered phase-locking solution very quickly, and thus allows us to construct neural network models with the ability to perform fast spike-based computations, such as coincidence detection and winner-take-all. These basic computational units are able to be accumulated to execute higher-level brain functions, the implementation of which will facilitate the realization of, for instance, binding in machine vision and perception.

Brief concluding remarks are offered in Chapter 10.

Chapter 2

Contraction and Partial Contraction

Basically, a nonlinear time-varying dynamic system will be called *contracting* if initial conditions or temporary disturbances are forgotten exponentially fast, i.e., if trajectories of the perturbed system return to their nominal behavior with an exponential convergence rate. The concept of *partial contraction* allows to extend the applications of contraction analysis to include convergence to behaviors or to specific properties (such as equality of state components, or convergence to a manifold) rather than trajectories.

2.1 Contraction Theory

Contraction Theory is a new nonlinear analysis tool, which investigates the stability with respect to trajectories. Here we briefly summarize its basic definitions and main results, details of which can be found in [81, 82].

Consider a nonlinear system

$$\dot{\mathbf{x}} = \mathbf{f}(\mathbf{x}, t) \tag{2.1}$$

where $\mathbf{x} \in \mathbb{R}^{m \times 1}$ is a state vector and $\mathbf{f}$ is an $m \times 1$ vector function. Assuming $\mathbf{f}(\mathbf{x}, t)$ is continuously differentiable, we have

$$\frac{d}{dt}(\delta\mathbf{x}^T \delta\mathbf{x}) = 2\ \delta\mathbf{x}^T \delta\dot{\mathbf{x}} = 2\ \delta\mathbf{x}^T \frac{\partial \mathbf{f}}{\partial \mathbf{x}}\ \delta\mathbf{x} \leq 2\ \lambda_{max}\ \delta\mathbf{x}^T \delta\mathbf{x}$$

where $\delta\mathbf{x}$ is a virtual displacement between two neighboring solution trajectories, and $\lambda_{max}(\mathbf{x}, t)$ is the largest eigenvalue of the symmetric part of the Jacobian $\mathbf{J} = \frac{\partial \mathbf{f}}{\partial \mathbf{x}}$. Hence, if $\lambda_{max}(\mathbf{x}, t)$ is uniformly strictly negative, any infinitesimal length $\|\delta\mathbf{x}\|$ converges exponentially to zero. By path integration at fixed time, this implies in turn that all the solutions of the system (2.1) converge exponentially to a single trajectory, independently of the initial conditions.

More generally, consider a coordinate transformation

$$\delta\mathbf{z} = \mathbf{\Theta}\delta\mathbf{x} \tag{2.2}$$

where $\Theta(\mathbf{x}, t)$ is a uniformly invertible square matrix. One has

$$\frac{d}{dt}(\delta \mathbf{z}^T \delta \mathbf{z}) = 2\ \delta \mathbf{z}^T \delta \dot{\mathbf{z}} = 2\ \delta \mathbf{z}^T\ (\dot{\Theta} + \Theta \frac{\partial \mathbf{f}}{\partial \mathbf{x}}) \Theta^{-1}\ \delta \mathbf{z}$$

so that exponential convergence of $\|\delta \mathbf{z}\|$ to zero is guaranteed if the *generalized Jacobian matrix*

$$\mathbf{F} = (\dot{\Theta} + \Theta \frac{\partial \mathbf{f}}{\partial \mathbf{x}}) \Theta^{-1} \tag{2.3}$$

is uniformly negative definite. Again, this implies in turn that all the solutions of the original system (2.1) converge exponentially to a single trajectory, independently of the initial conditions.

By convention, the system (2.1) is called *contracting*, $\mathbf{f}(\mathbf{x}, t)$ is called a *contracting function*, and the absolute value of the largest eigenvalue of the symmetric part of $\mathbf{F}$ is called the system's *contraction rate* with respect to the uniformly positive definite *metric* $\mathbf{M} = \Theta^T \Theta$.

Note that in a globally contracting autonomous system, all trajectories converge exponentially to a unique equilibrium point [81, 133].

2.2 Feedback Combination of Contracting Systems

One of the main features of contraction is that it is automatically preserved through a variety of system combination. Consider two contracting systems and an arbitrary feedback connection between them. The overall virtual dynamics can be written as

$$\frac{d}{dt} \begin{bmatrix} \delta \mathbf{z}_1 \\ \delta \mathbf{z}_2 \end{bmatrix} = \mathbf{F} \begin{bmatrix} \delta \mathbf{z}_1 \\ \delta \mathbf{z}_2 \end{bmatrix}$$

with the symmetric part of the generalized Jacobian in the form

$$\mathbf{F}_s = \frac{1}{2}\ (\mathbf{F}\ +\ \mathbf{F}^T) = \begin{bmatrix} \mathbf{F}_{1s} & \mathbf{G} \\ \mathbf{G}^T & \mathbf{F}_{2s} \end{bmatrix}$$

(the subscript symbol s represents the symmetric part of the matrix). By hypothesis the matrices $\mathbf{F}_{1s}$ and $\mathbf{F}_{2s}$ are uniformly negative definite. Then $\mathbf{F}$ is uniformly negative definite if and only if ([51], page 472)

$$\mathbf{F}_{2s} < \mathbf{G}^T\ \mathbf{F}_{1s}^{-1}\ \mathbf{G}$$

Thus, a sufficient condition for the overall system to be contracting is that

$$\lambda(\mathbf{F}_{1s})\ \lambda(\mathbf{F}_{2s})\ >\ \sigma^2(\mathbf{G}) \qquad \text{uniformly}\ \ \forall t \geq 0 \tag{2.4}$$

where $\lambda(\mathbf{F}_{is})$ is the contraction rate of $\mathbf{F}_{is}$ and $\sigma(\mathbf{G})$ is the largest singular value of $\mathbf{G}$. Indeed, condition (2.4) is equivalent to

$$\lambda_{max}(\mathbf{F}_{2s})\ <\ \lambda_{min}(\mathbf{F}_{1s}^{-1})\ \sigma^2(\mathbf{G})$$

and, for an arbitrary nonzero vector $\mathbf{v}$,

$$\begin{aligned} \mathbf{v}^T \mathbf{F}_{2s} \mathbf{v} &\leq \lambda_{max}(\mathbf{F}_{2s}) \ \mathbf{v}^T\mathbf{v} \\ &< \lambda_{min}(\mathbf{F}_{1s}^{-1}) \ \sigma^2(\mathbf{G}) \ \mathbf{v}^T\mathbf{v} \\ &\leq \lambda_{min}(\mathbf{F}_{1s}^{-1}) \ \mathbf{v}^T \mathbf{G}^T \mathbf{G} \mathbf{v} \\ &\leq \mathbf{v}^T \mathbf{G}^T \mathbf{F}_{1s}^{-1} \mathbf{G} \mathbf{v} \end{aligned}$$

A simple example was studied in [81] where

$$\mathbf{F} = \begin{bmatrix} \mathbf{F}_1 & \mathbf{G} \\ -\mathbf{G}^T & \mathbf{F}_2 \end{bmatrix}$$

The result (2.4) can be applied recursively to larger combinations. Note that, from the eigenvalue interlacing theorem [51],

$$\lambda(\mathbf{F}_s) \leq \min_i \lambda(\mathbf{F}_{is})$$

2.3 Partial Contraction Theory

The concept of partial contraction came out firstly when we worked on the study of network synchronization, since which its unique capacity and flexibility have been proved in more and more application fields.

Theorem 2.1 *Consider a nonlinear system of the form*

$$\dot{\mathbf{x}} = \mathbf{f}(\mathbf{x}, \mathbf{x}, t)$$

and assume that its auxiliary system

$$\dot{\mathbf{y}} = \mathbf{f}(\mathbf{y}, \mathbf{x}(t), t)$$

is contracting with respect to $\mathbf{y}$. *If a particular solution of the auxiliary* $\mathbf{y}$*-system verifies a smooth specific property, then all trajectories of the original* $\mathbf{x}$*-system verify this property exponentially. The original system is said to be partially contracting.*

Proof: The virtual, observer-like $\mathbf{y}$-system has two particular solutions, namely $\mathbf{y}(t) = \mathbf{x}(t)$ for all $t \geq 0$ and the solution with the specific property. For a contracting system, all solutions converge together exponentially regardless of the initial conditions. This implies that $\mathbf{x}(t)$ verifies the specific property exponentially. □

Note that contraction may be trivially regarded as a particular case of partial contraction. Consider for instance an original system in the form

$$\dot{\mathbf{x}} = \mathbf{c}(\mathbf{x}, t) + \mathbf{d}(\mathbf{x}, t)$$

where function $\mathbf{c}$ is contracting in a constant metric. The auxiliary contracting system may then be constructed as

$$\dot{\mathbf{y}} \;=\; \mathbf{c}(\mathbf{y},t) \;+\; \mathbf{d}(\mathbf{x}(t),t)$$

In this example, contraction is a particular case of partial contraction when $\mathbf{d} = \mathbf{0}$. If $\mathbf{d} \neq \mathbf{0}$, the specific property of interest may consist e.g. of an equilibrium point, or a relationship between state variables which we will illustrate through the following sections. Here we study a few simple examples.

Example 2.3.1: Consider the system taken from [60]

$$\begin{bmatrix} \dot{x}_1 \\ \dot{x}_2 \end{bmatrix} = \begin{bmatrix} -1 & x_1 \\ -x_1 & -1 \end{bmatrix} \begin{bmatrix} x_1 \\ x_2 \end{bmatrix}$$

to which we construct an auxiliary system

$$\begin{bmatrix} \dot{y}_1 \\ \dot{y}_2 \end{bmatrix} = \begin{bmatrix} -1 & x_1 \\ -x_1 & -1 \end{bmatrix} \begin{bmatrix} y_1 \\ y_2 \end{bmatrix}$$

The $\mathbf{y}$-system is contracting and has two particular solutions $\begin{bmatrix} y_1 \\ y_2 \end{bmatrix} = \begin{bmatrix} x_1 \\ x_2 \end{bmatrix}$ and $\begin{bmatrix} y_1 \\ y_2 \end{bmatrix} = \begin{bmatrix} 0 \\ 0 \end{bmatrix}$. Thus, according to Partial Contraction Theory, x_1 and x_2 will both tend to 0 exponentially. □

Example 2.3.2: Consider the system from [131]

$$\begin{cases} \dot{x}_1 \;=\; x_2 \;-\; x_1^7 \,(\, x_1^4 \;+\; 2x_2^2 \;-\; 10\,) \\ \dot{x}_2 \;=\; -\, x_1^3 \;-\; 3x_2^5 \,(\, x_1^4 \;+\; 2x_2^2 \;-\; 10\,) \end{cases}$$

which is equivalent to

$$\frac{d}{dt}(\, x_1^4 \;+\; 2x_2^2 \;-\; 10\,) \;=\; -\,(\, 4x_1^{10} \;+\; 12x_2^6\,)\,(\, x_1^4 \;+\; 2x_2^2 \;-\; 10\,)$$

and has an auxiliary system

$$\dot{y} \;=\; -\,(\, 4x_1^{10} \;+\; 12x_2^6\,)\, y$$

The y-system has two particular solutions $y = x_1^4 + 2x_2^2 - 10$ and $y = 0$, and is contracting as long as not both $x_1(t)$ and $x_2(t)$ equal to 0. It is then easy to show that, the system stays at the origin if $x_1(0) = x_2(0) = 0$. Otherwise it tends to reach

$$x_1(t)^4 \;+\; 2\, x_2(t)^2 \;=\; 10$$

exponentially. □

Example 2.3.3: Consider a convex combination or interpolation between contracting dynamics

$$\dot{\mathbf{x}} = \sum_i \alpha_i(\mathbf{x},t)\; \mathbf{f}_i(\mathbf{x},t)$$

where the individual systems $\dot{\mathbf{x}} = \mathbf{f}_i(\mathbf{x}, t)$ are contracting in a common metric $\mathbf{M}(\mathbf{x}) = \Theta^T(\mathbf{x})\Theta(\mathbf{x})$ and have a common trajectory $\mathbf{x}_o(t)$ (for instance an equilibrium), with all $\alpha_i(\mathbf{x}, t) \geq 0$ and $\sum_i \alpha_i(\mathbf{x}, t) = 1$. Then all trajectories of the system globally exponentially converge to the trajectory $\mathbf{x}_o(t)$. Indeed, the auxiliary system

$$\dot{\mathbf{y}} = \sum_i \alpha_i(\mathbf{x}, t)\ \mathbf{f}_i(\mathbf{y}, t)$$

is contracting (with metric $\mathbf{M}(\mathbf{y})$) and has $\mathbf{x}(t)$ and $\mathbf{x}_o(t)$ as particular solutions. □

The notion of building a virtual contracting system to prove exponential convergence applies also to control problems[60, 135]. Consider for instance a nonlinear system of the form

$$\dot{\mathbf{x}} = \mathbf{f}(\mathbf{x}, \mathbf{x}, \mathbf{u}, t)$$

and assume that the control input $\mathbf{u}(\mathbf{x}, \mathbf{x}_d, t)$ can be chosen such that

$$\dot{\mathbf{x}}_d = \mathbf{f}(\mathbf{x}_d, \mathbf{x}, \mathbf{u}, t)$$

where $\mathbf{x}_d(t)$ is the desired state. Construct now the auxiliary system

$$\dot{\mathbf{y}} = \mathbf{f}(\mathbf{y}, \mathbf{x}, \mathbf{u}, t)$$

If the $\mathbf{y}$-system is contracting, then $\mathbf{x}$ tends $\mathbf{x}_d$ exponentially.

Example 2.3.4: Consider a rigid robot model

$$\mathbf{H}(\mathbf{q})\ddot{\mathbf{q}} + \mathbf{C}(\mathbf{q}, \dot{\mathbf{q}})\dot{\mathbf{q}} + \mathbf{g}(\mathbf{q}) = \tau$$

and the energy-based controller [131]

$$\mathbf{H}(\mathbf{q})\ddot{\mathbf{q}}_\mathbf{r} + \mathbf{C}(\mathbf{q}, \dot{\mathbf{q}})\dot{\mathbf{q}}_\mathbf{r} + \mathbf{g}(\mathbf{q}) - \mathbf{K}(\dot{\mathbf{q}} - \dot{\mathbf{q}}_\mathbf{r}) = \tau$$

with $\mathbf{K}$ a constant symmetric positive-definite matrix. The virtual $\mathbf{y}$-system

$$\mathbf{H}(\mathbf{q})\dot{\mathbf{y}} + \mathbf{C}(\mathbf{q}, \dot{\mathbf{q}})\mathbf{y} + \mathbf{g}(\mathbf{q}) - \mathbf{K}(\dot{\mathbf{q}} - \mathbf{y}) = \tau$$

has $\dot{\mathbf{q}}$ and $\dot{\mathbf{q}}_\mathbf{r}$ as two particular solutions, and furthermore is contracting, since the skew-symmetry of the matrix $\dot{\mathbf{H}} - \mathbf{2C}$ implies

$$\frac{\mathbf{d}}{\mathbf{dt}}\ \delta\mathbf{y}^\mathbf{T}\mathbf{H}\delta\mathbf{y} = -\mathbf{2}\delta\mathbf{y}^\mathbf{T}(\mathbf{C} + \mathbf{K})\delta\mathbf{y} + \delta\mathbf{y}^\mathbf{T}\dot{\mathbf{H}}\delta\mathbf{y} = -\mathbf{2}\delta\mathbf{y}^\mathbf{T}\mathbf{K}\delta\mathbf{y}$$

Thus $\dot{\mathbf{q}}$ tends to $\dot{\mathbf{q}}_\mathbf{r}$ exponentially. Making then the usual choice $\dot{\mathbf{q}}_\mathbf{r} = \dot{\mathbf{q}}_\mathbf{d} - \lambda(\mathbf{q} - \mathbf{q}_\mathbf{d})$ creates a hierarchy and implies in turn that $\mathbf{q}$ tends to $\mathbf{q}_\mathbf{d}$ exponentially. □

2.4 Line-Attractor

Recent research in computational neuroscience points out the importance of continuous attractors [127, 71]. If a system contains a global stable equilibrium point, all

solutions converge to this point attractor regardless of initial conditions. If a system contains a line attractor, all solutions will converge to this line, and the resting point on this line depends on initial conditions. Figure 2-1 illustrates the difference between these two types of attractors. In this section, we use partial contraction theory to study line attractor.

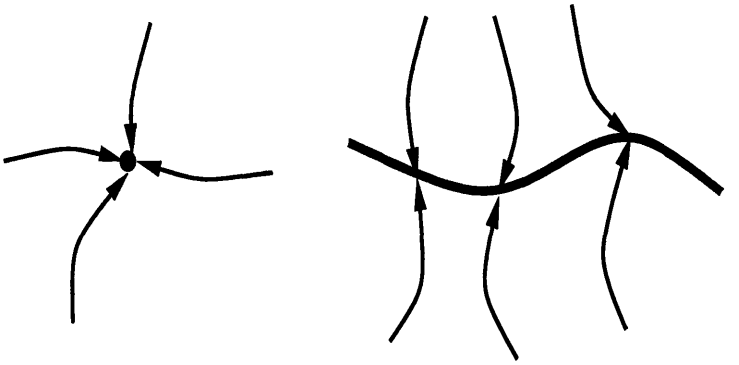

Figure 2-1: Illustration of equilibrium point and line attractor.

2.4.1 Line-Attractor

Consider [47] a nonlinear neural network model

$$\tau \dot{x}_i \; + \; x_i \; = \; [\sum_j w_{ji} \, x_j \; + \; b_i \;]^+ \qquad\qquad i = 1, \ldots, n$$

with $[a]^+ = \max(0, a)$ and constant $\tau > 0$, or in matrix form

$$\tau \dot{\mathbf{x}} \; + \; \mathbf{x} \; = \; [\; \mathbf{W}\mathbf{x} \; + \; \mathbf{b} \;]^+$$

with $\mathbf{W}^T = \mathbf{W} = [w_{ij}]$. If $\mathbf{I} - \mathbf{W}$ is positive semi-definite and $\mathbf{b}$ is in its range space, a line attractor exists [47]. To prove global exponential stability of this line attractor, arrange the eigenvalues λ_i of $\mathbf{I} - \mathbf{W}$ in increasing order, with $\lambda_2 > \lambda_1 = 0$. The corresponding eigenvectors $\mathbf{u}_i$ represent an orthonormal basis of the state space. Consider now the auxiliary system

$$\tau \dot{\mathbf{y}} \; + \; \mathbf{y} \; = \; [\; \mathbf{W}\mathbf{y} \; + \; \mathbf{b} \;]^+ \; + \; \lambda_2 \, \mathbf{u}_1 \mathbf{u}_1^T \; (\; \mathbf{x}(t) - \mathbf{y} \;) \qquad (2.5)$$

Note that given positive initial conditions, all components of $\mathbf{x}$ and $\mathbf{y}$ remain positive. To apply partial contraction analysis, we need to do two things: first prove the auxiliary system is contracting, and then find a specific property for $\mathbf{y}$.
contraction proof:
To prove the auxiliary system (2.5) is contracting, we use contraction analysis results for continuously switching systems [82, 84]. Consider an arbitrary number of

continuously differentiable flow fields

$$\dot{\mathbf{x}} = \mathbf{f}_i(\mathbf{x}, t)$$

which are all contracting with respect to the *same* continuous $\boldsymbol{\Theta}(\mathbf{x}, t)$. Now switch arbitrarily among these different flow fields $\mathbf{f}_i$. If the resulting flow is continuous in $\mathbf{x}$ for any time $t \geq 0$, the overall system is contracting. A detailed proof for system (2.5) to be contracting can be found in Appendix. The overall contraction rate is lower bounded by $\frac{\lambda_2}{2\tau}$.
specific property:
Besides $\mathbf{y} = \mathbf{x}(t)$, there exists another particular solution for the auxiliary system (2.5) which is

$$\mathbf{y} = \mathbf{e} + y_\infty \, \mathbf{u}_1$$

Here $\mathbf{e}$ is a constant vector satisfying $(\mathbf{I} - \mathbf{W})\ \mathbf{e} = \mathbf{b}$ and y_∞ is a scalar variable defined by

$$\tau \dot{y}_\infty + \ \lambda_2 y_\infty \ = \ \lambda_2 \ \mathbf{u}_1^T \ (\mathbf{x} - \mathbf{e})$$

Note that we used $\mathbf{u}_1^T \mathbf{u}_1 = 1$ and the fact that, given positive initial conditions, one has

$$[\ \mathbf{W}\mathbf{y} + \mathbf{b}\ ]^+ = [\ \mathbf{y} + \mathbf{b} - (\mathbf{I} - \mathbf{W})(\mathbf{e} + y_\infty \ \mathbf{u}_1)\ ]^+ = [\ \mathbf{y}\ ]^+ \ = \ \mathbf{y}$$

Thus, according to partial contraction theory, $\mathbf{x}(t)$ verifies exponentially the specific property that $(\mathbf{x}(t) - \mathbf{e})$ is aligned with $\mathbf{u}_1$. Hence all solutions of the original system converge exponentially to a line attractor of the form

$$\mathbf{x} = \mathbf{e} + x_\infty \ \mathbf{u}_1$$

where $\dot{x}_\infty = 0$ using the original $\mathbf{x}$ dynamics. The actual value of x_∞ is determined by the initial conditions.

2.4.2 Generalized Line-Attractor

In this section, we study a generalized non-switching line-attractor model. Consider a nonlinear system

$$\dot{\mathbf{x}} = \mathbf{f}(\mathbf{x}, t)$$

with Jacobian $\mathbf{J}(\mathbf{x}, t) = \frac{\partial \mathbf{f}}{\partial \mathbf{x}}$. We assume $\mathbf{J}(\mathbf{x}, t)$ that is symmetric, and arrange its eigenvalues $\lambda_i = \lambda_i(\mathbf{x}, t)$ $i = 1, \ldots, n$ in increasing order. The corresponding eigenvectors $\mathbf{u}_i = \mathbf{u}_i(\mathbf{x}, t)$ represent an orthonormal basis of the state space.

Theorem 2.2 *For the general nonlinear model described above, if* $\forall\, i = 2, \ldots, n,\ \lambda_i < 0$, λ_1 *is upper bounded, and* $\mathbf{u}_1$ *is constant, then all solutions of the original system will converge to an attractor of the form*

$$\mathbf{x}(t) = \mathbf{e}(t) + x_\infty(t) \ \mathbf{u}_1 \tag{2.6}$$

where $x_\infty(t)$ may depend on initial conditions. The convergence rate is lower bounded by $|\lambda_2|$.

Proof: The virtual dynamics of the original system is

$$\delta\dot{\mathbf{x}} \;=\; \mathbf{J}(\mathbf{x},t)\;\delta\mathbf{x} \tag{2.7}$$

Consider an auxiliary virtual dynamics of the form

$$\delta\dot{\mathbf{y}} \;=\; \mathbf{J}(\mathbf{x},t)\;\delta\mathbf{y} \;+\; k_o(\mathbf{x},t)\;\mathbf{u}_1\mathbf{u}_1^T\;(\delta\mathbf{y} \;-\; \delta\mathbf{x}) \tag{2.8}$$

and choose $k_o(\mathbf{x},t) = \lambda_2(\mathbf{x},t) - \lambda_1(\mathbf{x},t)$. Then this auxiliary dynamics is contracting, since

$$\mathbf{J}(\mathbf{x},t) \;+\; k_o(\mathbf{x},t)\;\mathbf{u}_1\mathbf{u}_1^T \;=\; \sum_{i=1}^{n}\lambda_i\;\mathbf{u}_i\mathbf{u}_i^T + \;k_o\;\mathbf{u}_1\mathbf{u}_1^T \;\leq\; \lambda_2(\mathbf{x},t)\;\mathbf{I}$$

Next, a particular solution of the auxiliary system (2.8) is $\delta\mathbf{y} = \mathbf{u}_1\delta y_\infty$, where

$$\begin{aligned}\delta\dot{y}_\infty \;&=\; (\lambda_1 \;+\; k_o)\;\delta y_\infty \;-\; k_o\;\mathbf{u}_1^T\;\delta\mathbf{x}\\ &=\; \lambda_2\;\delta y_\infty \;-\; (\lambda_2 - \lambda_1)\;\mathbf{u}_1^T\;\delta\mathbf{x}\end{aligned}$$

Thus, from partial contraction, $\delta\mathbf{x}$ converges exponentially to the form $\delta\mathbf{x} = \mathbf{u}_1\delta x_\infty$, where, by replacing in (2.7),

$$\delta\dot{x}_\infty = \lambda_1\;\delta x_\infty$$

Hence all solutions $\mathbf{x}(t)$ of the original system exponentially satisfy (2.6), where $\mathbf{e}(t)$ depends on the explicit form of $\mathbf{f}$. Note that if $\lambda_1 > 0$, the dynamics on the line attractor is unstable. □

2.5 Appendix: Contraction Analysis of (2.5)

To prove that the system (2.5) is contracting, we assume $\forall\; i,j,\; w_{ij} \geq 0$. This implies that all couplings are excitatory. Such a matrix $\mathbf{W} = [w_{ij}]$ is named a *nonnegative matrix* [51].

Lemma 2.1 *If $\mathbf{W}$ is nonnegative and $\mathbf{I} - \mathbf{W}$ is positive semi-definite, then $\mathbf{I} + \mathbf{W}$, and all their principle submatrices are positive semi-definite.*

Proof:
Since $\lambda_i(\mathbf{I} - \mathbf{W}) = 1 - \lambda_i(\mathbf{W})$, we have

$$\forall\; i = 1,\ldots,n \qquad \lambda_i(\mathbf{W}) \;\leq 1 \quad \text{with} \quad \lambda_{max}(\mathbf{W}) \;=\; 1$$

According to extended Perron's Theorem [51](page 503), if $\mathbf{W}$ is nonnegative, then its spectral radius $\rho(\mathbf{W})$ is an eigenvalue of $\mathbf{W}$, which implies that $\rho(\mathbf{W}) = 1$ in this case. Thus $\lambda_i(\mathbf{I} + \mathbf{W}) = 1 + \lambda_i(\mathbf{W}) \geq 0$, i.e., $\mathbf{I} + \mathbf{W}$ is positive semi-definite. Furthermore, all submatrices of $\mathbf{I} - \mathbf{W}$ and $\mathbf{I} + \mathbf{W}$ are positive semi-definite, which can be concluded from Interlacing Theorem. □

To conduct contraction analysis for system (2.5), we first study the case when $\forall i = 1, \ldots, n$, $[\ \sum_i w_{ji}\ y_j + b_i\ ]^+ > 0$. Thus the system's dynamics is actually

$$\tau\dot{\mathbf{y}} \ + \ \mathbf{y} \ = \ \mathbf{W}\mathbf{y} \ + \ \mathbf{b} \ + \ \lambda_2 \ \mathbf{u}_1\mathbf{u}_1^T \ (\ \mathbf{x}(t) - \mathbf{y} \ )$$

which is contracting since $\forall \mathbf{v} \neq 0$, $\mathbf{v} = \sum_{i=1}^n k_i\mathbf{u}_i$, and

$$\begin{aligned}
\mathbf{v}^T(\mathbf{I} - \mathbf{W} + \lambda_2 \ \mathbf{u}_1\mathbf{u}_1^T)\mathbf{v} \ &= \ \mathbf{v}^T(\mathbf{I} - \mathbf{W})\mathbf{v} + \lambda_2 \ \mathbf{v}^T\mathbf{u}_1\mathbf{u}_1^T\mathbf{v} \\
&= \ \sum_{i=2}^{n}(k_i\mathbf{u}_i)^T(\mathbf{I} - \mathbf{W})(k_i\mathbf{u}_i) + \lambda_2(k_1\mathbf{u}_i)^T\mathbf{u}_1\mathbf{u}_1^T(k_1\mathbf{u}_i) \\
&= \ \sum_{i=2}^{n}\lambda_i k_i^2 + \lambda_2 k_1^2 \ > \ 0
\end{aligned}$$

Moreover,

$$\begin{aligned}
\lambda_{min}(\mathbf{I} - \mathbf{W} + \lambda_2 \ \mathbf{u}_1\mathbf{u}_1^T) \ &= \ \min_{\mathbf{v}^T\mathbf{v}\neq 0} \frac{\mathbf{v}^T(\mathbf{I} - \mathbf{W} + \lambda_2 \ \mathbf{u}_1\mathbf{u}_1^T)\mathbf{v}}{\mathbf{v}^T\mathbf{v}} \\
&= \ \frac{\sum_{i=2}^n \lambda_i k_i^2 + \lambda_2 k_1^2}{\sum_{i=1}^n k_i^2} \ \geq \ \lambda_2
\end{aligned}$$

Next, by assuming $\mathbf{W} = [w_{ij}] = \begin{bmatrix} \mathbf{W}_{n-1} & \mathbf{w}_n \\ \mathbf{w}_n^T & w_{nn} \end{bmatrix}$ with $\mathbf{w}_n = [w_{1n} \ \ldots \ w_{(n-1)n}]^T$, and setting $\mathbf{v}^T = [\mathbf{v}_{n-1}^T \ v_n]$, one has

$$\begin{aligned}
& \mathbf{v}^T(\mathbf{I} - \mathbf{W} + \lambda_2 \ \mathbf{u}_1\mathbf{u}_1^T)\mathbf{v} \\
= \ & \mathbf{v}^T(\begin{bmatrix} \mathbf{I} - \mathbf{W}_{n-1} & -\mathbf{w}_n \\ -\mathbf{w}_n^T & 1 - w_{nn} \end{bmatrix} + \lambda_2 \ \mathbf{u}_1\mathbf{u}_1^T)\mathbf{v} \\
= \ & \mathbf{v}_{n-1}^T(\mathbf{I} - \mathbf{W}_{n-1})\mathbf{v}_{n-1} + v_n^T(1 - w_{nn})v_n - 2v_n(\mathbf{v}_{n-1}^T\mathbf{w}_n) + \lambda_2\mathbf{v}^T\mathbf{u}_1\mathbf{u}_1^T\mathbf{v} \\
\geq \ & \lambda_2\mathbf{v}^T\mathbf{v}
\end{aligned}$$

Thus, if for element n(or any other one) $[\ \sum_n w_{jn}\ y_j + b_n\ ]^+ = 0$, the Jacobian of (2.5) changes to $\mathbf{F} = -(\mathbf{I} - \begin{bmatrix} \mathbf{W}_{n-1} & \mathbf{w}_n \\ \mathbf{0} & 0 \end{bmatrix} + \lambda_2 \ \mathbf{u}_1\mathbf{u}_1^T)$, which is still contracting since

$$\begin{aligned}
-\ \mathbf{v}^T\mathbf{F}\mathbf{v} \ &= \ \mathbf{v}^T(\begin{bmatrix} \mathbf{I} - \mathbf{W}_{n-1} & -\frac{1}{2}\mathbf{w}_n \\ -\frac{1}{2}\mathbf{w}_n^T & 1 \end{bmatrix} + \lambda_2 \ \mathbf{u}_1\mathbf{u}_1^T)\mathbf{v} \\
&= \ \frac{1}{2}\mathbf{v}^T(\mathbf{I} - \mathbf{W} + \lambda_2 \ \mathbf{u}_1\mathbf{u}_1^T)\mathbf{v} + \frac{1}{2}\mathbf{v}^T(\begin{bmatrix} \mathbf{I} - \mathbf{W}_{n-1} & \mathbf{0} \\ \mathbf{0} & 1 + w_{nn} \end{bmatrix} + \lambda_2 \ \mathbf{u}_1\mathbf{u}_1^T)\mathbf{v} \\
&\geq \ \frac{1}{2}\mathbf{v}^T(\mathbf{I} - \mathbf{W} + \lambda_2 \ \mathbf{u}_1\mathbf{u}_1^T)\mathbf{v} \ \geq \ \frac{1}{2}\lambda_2\mathbf{v}^T\mathbf{v}
\end{aligned}$$

The analysis can be easily extended. For instance, one can assume

$$\mathbf{W} = [w_{ij}] = \begin{bmatrix} \mathbf{W}_{n-2} & \mathbf{w}_{n-1} & \bar{\mathbf{w}}_n \\ \mathbf{w}_{n-1}^T & w_{(n-1)(n-1)} & w_{n(n-1)} \\ \bar{\mathbf{w}}_n^T & w_{(n-1)n} & w_{nn} \end{bmatrix}$$

If for both elements $n-1$ and n $[\ \sum_i w_{ji}\ y_j + b_i\ ]^+ = 0$, the Jacobian is

$$\mathbf{F} = -(\mathbf{I} - \begin{bmatrix} \mathbf{W}_{n-2} & \mathbf{w}_{n-1} & \bar{\mathbf{w}}_n \\ \mathbf{0} & \mathbf{0} & \mathbf{0} \\ \mathbf{0} & \mathbf{0} & \mathbf{0} \end{bmatrix} + \lambda_2\ \mathbf{u}_1\mathbf{u}_1^T)$$

which is contracting since

$$\begin{aligned} -\mathbf{v}^T\mathbf{F}\mathbf{v} &= \frac{1}{2}\mathbf{v}^T(\mathbf{I} - \mathbf{W} + \lambda_2\ \mathbf{u}_1\mathbf{u}_1^T)\mathbf{v}\ + \\ &\quad \frac{1}{2}\mathbf{v}^T(\begin{bmatrix} \mathbf{I} - \mathbf{W}_{n-2} & \mathbf{0} \\ \mathbf{0} & \mathbf{I} + \begin{bmatrix} w_{(n-1)(n-1)} & w_{n(n-1)} \\ w_{(n-1)n} & w_{nn} \end{bmatrix} \end{bmatrix} + \lambda_2\ \mathbf{u}_1\mathbf{u}_1^T)\mathbf{v} \\ &\geq \frac{1}{2}\lambda_2\mathbf{v}^T\mathbf{v} \end{aligned}$$

We conclude that, system (2.5) as a continuous switching system is contracting because each of its piece-wise system is contracting based on an identity metric. Furthermore, the overall system's contracting rate is lower bounded by $\frac{\lambda_2}{2\tau}$.

Chapter 3

Two Coupled Oscillators

Initiated by Huygens in the 17th century, the study of coupled oscillators involves today a variety of research fields, such as mathematics [24, 120, 141, 142], biology [21, 99, 140], neuroscience [14, 50, 67, 89, 101, 130, 177, 182], robotics [10, 53, 64, 68], and electronics [20], to cite just a few. Theoretical analysis of coupled oscillators can be performed either in the phase-space, as e.g. in the classical Kuramoto model [69, 142, 175], or in the state-space, as e.g. in the fast threshold modulation model [66, 137, 138]. While nonlinear state-space models are much closer to physical reality, there still does not exist a general and explicit analysis tool to study them. Starting from this chapter, we develop a new method based on partial contraction theory.

The analysis is carried out in two steps. First, we prove that the whole coupled system is contracting or partially contracting, implying for instance that all subsystems converge together regardless of the initial conditions. In a second, easy step, the final behavior is determined. We illustrate the idea in this chapter by investigating the coupled networks composed by two oscillators. The theoretical results are then simulated with general Van der Pol oscillators [99, 141], whose relaxation behavior can be made to resemble closely some standard neuron models. In contrast with previous approaches such as e.g., [17, 119, 139], our results are exact and global. In fact, the analysis method we developed is not limited by individual systems' dynamics. It can also be applied to study any other coupled systems rather than oscillators.

3.1 One-Way Coupling Configuration

Consider a pair of one-way (unidirectional) coupled identical oscillators

$$\begin{cases} \dot{\mathbf{x}}_1 = \mathbf{f}(\mathbf{x}_1, t) \\ \dot{\mathbf{x}}_2 = \mathbf{f}(\mathbf{x}_2, t) + \mathbf{u}(\mathbf{x}_1) - \mathbf{u}(\mathbf{x}_2) \end{cases} \tag{3.1}$$

where $\mathbf{x}_1$, $\mathbf{x}_2 \in \mathbb{R}^m$ are the state vectors, $\mathbf{f}(\mathbf{x}_i, t)$ the dynamics of the uncoupled oscillators, and $\mathbf{u}(\mathbf{x}_1) - \mathbf{u}(\mathbf{x}_2)$ the coupling force.

Theorem 3.1 *If the function* $\mathbf{f} - \mathbf{u}$ *is contracting in (3.1), two systems* $\mathbf{x}_1$ *and* $\mathbf{x}_2$ *will reach synchrony exponentially regardless of the initial conditions.*

Proof: The second subsystem, with $\mathbf{u}(\mathbf{x}_1)$ as input, is contracting, and $\mathbf{x}_2(t) = \mathbf{x}_1(t)$ is particular solution. □

Example 3.1.1: Consider two coupled identical Van der Pol oscillators

$$\begin{cases} \ddot{x}_1 + \alpha(x_1^2 - 1)\dot{x}_1 + \omega^2 x_1 = 0 \\ \ddot{x}_2 + \alpha(x_2^2 - 1)\dot{x}_2 + \omega^2 x_2 = \alpha\kappa(\dot{x}_1 - \dot{x}_2) \end{cases}$$

where α, ω and κ are strictly positive constants (this assumption holds for all the Van der Pol examples). Since the system

$$\ddot{x} + \alpha(x^2 + \kappa - 1)\dot{x} + \omega^2 x = u(t)$$

is semi-contracting for $\kappa > 1$ (see Appendix 3.3), x_2 will synchronize to x_1 asymptotically. □

Note that a typical engineering application with an one-way coupling configuration is observer design, in which case $\mathbf{x}_1$ represents the plant state needed to be measured. The result of Theorem 3.1 can be easily extended to a network containing n oscillators with a chain structure (or more generally, a tree structure)

$$\begin{cases} \dot{\mathbf{x}}_1 = \mathbf{f}(\mathbf{x}_1, t) \\ \dot{\mathbf{x}}_2 = \mathbf{f}(\mathbf{x}_2, t) + \mathbf{u}(\mathbf{x}_1) - \mathbf{u}(\mathbf{x}_2) \\ \cdots \\ \dot{\mathbf{x}}_n = \mathbf{f}(\mathbf{x}_n, t) + \mathbf{u}(\mathbf{x}_{n-1}) - \mathbf{u}(\mathbf{x}_n) \end{cases} \tag{3.2}$$

where the synchronization condition is the same as that for system (3.1).

3.2 Two-Way Coupling Configuration

The meaning of synchronization may vary in different contexts. In this thesis, we define synchronization of two (or more) oscillators $\mathbf{x}_1$, $\mathbf{x}_2$ as corresponding to a complete match, i.e., $\mathbf{x}_1 = \mathbf{x}_2$. Similarly, we define anti-synchronization as $\mathbf{x}_1 = -\mathbf{x}_2$. These two behaviors are called in-phase synchronization and anti-phase synchronization in many communities.

3.2.1 Synchronization

Theorem 3.2 *Consider two coupled systems. If the dynamics equations verify*

$$\dot{\mathbf{x}}_1 - \mathbf{h}(\mathbf{x}_1, t) = \dot{\mathbf{x}}_2 - \mathbf{h}(\mathbf{x}_2, t)$$

where the function $\mathbf{h}$ *is contracting, then* $\mathbf{x}_1$ *and* $\mathbf{x}_2$ *will converge to each other exponentially, regardless of the initial conditions.*

Proof: Given initial conditions $\mathbf{x}_1(0)$ and $\mathbf{x}_2(0)$, denote by $\mathbf{x}_1(t)$ and $\mathbf{x}_2(t)$ the solutions of the two coupled systems. Define

$$\mathbf{g}(\mathbf{x}_1, \mathbf{x}_2, t) = \dot{\mathbf{x}}_1 - \mathbf{h}(\mathbf{x}_1, t) = \dot{\mathbf{x}}_2 - \mathbf{h}(\mathbf{x}_2, t)$$

and construct the auxiliary system

$$\dot{\mathbf{y}} = \mathbf{h}(\mathbf{y}, t) + \mathbf{g}(\mathbf{x}_1(t), \mathbf{x}_2(t), t)$$

This system is contracting since the function $\mathbf{h}$ is contracting, and therefore all solutions of $\mathbf{y}$ converge together exponentially. Since $\mathbf{y} = \mathbf{x}_1(t)$ and $\mathbf{y} = \mathbf{x}_2(t)$ are two particular solutions, this implies that $\mathbf{x}_1(t)$ and $\mathbf{x}_2(t)$ converge together exponentially. □

A few remarks on Theorem 3.2:

- Theorem 3.2 can also be proved by construct another auxiliary system

$$\begin{cases} \dot{\mathbf{y}}_1 = \mathbf{h}(\mathbf{y}_1, t) + \mathbf{g}(\mathbf{x}_1, \mathbf{x}_2, t) \\ \dot{\mathbf{y}}_2 = \mathbf{h}(\mathbf{y}_2, t) + \mathbf{g}(\mathbf{x}_1, \mathbf{x}_2, t) \end{cases}$$

  which has a particular solution verifying the specific property $\mathbf{y}_1 = \mathbf{y}_2$. In fact, this auxiliary system is composed of two independent subsystems driven by the same inputs. Thus, the proof can be simplified by reduce the dimension of the $\mathbf{y}$-system.

- Theorem 3.1 is a particular case of Theorem 3.2. So is, for instance, a system of two-way coupled identical oscillators of the form

$$\begin{cases} \dot{\mathbf{x}}_1 = \mathbf{f}(\mathbf{x}_1, t) + \mathbf{u}(\mathbf{x}_2) - \mathbf{u}(\mathbf{x}_1) \\ \dot{\mathbf{x}}_2 = \mathbf{f}(\mathbf{x}_2, t) + \mathbf{u}(\mathbf{x}_1) - \mathbf{u}(\mathbf{x}_2) \end{cases} \tag{3.3}$$

  In such a system $\mathbf{x}_1$ tends to $\mathbf{x}_2$ exponentially if $\mathbf{f} - 2\mathbf{u}$ is contracting. Furthermore, because the coupling forces vanish exponentially, both oscillators tend to their original limit cycle behavior, but with a common phase.

- Although contraction properties are central to the analysis, the overall system itself in general is not contracting, and the common phase of the steady states is determined by the initial conditions $\mathbf{x}_1(0)$ and $\mathbf{x}_2(0)$. This point indicates the difference between contraction and partial contraction.

- The result of Theorem 3.2 can be easily extended to coupled discrete-time systems, using discrete versions [81] of contraction analysis, to coupled hybrid systems, and to coupled systems expressed by partial-differential-equations(PDE).

Example 3.2.1: Consider again two coupled identical Van der Pol oscillators

$$\begin{cases} \ddot{x}_1 + \alpha(x_1^2 - 1)\dot{x}_1 + \omega^2 x_1 = \alpha\kappa_1(\dot{x}_2 - \dot{x}_1) \\ \ddot{x}_2 + \alpha(x_2^2 - 1)\dot{x}_2 + \omega^2 x_2 = \alpha\kappa_2(\dot{x}_1 - \dot{x}_2) \end{cases}$$

One has

$$\ddot{x}_1 + \alpha(x_1^2 + \kappa_1 + \kappa_2 - 1)\dot{x}_1 + \omega^2 x_1 = \ddot{x}_2 + \alpha(x_2^2 + \kappa_1 + \kappa_2 - 1)\dot{x}_2 + \omega^2 x_2$$

According to Theorem 3.2 and the result in Appendix 3.3, we know that these two oscillators will reach synchrony asymptotically if

$$\kappa_1 + \kappa_2 > 1$$

for non-zero initial conditions. Figure 3-1 shows a simulation result, where initial conditions are chosen randomly. □

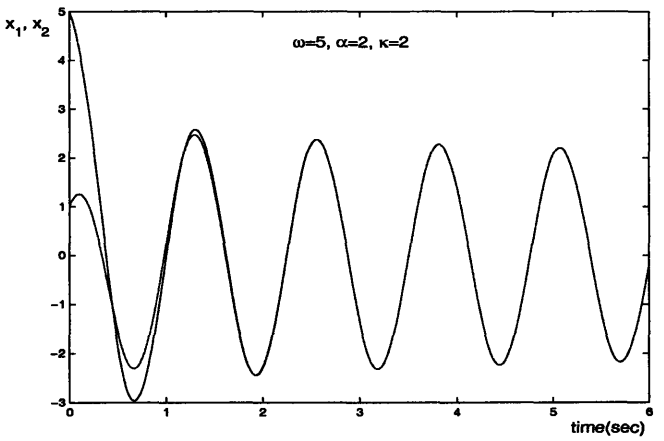

Figure 3-1: Two bidirectionally coupled Van der Pol oscillators synchronize.

3.2.2 Anti-Synchronization

In a seminal paper [136] inspired by Turing's work [99, 153], Smale describes a mathematical model where two identical biological cells, inert by themselves, can be excited into oscillations through diffusion interaction across their membranes. Using Theorem 3.2, we can build a coupled system

$$\begin{cases} \dot{\mathbf{x}}_1 = \mathbf{h}(\mathbf{x}_1, t) + \mathbf{u}(\mathbf{x}_2, t) - \mathbf{u}(\mathbf{x}_1, t) \\ \dot{\mathbf{x}}_2 = \mathbf{h}(\mathbf{x}_2, t) + \mathbf{u}(\mathbf{x}_1, t) - \mathbf{u}(\mathbf{x}_2, t) \end{cases} \tag{3.4}$$

to describe Smale's model.

Theorem 3.3 *If the uncoupled dynamics* $\mathbf{h}$ *in (3.4) is contracting and odd in* $\mathbf{x}$, $\mathbf{x}_1 + \mathbf{x}_2$ *will converge to zero exponentially regardless of the initial conditions. Moreover, for non-zero initial conditions,* $\mathbf{x}_1$ *and* $\mathbf{x}_2$ *will oscillate and reach anti-synchrony if the system*

$$\dot{\mathbf{z}} = \mathbf{h}(\mathbf{z}, t) - 2\mathbf{u}(\mathbf{z}, t)$$

has a stable limit-cycle.

Proof: Theorem 3.3 can be proved by change the sign of $\mathbf{x}_2$ in Theorem 3.2, or by construct an auxiliary system

$$\begin{cases} \dot{\mathbf{y}}_1 &= \mathbf{h}(\mathbf{y}_1, t) + \mathbf{g}(\mathbf{x}_1, \mathbf{x}_2, t) \\ \dot{\mathbf{y}}_2 &= \mathbf{h}(\mathbf{y}_2, t) - \mathbf{g}(\mathbf{x}_1, \mathbf{x}_2, t) \end{cases}$$

with $\mathbf{g}(\mathbf{x}_1, \mathbf{x}_2, t) = \mathbf{u}(\mathbf{x}_2, t) - \mathbf{u}(\mathbf{x}_1, t)$. The $\mathbf{y}$-system has a particular solution verifying the specific property $\mathbf{y}_1 = -\mathbf{y}_2$. □

Example 3.2.2: Consider specifically Smale's example [136], where

$$\mathbf{h}(\mathbf{x}, t) = \mathbf{A} \begin{bmatrix} x_1 \\ x_2 \\ x_3 \\ x_4 \end{bmatrix} + \begin{bmatrix} -x_1^3 \\ 0 \\ 0 \\ 0 \end{bmatrix} \qquad \mathbf{u}(\mathbf{x}) = \frac{1}{2}\,\mathbf{K} \begin{bmatrix} x_1 \\ x_2 \\ x_3 \\ x_4 \end{bmatrix}$$

with

$$\mathbf{A} = \begin{bmatrix} 1+a & 1 & \gamma a & 0 \\ -1 & a & 0 & \gamma a \\ -\gamma a & 0 & 2a & 0 \\ 0 & -\gamma a & 0 & 2a \end{bmatrix} \qquad \mathbf{K} = \begin{bmatrix} a & 0 & \gamma a & 0 \\ 0 & a & 0 & \gamma a \\ -\gamma a & 0 & -2a & 0 \\ 0 & -\gamma a & 0 & -2a \end{bmatrix}$$

For $a < -1$, $\mathbf{h}$ has a negative definite Jacobian and thus is contracting, and $\mathbf{h} - 2\mathbf{u}$ yields a stable limit-cycle, so that the two originally stable cells are excited into oscillations for non-zero initial conditions. Requiring in addition that $\sqrt{2} < \gamma < 3/2$ guarantees that all the eigenvalues of $\mathbf{K}$ are real and strictly positive, so that $\mathbf{K}$ can be transformed into a diagonal diffusion matrix through a linear change of coordinates. □

Example 3.2.3: Smale's example can be simplified by directly using two damped Van der Pol oscillators

$$\begin{cases} \ddot{x}_1 + \alpha(x_1^2 + 2\kappa - 1)\dot{x}_1 + \omega^2 x_1 = -\alpha\kappa(\dot{x}_2 - \dot{x}_1) \\ \ddot{x}_2 + \alpha(x_2^2 + 2\kappa - 1)\dot{x}_2 + \omega^2 x_2 = -\alpha\kappa(\dot{x}_1 - \dot{x}_2) \end{cases}$$

with the simulation result plotted in Figure 3-2. □

3.2.3 Oscillator-Death

Inverse to Smale's effect, there is a phenomenon called oscillator-death (or amplitude-death) [5, 8, 121] where oscillators stop oscillating and stabilize at constant steady states after they are coupled.

Theorem 3.4 *Oscillator-death happens if the dynamics of the whole coupled network is contracting and autonomous.*

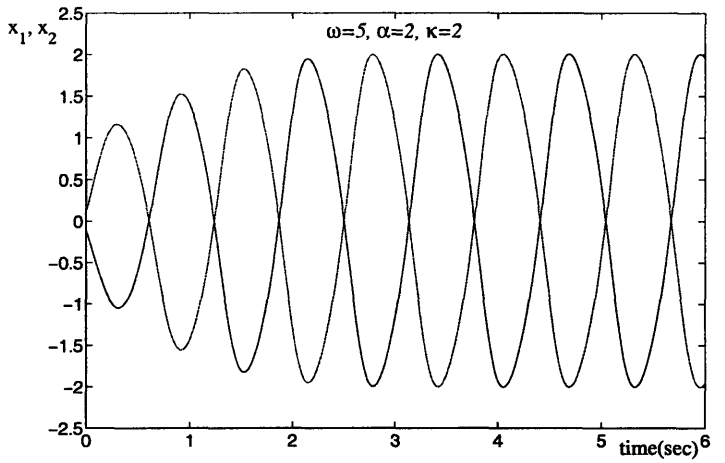

Figure 3-2: Two Smale's cells anti-synchronize through diffusion interactions.

Example 3.2.4: Couple two Van der Pol oscillators with asymmetric forces

$$\begin{cases} \ddot{x}_1 + \alpha(x_1^2 - 1)\dot{x}_1 + \omega^2 x_1 = \alpha\kappa(\dot{x}_2 - \dot{x}_1) \\ \ddot{x}_2 + \alpha(x_2^2 - 1)\dot{x}_2 + \omega^2 x_2 = \alpha\kappa(-\dot{x}_1 - \dot{x}_2) \end{cases} \tag{3.5}$$

where $\kappa > 1$. By introducing new variables y_1 and y_2 as that in system (3.8), we get a generalized Jacobian

$$\mathbf{F} = \begin{bmatrix} -\alpha(x_1^2 + \kappa - 1) & \omega & \alpha\kappa & 0 \\ -\omega & 0 & 0 & 0 \\ -\alpha\kappa & 0 & -\alpha(x_2^2 + \kappa - 1) & \omega \\ 0 & 0 & -\omega & 0 \end{bmatrix} \leq \mathbf{0}$$

whose symmetric part is simply that of two uncoupled damped Van der Pol oscillators. Thus both systems will tend to zero asymptotically. □

3.2.4 Coupled Van der Pol Oscillators - a general study

As a conclusion of this section, we now consider two identical Van der Pol oscillators coupled in a very general way:

$$\begin{cases} \ddot{x}_1 + \alpha(x_1^2 - 1)\dot{x}_1 + \omega^2 x_1 = \alpha\ (\gamma\dot{x}_2 - \kappa\dot{x}_1) \\ \ddot{x}_2 + \alpha(x_2^2 - 1)\dot{x}_2 + \omega^2 x_2 = \alpha\ (\gamma\dot{x}_1 - \kappa\dot{x}_2) \end{cases} \tag{3.6}$$

where α is a positive constant. It can be proved that, as long as the condition

$$|\ \gamma\ | > 1 - \kappa$$

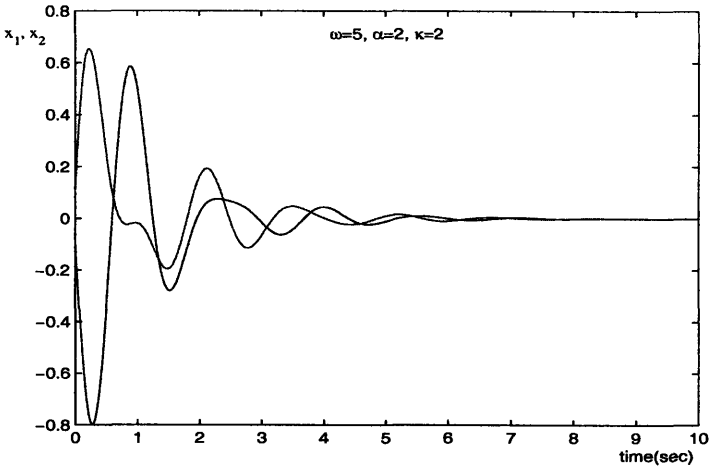

Figure 3-3: Two Van der Pol oscillators die through interactions.

is satisfied, x_1 converges to x_2 asymptotically for all $\gamma \geq 0$ while x_1 converges to $-x_2$ asymptotically for all $\gamma \leq 0$. Note that if $\gamma = 0$ we get two independent stable subsystems. Both x_1 and x_2 tend to the origin, which can be considered as a continuous connection between $\gamma > 0$ and $\gamma < 0$. This result agrees with the common intuition that excitatory coupling leads to synchrony while inhibitory coupling to anti-synchrony.

Next we need to study the stable behavior of the coupled systems in order to make sure that if they keep oscillating or tend to a stationary equilibrium. Assume first that $\gamma > 0$, we have

$$\ddot{x}_i + \alpha(x_i^2 - 1)\dot{x}_i + \omega^2 x_i \;\rightarrow\; \alpha\,(\gamma - \kappa)\dot{x}_i \qquad i = 1, 2$$

which gives the stable dynamics of x_1 and x_2 as

$$\ddot{x}_i + \alpha(x_i^2 + \kappa - \gamma - 1)\dot{x}_i + \omega^2 x_i = 0.$$

This dynamic equation has a stable limit cycle if $\gamma > \kappa - 1$ or a stable equilibrium point at origin otherwise. A similar result can be derived for $\gamma < 0$, where x_1 and x_2 reach anti-synchrony if $\gamma < 1 - \kappa$ or tend to zero otherwise.

Also note that:

- Setting $\kappa = 1$, x_1 and x_2 will keep oscillating for all $\gamma \neq 0$. Oscillator-death as a transition state between synchronized and anti-synchronized solutions does not exist except when $\gamma = 0$.

- In general, a positive value of γ represents a force to drive synchrony while a negative value to drive anti-synchrony. Hence it is easy to understand the behavior of system (3.5) where the coupling to the first oscillator tries to syn-

chronize but the coupling to the second tries to anti-synchronize, with equal strength. A neutral result is thus obtained. In fact, if we look at a coupled system with non-symmetric couplings

$$\begin{cases} \ddot{x}_1 + \alpha(x_1^2 - 1)\dot{x}_1 + \omega^2 x_1 = \alpha\ (\gamma_1 \dot{x}_2 - \kappa_1 \dot{x}_1) \\ \ddot{x}_2 + \alpha(x_2^2 - 1)\dot{x}_2 + \omega^2 x_2 = \alpha\ (\gamma_2 \dot{x}_1 - \kappa_2 \dot{x}_2) \end{cases}$$

the condition for oscillator-death is

$$\kappa_1 > 1\ ,\ \kappa_2 > 1\ \ ,\ (\kappa_1 - 1)(\kappa_2 - 1) \geq (\gamma_1 + \gamma_2)^2/4.$$

- If we add extra diffusion coupling associated to the states x_1 and x_2 to system (3.6)

$$\begin{cases} \ddot{x}_1 + \alpha(x_1^2 - 1)\dot{x}_1 + \omega^2 x_1 = \alpha\ (\gamma \dot{x}_2 - \kappa \dot{x}_1) + \alpha\ (\bar{\gamma} x_2 - \bar{\kappa} x_1) \\ \ddot{x}_2 + \alpha(x_2^2 - 1)\dot{x}_2 + \omega^2 x_2 = \alpha\ (\gamma \dot{x}_1 - \kappa \dot{x}_2) + \alpha\ (\bar{\gamma} x_1 - \bar{\kappa} x_2) \end{cases}$$

where κ and $\bar{\kappa}$ are both positive, the main result preserves as long as $\gamma\bar{\gamma} > 0$. If the condition $\mid \gamma \mid > 1 - \kappa$ is satisfied, x_1 converges to x_2 asymptotically for all $\gamma \geq 0$ while x_1 converges to $-x_2$ asymptotically for all $\gamma \leq 0$. The second coupling term does not change the qualitative results (but only the amplitude and frequency of the final behavior) as long as

$$\omega^2 + \alpha(\ \bar{\kappa} - \mid \bar{\gamma} \mid\ ) > 0\ .$$

These results can be regarded as a global generalization of the dynamics analysis of two identical Van der Pol oscillators in [119, 139].

3.3 Appendix: Driven damped Van der Pol oscillator

Consider the second-order system

$$\ddot{x} + (\beta + \alpha x^2)\dot{x} + \omega^2 x = u(t) \tag{3.7}$$

driven by an external input $u(t)$, where α, β, ω are strictly positive constants. Introducing a new variable y, this system can be written

$$\begin{cases} \dot{x} = \omega y - \frac{\alpha}{3}x^3 - \beta x \\ \dot{y} = -\omega x + \frac{u(t)}{\omega} \end{cases} \tag{3.8}$$

The corresponding Jacobian matrix

$$\mathbf{F} = \begin{bmatrix} -(\beta + \alpha x^2) & \omega \\ -\omega & 0 \end{bmatrix}$$

is negative semi-definite. Therefore,

$$\frac{d}{dt}(\delta \mathbf{z}^T \delta \mathbf{z}) = 2\ \delta \mathbf{z}^T\ \mathbf{F}\ \delta \mathbf{z} \leq 0$$

where $\delta \mathbf{z} = [\delta x, \delta y]^T$ is the generalized virtual displacement. Thus $\delta \mathbf{z}^T \delta \mathbf{z}$ tends to a lower limit asymptotically. Now check its high-order Taylor expansion:
if $\delta x \neq 0$,

$$\delta \mathbf{z}^T \delta \mathbf{z}(t + dt) - \delta \mathbf{z}^T \delta \mathbf{z}(t) = -2\ (\beta + \alpha x^2)(\delta x)^2\ dt + O((dt)^2)$$

while if $\delta x = 0$,

$$\delta \mathbf{z}^T \delta \mathbf{z}(t + dt) - \delta \mathbf{z}^T \delta \mathbf{z}(t) = -4\ (\beta + \alpha x^2)(\delta \dot{x})^2\ \frac{(dt)^3}{3!} + O((dt)^4)$$

So the fact that $\delta \mathbf{z}^T \delta \mathbf{z}$ tends to a lower limit implies that δx and $\delta \dot{x}$ both tend to 0. System (3.7) is called *semi-contracting*, and for any external input all its solutions converge asymptotically to a single trajectory, independent of the initial conditions.

Note that if $\beta < 0$ and $u(t) = 0$, system (3.7) has a unique, stable limit cycle.

Chapter 4

Nonlinear Networked Systems

Most coupled oscillators in the natural world are organized in large networks, such as pacemaker cells in heart, neural networks in brain, fireflies with synchronized flashes, crickets with synchronized chirping, etc.[140, 144]. System (3.2) represents such an instance with a chain structure. In fact, there are many many other instances such as the three symmetric ones we illustrate in Figure 4-1.

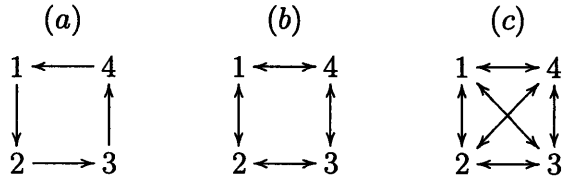

Figure 4-1: An $n = 4$ network with different symmetric structures.

In this chapter, we show that, partial contraction analysis can be applied to study the synchronization phenomenon in networked systems, not limited as oscillators, with various structures or arbitrary sizes. Either individual system's dynamics or coupling forces could be nonlinear.

4.1 Networks with All-To-All Symmetry

As the beginning, we study a network with all-to-all symmetry, that is, each element inside is coupled to all the others. Such a special example can be analyzed using an immediate extension of Theorem 3.2.

Theorem 4.1 *Consider n coupled systems. If a contracting function $\mathbf{h}(\mathbf{x}_i, t)$ exists such that*

$$\dot{\mathbf{x}}_1 - \mathbf{h}(\mathbf{x}_1, t) = \cdots = \dot{\mathbf{x}}_n - \mathbf{h}(\mathbf{x}_n, t)$$

then all the systems will synchronize exponentially regardless of the initial conditions.

For instance, for identical oscillators coupled with diffusion-type force

$$\dot{\mathbf{x}}_i \;=\; \mathbf{f}(\mathbf{x}_i, t) \;+\; \sum_{j=1}^{n} \left(\mathbf{u}(\mathbf{x}_j) - \mathbf{u}(\mathbf{x}_i) \right) \qquad i = 1, 2, \ldots, n \tag{4.1}$$

contraction of $\mathbf{f} - n\mathbf{u}$ guarantees synchronization of the whole network.

Example 4.1.1: Consider an all-to-all network containing four identical Van der Pol oscillators

$$\ddot{x}_i + \alpha(x_i^2 - 1)\dot{x}_i + \omega^2 x_i \;=\; \alpha\kappa \sum_{j=1}^{4} (\dot{x}_j - \dot{x}_i) \qquad i = 1, 2, 3, 4 \tag{4.2}$$

which can be re-written as

$$\ddot{x}_i + \alpha(x_i^2 + 4\kappa - 1)\dot{x}_i + \omega^2 x_i \;=\; \alpha\kappa \sum_{j=1}^{4} \dot{x}_j \qquad i = 1, 2, 3, 4.$$

Thus, these four oscillators will reach synchrony if $\kappa > \frac{1}{4}$, for non-zero initial conditions. □

In [96], Mirollo and Strogatz study an all-to-all network of pulse-coupled integrate-and-fire oscillators, and derive a result on global synchronization. Their analysis is based on an event called *absorption* which is unique to all-to-all coupled networks.

4.2 Networks with Less Symmetry

Besides its direct meaning to all-to-all networks, Theorem 4.1 may also be applied to study networks with less symmetry.

Example 4.2.1: Consider an $n = 4$ network with two-way-ring symmetry (as illustrated in Figure 4-1(b))

$$\dot{\mathbf{x}}_i \;=\; \mathbf{f}(\mathbf{x}_i, t) \;+\; (\mathbf{u}(\mathbf{x}_{i-1}) - \mathbf{u}(\mathbf{x}_i)) \;+\; (\mathbf{u}(\mathbf{x}_{i+1}) - \mathbf{u}(\mathbf{x}_i)) \qquad i = 1, 2, 3, 4$$

where the subscripts $i - 1$ and $i + 1$ are computed circularly. Combining these four oscillators into two groups $(\mathbf{x}_1, \mathbf{x}_2)$ and $(\mathbf{x}_3, \mathbf{x}_4)$, we find

$$\begin{bmatrix} \dot{\mathbf{x}}_1 - \mathbf{f}(\mathbf{x}_1, t) + 2\mathbf{u}(\mathbf{x}_1) \\ \dot{\mathbf{x}}_2 - \mathbf{f}(\mathbf{x}_2, t) + 2\mathbf{u}(\mathbf{x}_2) \end{bmatrix} = \begin{bmatrix} \dot{\mathbf{x}}_3 - \mathbf{f}(\mathbf{x}_3, t) + 2\mathbf{u}(\mathbf{x}_3) \\ \dot{\mathbf{x}}_4 - \mathbf{f}(\mathbf{x}_4, t) + 2\mathbf{u}(\mathbf{x}_4) \end{bmatrix} = \begin{bmatrix} \mathbf{u}(\mathbf{x}_2) + \mathbf{u}(\mathbf{x}_4) \\ \mathbf{u}(\mathbf{x}_1) + \mathbf{u}(\mathbf{x}_3) \end{bmatrix}.$$

Thus, if the function $\mathbf{f} - 2\mathbf{u}$ is contracting, $(\mathbf{x}_1, \mathbf{x}_2)$ converges to $(\mathbf{x}_3, \mathbf{x}_4)$ exponentially, and hence

$$\begin{cases} \dot{\mathbf{x}}_1 - \mathbf{f}(\mathbf{x}_1, t) + 2\mathbf{u}(\mathbf{x}_1) \;\to\; 2\mathbf{u}(\mathbf{x}_2) \\ \dot{\mathbf{x}}_2 - \mathbf{f}(\mathbf{x}_2, t) + 2\mathbf{u}(\mathbf{x}_2) \;\to\; 2\mathbf{u}(\mathbf{x}_1) \end{cases}$$

so that in turn $\mathbf{x}_1$ converges to $\mathbf{x}_2$ exponentially if the function $\mathbf{f} - 4\mathbf{u}$ is contracting. The four oscillators then reach synchrony exponentially regardless of the initial conditions.

For four Van der Pol oscillators,

$$\ddot{x}_i + \alpha(x_i^2 - 1)\dot{x}_i + \omega^2 x_i \;=\; \alpha\kappa \;(\; (\dot{x}_{i-1} - \dot{x}_i) + (\dot{x}_{i+1} - \dot{x}_i) \;) \tag{4.3}$$

a sufficient condition to reach synchrony is $\kappa > \frac{1}{2}$. □

An extended partial contraction analysis can be used to study the example below, the idea of which will be generalized in the following section.

Definition 4.1 *Consider n square matrices* $\mathbf{K}_i$ *of identical dimensions, and define*

$$\mathbf{I}^n_{\mathbf{K}_i} = \begin{bmatrix} \mathbf{K}_1 & 0 & \cdots & 0 \\ 0 & \mathbf{K}_2 & \cdots & 0 \\ \vdots & \vdots & \ddots & \vdots \\ 0 & 0 & \cdots & \mathbf{K}_n \end{bmatrix}$$

One has $\mathbf{I}^n_{\mathbf{K}_i} > \mathbf{0}$ *if and only if* $\mathbf{K}_i > \mathbf{0}$, $\forall i$.

Definition 4.2 *Consider a square symmetric matrix* $\mathbf{K}$, *and define*

$$\mathbf{U}^n_{\mathbf{K}} = \begin{bmatrix} \mathbf{K} & \mathbf{K} & \cdots & \mathbf{K} \\ \mathbf{K} & \mathbf{K} & \cdots & \mathbf{K} \\ \vdots & \vdots & \ddots & \vdots \\ \mathbf{K} & \mathbf{K} & \cdots & \mathbf{K} \end{bmatrix}_{n \times n}$$

One has $\mathbf{U}^n_{\mathbf{K}} \geq 0$ *if and only if* $\mathbf{K} \geq 0$.

Example 4.2.2: Consider an $n = 4$ network with one-way-ring symmetry (as illustrated in Figure 4-1(a))

$$\dot{\mathbf{x}}_i \;=\; \mathbf{f}(\mathbf{x}_i, t) \;+\; \mathbf{K}\;(\;\mathbf{x}_{i-1} \;-\; \mathbf{x}_i\;) \qquad i = 1,2,3,4$$

where $\mathbf{K} = \mathbf{K}^T \geq 0$ and the subscripts are calculated circularly. This system is equivalent to

$$\dot{\mathbf{x}}_i \;=\; \mathbf{f}(\mathbf{x}_i, t) \;-\; \mathbf{K}(2\mathbf{x}_i + \mathbf{x}_{i+1} + \mathbf{x}_{i+2}) \;+\; \mathbf{K}\sum_{j=1}^{4} \mathbf{x}_j$$

Construct an auxiliary system driven by the input $\mathbf{K}\sum_{j=1}^{4} \mathbf{x}_j(t)$

$$\dot{\mathbf{y}}_i = \mathbf{f}(\mathbf{y}_i, t) - \mathbf{K}(2\mathbf{y}_i + \mathbf{y}_{i+1} + \mathbf{y}_{i+2}) + \mathbf{K}\sum_{j=1}^{4} \mathbf{x}_j(t) \qquad i = 1,2,3,4$$

The auxiliary system admits the particular solution $\mathbf{y}_1 = \mathbf{y}_2 = \mathbf{y}_3 = \mathbf{y}_4 = \mathbf{y}_\infty$ with

$$\dot{\mathbf{y}}_\infty \;=\; \mathbf{f}(\mathbf{y}_\infty, t) \;-\; 4\,\mathbf{K}\,\mathbf{y}_\infty \;+\; \mathbf{K}\sum_{j=1}^{4} \mathbf{x}_j(t)$$

To apply Theorem 2.1 for the specific property $\mathbf{y}_1 = \mathbf{y}_2 = \mathbf{y}_3 = \mathbf{y}_4$ and prove that all $\mathbf{x}_i$ synchronize regardless of the initial conditions, there only remains to study the Jacobian matrix

$$\mathbf{J} = \begin{bmatrix} \mathbf{J}_1 - 2\mathbf{K} & -\mathbf{K} & -\mathbf{K} & 0 \\ 0 & \mathbf{J}_2 - 2\mathbf{K} & -\mathbf{K} & -\mathbf{K} \\ -\mathbf{K} & 0 & \mathbf{J}_3 - 2\mathbf{K} & -\mathbf{K} \\ -\mathbf{K} & -\mathbf{K} & 0 & \mathbf{J}_4 - 2\mathbf{K} \end{bmatrix}$$

where $\mathbf{J}_i = \frac{\partial \mathbf{f}}{\partial \mathbf{y}}(\mathbf{y}_i, t)$. The symmetric part of the Jacobian is

$$\begin{aligned} \mathbf{J}_s &= \begin{bmatrix} \mathbf{J}_{1s} - 2\mathbf{K} & -\frac{\mathbf{K}}{2} & -\mathbf{K} & -\frac{\mathbf{K}}{2} \\ -\frac{\mathbf{K}}{2} & \mathbf{J}_{2s} - 2\mathbf{K} & -\frac{\mathbf{K}}{2} & -\mathbf{K} \\ -\mathbf{K} & -\frac{\mathbf{K}}{2} & \mathbf{J}_{3s} - 2\mathbf{K} & -\frac{\mathbf{K}}{2} \\ -\frac{\mathbf{K}}{2} & -\mathbf{K} & -\frac{\mathbf{K}}{2} & \mathbf{J}_{4s} - 2\mathbf{K} \end{bmatrix} \\ &= \mathbf{I}^4_{(\mathbf{J}_{is} - \mathbf{K})} - \frac{1}{2}\,\mathbf{U}^4_{\mathbf{K}} - \frac{1}{2}\,\mathbf{J}_+ \end{aligned}$$

where

$$\mathbf{J}_+ = \begin{bmatrix} \mathbf{K} & 0 & \mathbf{K} & 0 \\ 0 & \mathbf{K} & 0 & \mathbf{K} \\ \mathbf{K} & 0 & \mathbf{K} & 0 \\ 0 & \mathbf{K} & 0 & \mathbf{K} \end{bmatrix}$$

We know that if $\forall i$, $\mathbf{J}_{is} - \mathbf{K} < \mathbf{0}$, then $\mathbf{I}^4_{(\mathbf{J}_{is} - \mathbf{K})} < 0$, and if $\mathbf{K} \geq 0$ then $\mathbf{U}^4_{\mathbf{K}} \geq 0$ and $\mathbf{J}_+ \geq 0$. If both conditions are satisfied, the Jacobian $\mathbf{J}_s$ is negative definite.

A corresponding Van der Pol example is

$$\ddot{x}_i + \alpha(x_i^2 - 1)\dot{x}_i + \omega^2 x_i = \alpha\kappa(\dot{x}_{i-1} - \dot{x}_i) \qquad i = 1, 2, 3, 4 \tag{4.4}$$

where the sufficient condition to reach synchrony asymptotically is $\kappa > 1$. □

Note that up to now, we have studied the synchronization behaviors of coupled networks containing four oscillators with chain, one-way-ring, two-way-ring and all-to-all structures. Figure 4-2 lists simulation results of coupled Van der Pol oscillators, whose dynamics are based on equations (3.2), (4.4), (4.3) and (4.2). The asymptotic synchronization conditions are $\kappa > 1$, $\kappa > 1$, $\kappa > \frac{1}{2}$, $\kappa > \frac{1}{4}$, respectively. Given the same parameters ($\alpha = 0.5$, $\omega = 2$, $\kappa = 1.5$) and the same initial conditions (chosen randomly), we see from the figures that the synchronization rate increases in such an order as

$$\text{chain} \longrightarrow \text{one-way-ring} \longrightarrow \text{two-way-ring} \longrightarrow \text{all-to-all}$$

We will explain this observation in Section 4.5. Note that in each figure, the ordinate is x_i and the abscissa is time. The solid curve represents $x_1(t)$, the state of the first oscillator which is the independent one in the chain structure.

4.3 Networks with General Structure

Based on partial contraction analysis, we now study networked systems coupled in a very general structure. For notation simplicity, we first assume that coupling forces

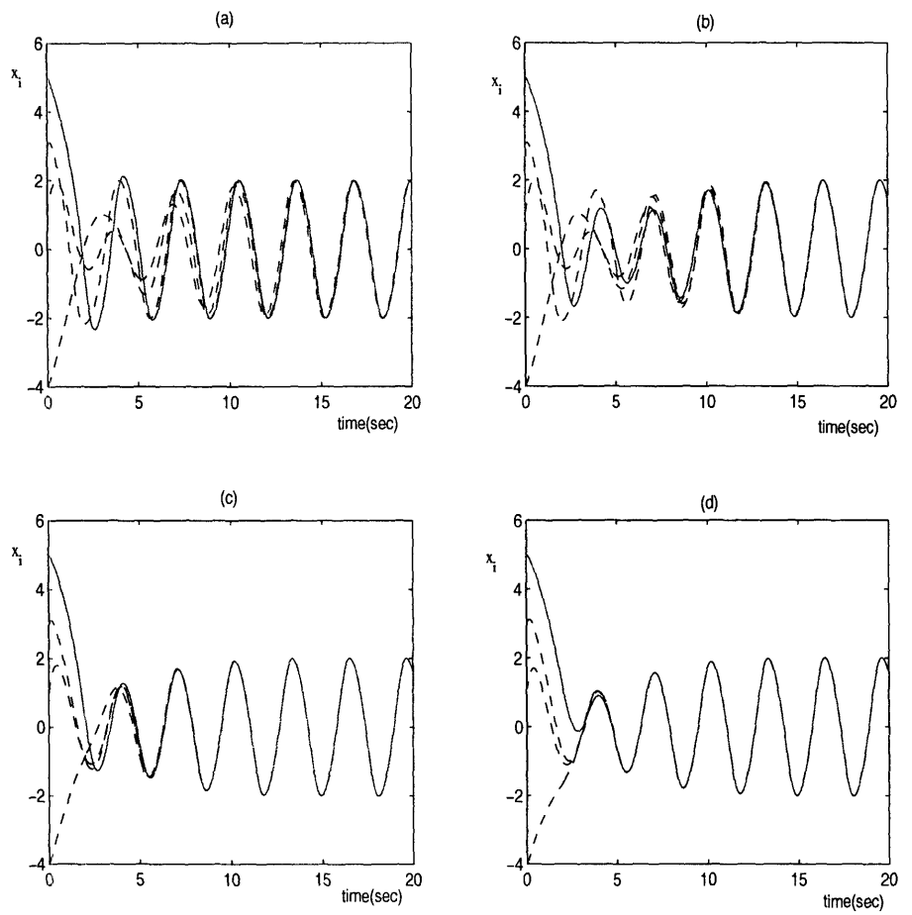

Figure 4-2: Four coupled Van der Pol oscillators synchronize with (a) chain, (b) one-way-ring, (c) two-way-ring, (d) all-to-all structure.

are linear diffusive with gains $\mathbf{K}_{ij}$ (associated with coupling from node i to j) positive definite, i.e., $(\mathbf{K}_{ij})_s = \mathbf{K}_{ijs} > 0$. We further assume that coupling links are bidirectional and symmetric in different directions, i.e., $\mathbf{K}_{ij} = \mathbf{K}_{ji}$. All these assumptions can be relaxed as we will show later.

Consider now a network containing n identical elements

$$\dot{\mathbf{x}}_i = \mathbf{f}(\mathbf{x}_i, t) + \sum_{j \in \mathcal{N}_i} \mathbf{K}_{ji} (\mathbf{x}_j - \mathbf{x}_i) \qquad i = 1, \ldots, n \tag{4.5}$$

where $\mathcal{N}_i$ denotes the set of indices of the active links of element i. It is equivalent to

$$\dot{\mathbf{x}}_i = \mathbf{f}(\mathbf{x}_i, t) + \sum_{j \in \mathcal{N}_i} \mathbf{K}_{ji} (\mathbf{x}_j - \mathbf{x}_i) - \mathbf{K}_0 \sum_{j=1}^{n} \mathbf{x}_j + \mathbf{K}_0 \sum_{j=1}^{n} \mathbf{x}_j$$

where $\mathbf{K}_0$ is chosen to be a constant symmetric positive definite matrix (we will discuss its function later). As usual, we construct an auxiliary system

$$\dot{\mathbf{y}}_i = \mathbf{f}(\mathbf{y}_i, t) + \sum_{j \in \mathcal{N}_i} \mathbf{K}_{ji} (\mathbf{y}_j - \mathbf{y}_i) - \mathbf{K}_0 \sum_{j=1}^{n} \mathbf{y}_j + \mathbf{K}_0 \sum_{j=1}^{n} \mathbf{x}_j(t) \tag{4.6}$$

which has a particular solution $\mathbf{y}_1 = \cdots = \mathbf{y}_n = \mathbf{y}_\infty$ with

$$\dot{\mathbf{y}}_\infty = \mathbf{f}(\mathbf{y}_\infty, t) - n\, \mathbf{K}_0\, \mathbf{y}_\infty + \mathbf{K}_0 \sum_{j=1}^{n} \mathbf{x}_j(t)$$

According to Partial Contraction Theory 2.1, if the auxiliary system (4.6) is contracting, all system trajectories will verify the independent property $\mathbf{x}_1 = \cdots = \mathbf{x}_n$ exponentially.

Next, we compute $\mathbf{J}_s$, the symmetric part of the Jacobian matrix of the auxiliary system.

Definition 4.3 *Consider a square symmetric matrix* $\mathbf{K}$*, and define*

$$\mathbf{T}_{\mathbf{K}}^n = \begin{bmatrix} \ddots & \vdots & & \vdots & \\ \cdots & \mathbf{K} & \cdots & -\mathbf{K} & \cdots \\ & \vdots & \ddots & \vdots & \\ \cdots & -\mathbf{K} & \cdots & \mathbf{K} & \cdots \\ & \vdots & & \vdots & \ddots \end{bmatrix}_{n \times n}$$

where all the elements in $\mathbf{T}_{\mathbf{K}}^n$ *except those already displayed in the four intersection points of* i*th and* j*th rows and* i*th and* j*th columns are zero.* $\mathbf{T}_{\mathbf{K}}^n \geq 0$ *if* $\mathbf{K} \geq 0$.

Definition 4.4 *Define the set*

$$\mathcal{N} = \cup_{i=1}^{n} \mathcal{N}_i$$

including all the active links in the network.

Definition 4.5 *Define*

$$\mathbf{L_K} = \sum_{(i,j)\in\mathcal{N}} \mathbf{T}^n_{\mathbf{K}_{ijs}}$$

In fact, if we view the network as a graph, $\mathbf{L_K}$ *is the symmetric part of the weighted Laplacian matrix [40]. The standard laplacian matrix is denoted as* $\mathbf{L}$.

Thus, we have

$$\mathbf{J}_s = \mathbf{I}^n_{\mathbf{J}_{is}} - \mathbf{L_K} - \mathbf{U}^n_{\mathbf{K}_0}$$

where $\mathbf{J}_{is} = (\frac{\partial \mathbf{f}}{\partial \mathbf{y}}(\mathbf{y}_i, t))_s$.

Lemma 4.1 *Define*

$$\mathbf{J}_r = -\mathbf{L_K} - \mathbf{U}^n_{\mathbf{K}_0}$$

If $\mathbf{K}_0 > \mathbf{0}$, $\mathbf{K}_{ij} > \mathbf{0}$, $\forall (i,j) \in \mathcal{N}$, *and the network is connected, then* $\mathbf{J}_r < \mathbf{0}$.

Proof: Note that each of the two parts in $\mathbf{J}_r$ is only negative semi-definite. Given an arbitrary nonzero vector $\mathbf{v} = [\mathbf{v}_1, \ldots, \mathbf{v}_n]^T$, one has

$$\begin{aligned} \mathbf{v}^T \mathbf{J}_r \mathbf{v} &= -\sum_{(i,j)\in\mathcal{N}} (\mathbf{v}_i - \mathbf{v}_j)^T \mathbf{K}_{ijs} (\mathbf{v}_i - \mathbf{v}_j) - (\sum_{i=1}^n \mathbf{v}_i)^T \mathbf{K}_0 (\sum_{i=1}^n \mathbf{v}_i) \\ &< 0 \end{aligned}$$

because the condition that the network is connected guarantees that

$$\mathbf{v}^T \mathbf{J}_r \mathbf{v} = 0 \quad \text{if and only if} \quad \mathbf{v}_1 = \cdots = \mathbf{v}_n = 0.$$

Furthermore, the largest eigenvalue of $\mathbf{J}_r$ can be calculated as

$$\lambda_{max}(\mathbf{J}_r) = \max_{\|\mathbf{v}\|=1} \mathbf{v}^T \mathbf{J}_r \mathbf{v} = \max_{\|\mathbf{v}\|=1} (-\mathbf{v}^T \mathbf{L_K} \mathbf{v} - \mathbf{v}^T \mathbf{U}^n_{\mathbf{K}_0} \mathbf{v})$$

Since $-\mathbf{v}^T \mathbf{U}^n_{\mathbf{K}_0} \mathbf{v}$ keeps decreasing as $\mathbf{K}_0$ increases except on the set $\sum_{i=1}^n \mathbf{v}_i = 0$, we can choose $\mathbf{K}_0$ large enough and get

$$\lambda_{max}(\mathbf{J}_r) = -\min_{\substack{\|\mathbf{v}\|=1 \\ \sum_{i=1}^n \mathbf{v}_i = 0}} \mathbf{v}^T \mathbf{L_K} \mathbf{v} = -\lambda_{m+1}(\mathbf{L_K})$$

according to the Courant-Fischer Theorem [51] – note that $\mathbf{K}_0$ is a virtual quantity used to make $\mathbf{J}_r < 0$ in the partial contracting analysis, and thus it cannot affect the real system's synchronization rate. Here the eigenvalues are arranged in an increasing order, and $\lambda_1(\mathbf{L_K}) = \cdots = \lambda_m(\mathbf{L_K}) = 0$, where m is the dimension of each individual element.

Note that in the particular case $m = 1$, and $\forall \mathbf{K}_{ij} = 1$, eigenvalue $\lambda_2(\mathbf{L_K}) = \lambda_2(\mathbf{L})$ is a fundamental quantity in graph theory named *algebraic connectivity* [34], which is equal to zero if and only if the graph is not connected. □

The above results imply immediately

Theorem 4.2 *Regardless of initial conditions, all the elements within a generally coupled network (4.5) will reach synchrony or group agreement exponentially if*

$$\lambda_{m+1}(\mathbf{L_K}) > \max_i \lambda_{max}(\mathbf{J}_{is}) \quad \text{uniformly} \tag{4.7}$$

or, in words, if

- *the network is connected,*
- $\lambda_{max}(\mathbf{J}_{is})$ *is upper bounded,*
- *the coupling strengths are strong enough.*

Proof: The auxiliary system (4.6) is contracting if the condition (4.7) is true. □

A few remarks on Theorem 4.2:

- The conditions given in Theorem 4.2 to guarantee synchronization represent the requirements on both individual system's internal dynamics and the network's geometric structure. A lower bound on the corresponding threshold of the coupling strength can be computed through eigenvalue analysis if a special network is given.

- Theorem 4.2 can also be used to find the threshold for symmetric subgroups in a network to reach synchrony, such as what we have illustrated in the simple Example 4.2.1.

- Partial contraction analysis does not add any restriction on the uncoupled dynamics $\mathbf{f}(\mathbf{x}, t)$ other than requiring $\lambda_{max}(\mathbf{J}_{is})$ to be upper bounded, which is easy to be satisfied if for instance individual elements are oscillators. As an example, $\lambda_{max}(\mathbf{J}_{is}) = \alpha$ for the Van der Pol oscillator. In fact, different qualitative choices exist for $\mathbf{f}$, which can be an oscillator, a contracting system, zero, or even a chaotic system [113, 133, 144]. For a group of contracting systems, if $\mathbf{\Theta} = \mathbf{I}$, the contraction property of the overall group will be enhanced by the diffusion couplings, and all the coupled systems are expected to converge to a common equilibrium point exponentially if $\mathbf{f}$ is autonomous. If $\mathbf{\Theta} \neq \mathbf{I}$, however, the situation is more complicated. A transformation process must be done in order to guarantee exponential convergence of the virtual dynamics. The coupling gain may lose positivity through the transformation, and the stability of the equilibrium point may be destroyed with strong enough coupling strengths. This kind of bifurcation is interesting especially if the otherwise silent systems behave as oscillators after coupling, a phenomenon of Smale's cells [79, 136, 153]. A simple example when $n = 2$ has been discussed in Section 3.2.2.

- The definition of the "neighbor" sets $\mathcal{N}_i$ is quite flexible. While it may be based simply on position proximity (neighbors within a certain distance of each node), it can be chosen to reflect many other factors. Gestalt psychology [124], for instance, suggests that in human visual perception, grouping occurs not only by proximity, but also by similarity, closure, continuity, common region and connectedness. The coupling strengths can also be specified flexibly. For instance, using Schoenberg/Micchelli's theorems on positive definite functions [93], they can be chosen as smooth functions based on sums of gaussians.

- Partial contraction theory is derived from contraction theory. Thus many results from [81, 132] apply directly. Consider for instance a coupled network with constraints

$$\dot{\mathbf{x}}_i = \mathbf{f}(\mathbf{x}_i, t) + \mathbf{n}_i + \sum_{j \in \mathcal{N}_i} \mathbf{K}_{ji} \, (\mathbf{x}_j - \mathbf{x}_i) \qquad i = 1, \ldots, n$$

  where $\mathbf{n}_i$ represents a superimposed flow normal to the constraint manifold and has the same form to each system. Construct the corresponding auxiliary system

$$\dot{\mathbf{y}}_i = \mathbf{f}(\mathbf{y}_i, t) + \mathbf{n}_i + \sum_{j \in \mathcal{N}_i} \mathbf{K}_{ji} \, (\mathbf{y}_j - \mathbf{y}_i) - \mathbf{K}_0 \sum_{j=1}^{n} \mathbf{y}_j + \mathbf{K}_0 \sum_{j=1}^{n} \mathbf{x}_j \tag{4.8}$$

  Using [81], contraction of the unconstrained flow (4.6) implies local contraction of the constrained flow (4.8), which means group agreement can be achieved for constrained network in a finite region which can be computed explicitly. In same cases, the introduction of the constraint combined with the specific property of the particular solution implies that the constrained original system is actually contracting. Similarly, because the auxiliary system is contracting, robustness results in [81] apply directly.

4.4 Extensions

Besides the properties discussed above, here we make a few more technical remarks and extensions to Theorem 4.2. We shall relax those assumptions made earlier.

4.4.1 Nonlinear Couplings

The analysis carries on straightforwardly to nonlinear couplings. For instance,

$$\dot{\mathbf{x}}_i \;=\; \mathbf{f}(\mathbf{x}_i, t) \;+\; \sum_{j \in \mathcal{N}_i} \mathbf{u}_{ji} \, (\mathbf{x}_j, \mathbf{x}_i, \mathbf{x}, t)$$

where the couplings are of the form

$$\mathbf{u}_{ji} \;=\; \mathbf{u}_{ji} \, (\, \mathbf{x}_j - \mathbf{x}_i, \; \mathbf{x}, \; t \,)$$

with $\mathbf{u}_{ji}\ (\ \mathbf{0},\ \mathbf{x},\ t\ ) = \mathbf{0}\ \ \forall\ i,\ j,\ \mathbf{x}, t$. The whole proof is the same except that we define

$$\mathbf{K}_{ji}\ =\ \frac{\partial \mathbf{u}_{ji}\ (\ \mathbf{x}_j - \mathbf{x}_i,\ \mathbf{x},\ t\ )}{\partial(\mathbf{x}_j - \mathbf{x}_i)}\ >\ 0 \qquad \text{uniformly}$$

and assume $\mathbf{K}_{ji} = \mathbf{K}_{ij}$.

For instance, one may have

$$\mathbf{u}_{ji}\ =\ (\ \mathbf{C}_{ji}(t) + \ \mathbf{B}_{ji}(t)\ \|\mathbf{x}_j - \mathbf{x}_i\|\ )\ (\mathbf{x}_j - \mathbf{x}_i)$$

with $\mathbf{C}_{ji} = \mathbf{C}_{ij} > 0$ uniformly and $\mathbf{B}_{ji} = \mathbf{B}_{ij} \geq 0$.

Note that if the network is all-to-all coupled, the coupling forces can be even more general as we discussed in Section 4.1.

4.4.2 One-way Couplings

The bidirectional coupling assumption on each link is not always necessary. Consider a coupled network with one-way-ring structure and linear diffusion coupling force

$$\dot{\mathbf{x}}_i\ =\ \mathbf{f}(\mathbf{x}_i, t)\ +\ \mathbf{K}\ (\ \mathbf{x}_{i-1}\ -\ \mathbf{x}_i\ ) \qquad i = 1, \ldots, n$$

where by convention $i - 1 = n$ when $i = 1$. We assume that the coupling gain $\mathbf{K} = \mathbf{K}^T > 0$ is identical to all links. Hence,

$$\mathbf{J}_r\ =\ -\frac{1}{2}\mathbf{L}_{\mathbf{K}}\ -\ \mathbf{U}^n_{\mathbf{K}_0}$$

is negative definite with

$$\mathbf{L}_{\mathbf{K}}\ =\ \sum_{i=1}^{n} \mathbf{T}^n_{\mathbf{K}}(i,\ i+1)$$

Since

$$\begin{aligned}\lambda_{m+1}(\ \frac{1}{2}\sum_{i=1}^{n} \mathbf{T}^n_{\mathbf{K}}(i,\ i+1)\ )\ &=\ \frac{1}{2}\ \lambda_{min}(\mathbf{K})\ \lambda_2(\sum_{i=1}^{n} \mathbf{T}^n_1(i,\ i+1)\ ) \\ &=\ \lambda_{min}(\mathbf{K})\ (1 - \cos\frac{2\pi}{n})\ ,\end{aligned}$$

the threshold to reach synchrony exponentially is

$$\lambda_{min}(\mathbf{K})\ (1 - \cos\frac{2\pi}{n}) > \max_i \lambda_{max}(\mathbf{J}_{is}) \qquad \text{uniformly} \tag{4.9}$$

A special case was given in Example 4.2.2 with $n = 4$.

Thus, Theorem 4.2 can be extended to the network whose links are either bidirectional with $\mathbf{K}_{ji} = \mathbf{K}_{ij}$ or unidirectional but formed as rings with $\mathbf{K}^T = \mathbf{K}$ (where $\mathbf{K}$ is identical within the same ring but may differ between different rings). Synchronized groups with increasing complexity can be generated through accumulation of smaller

groups.

In this context, for notational simplicity we do not differentiate between bidirectional and unidirectional links throughout the remainder of the thesis.

4.4.3 Positive Semi-Definite Couplings

Generally, to apply Theorem 4.2, we need positive definite coupling gains. If this condition can not be satisfied as the coupling gain $\mathbf{K}_{ij}$ is only positive semi-definite, we have to add extra restriction to the uncoupled system dynamics to guarantee globally stable synchronization.

Without loss of generality, we assume

$$\mathbf{K}_{ijs} = \begin{bmatrix} \bar{\mathbf{K}}_{ijs} & 0 \\ 0 & 0 \end{bmatrix}$$

where $\bar{\mathbf{K}}_{ijs}$ is positive definite and has a common dimension to all links. Thus, we can divide the uncoupled dynamics $\mathbf{J}_{is}$ into the form

$$\mathbf{J}_{is} = \begin{bmatrix} \mathbf{J}_{11s} & \mathbf{J}_{12} \\ \mathbf{J}_{12}^T & \mathbf{J}_{22s} \end{bmatrix}_i$$

with each component having the same dimension as that of the corresponding one in $\mathbf{K}_{ijs}$. A sufficient condition to guarantee globally stable synchronization behavior in the region beyond a coupling strength threshold is that, $\forall i$, $\mathbf{J}_{22s}$ *is contracting and both* $\lambda_{max}(\mathbf{J}_{11s})$, $\sigma_{max}(\mathbf{J}_{12})$ *are bounded.*

To prove this result, we choose a nonzero vector $\mathbf{v} = [\mathbf{v}_1, \ldots, \mathbf{v}_n]^T$ and get

$$\begin{aligned} \mathbf{v}^T \mathbf{J}_s \mathbf{v} &= \sum_{i=1}^{n} \mathbf{v}_i^T \mathbf{J}_{is} \mathbf{v}_i + \mathbf{v}^T \mathbf{J}_r \mathbf{v} \\ &\leq \sum_{i=1}^{n} \mathbf{v}_i^T \begin{bmatrix} 0 & \mathbf{J}_{12} \\ \mathbf{J}_{12}^T & \mathbf{J}_{22s} \end{bmatrix}_i \mathbf{v}_i + \sum_{i=1}^{n} \mathbf{v}_i^T \begin{bmatrix} \lambda \mathbf{I} & 0 \\ 0 & 0 \end{bmatrix} \mathbf{v}_i \\ &= \sum_{i=1}^{n} \mathbf{v}_i^T \begin{bmatrix} \lambda \mathbf{I} & \mathbf{J}_{12} \\ \mathbf{J}_{12}^T & \mathbf{J}_{22s} \end{bmatrix}_i \mathbf{v}_i \end{aligned}$$

where

$$\lambda = \lambda_{max}(\bar{\mathbf{J}}_r) + \max_i \lambda_{max}(\mathbf{J}_{11s})$$

and $\bar{\mathbf{J}}_r$ is a new matrix by ruling out the rows and columns containing only zero in $\mathbf{J}_r$ (we set $\mathbf{K}_0$ to be positive semi-definite and have the same form as $\mathbf{K}_{ijs}$) and hence is negative definite. From feedback combination condition (2.4), we know that a negative λ with absolute value large enough, a contracting $\mathbf{J}_{22s}$ and a bounded $\sigma(\mathbf{J}_{12})$ for all i guarantee the contracting of $\mathbf{J}_s$. In fact, global contraction of $\mathbf{J}_{22s}$ is a very important necessary condition, without which the synchronization can not occur in an unbounded parameter region. Pecora first pointed this out in [9, 114, 115]

with a new concept called *desynchronizing bifurcation.* Recently, [118] independently studied the similar phenomena.

Example 4.4.1: Consider a network composed of identical Van der Pol oscillators in a general structure. The dynamics of the ith oscillator is given as

$$\ddot{x}_i + \alpha(x_i^2 - 1)\dot{x}_i + \omega^2 x_i = \sum_{j \in \mathcal{N}_i} \alpha\kappa(\dot{x}_j - \dot{x}_i)$$

Using partial contracting analysis, we have

$$\mathbf{J}_s = \mathbf{I}^n_{\mathbf{J}_{is}} + \mathbf{J}_r = \mathbf{I}^n_{\mathbf{J}_{is}} - \mathbf{L}_{\mathbf{K}} - \mathbf{U}^n_{\mathbf{K}_0}$$

with

$$\mathbf{J}_{is} = \begin{bmatrix} \alpha(1 - x_i^2) & 0 \\ 0 & 0 \end{bmatrix}, \quad \mathbf{K}_{ij} = \mathbf{K}_{ijs} = \begin{bmatrix} \alpha\kappa & 0 \\ 0 & 0 \end{bmatrix}.$$

By rule out the even rows and even columns in $\mathbf{J}_s$ where the components are all zero, we get a new result

$$\bar{\mathbf{J}}_s = \mathbf{I}^n_{\bar{\mathbf{J}}_{is}} - \mathbf{L}_{\bar{\mathbf{K}}} - \mathbf{U}^n_{\bar{\mathbf{K}}_0}$$

with

$$\bar{\mathbf{J}}_{is} = \alpha(1 - x_i^2), \quad \bar{\mathbf{K}}_{ij} = \bar{\mathbf{K}}_{ijs} = \alpha\kappa.$$

The condition for $\bar{\mathbf{J}}_s$ to be negative definite is

$$\frac{1}{\kappa} < \lambda_2(\sum_{i,j \in \mathcal{N}} \mathbf{T}^n_1) = \lambda_2(\mathbf{L})$$

which guarantees simultaneously that $\mathbf{J}_s$ is negative semi-definite. Using semi-contracting analysis, we know that synchrony will happen asymptotically.

An important application of coupled nonlinear oscillators is the modeling of central pattern generators [21, 22, 41, 42, 43]. Consider a two-way-ring neural network composed of four identical Van der Pol oscillators as given in Figure 4-1(b). Assume that the first oscillator is connected to the left front leg while the third to the right back one. The system dynamics is given as

$$\ddot{x}_i + \alpha(x_i^2 - 1)\dot{x}_i + \omega^2 x_i = \alpha\kappa(\ \gamma_{(i-1)i}\ \dot{x}_{i-1} - \dot{x}_i\ ) + \alpha\kappa(\ \gamma_{(i+1)i}\ \dot{x}_{i+1} - \dot{x}_i\ )$$

with $i = 1, 2, 3, 4$. Choosing different values of coupling coefficient γ_{ij}, this model is able to generate rhythmic signals to drive different quadrupedal gaits. We set $\gamma_{ij} = \gamma_{ji} = 1$ if we want the oscillators i and j to synchronize while set $\gamma_{ij} = \gamma_{ji} = -1$ if we want them to anti-synchronize. Thus, following the description of animal gaits in [21], we are able to realize the pace, trot, bound and pronk, the quadrupedal gaits which are highly symmetric and robust with relative phase lags of zero or half a period. For instance, the pace gait(left/right pairing) is achieved by setting

$$\gamma_{41} = \gamma_{14} = -1, \quad \gamma_{21} = \gamma_{12} = 1, \quad \gamma_{32} = \gamma_{23} = -1, \quad \gamma_{43} = \gamma_{34} = 1$$

and coupling gain $\kappa > \frac{1}{2}$. The convergence from one gait to another is global. Once all the γ_{ij} are set to be zero, we get the stand.

A similar model can be used to study the locomotion of other numbers of legs. For instance, consider a two-way-ring network composed of six oscillators. By setting $\kappa > 1$ and all the γ_{ij} to be -1, we are able to generate the tripod gait, a common hexapodal gait in which the front and rear legs on one side, and the middle leg on the other, move together, followed by the remaining three legs half a period later [22].

Note that there are two different interpretations of locomotion, one of which believes that the rhythmic signals are generated by coupled neural cells in a Central Pattern Generator while another by interact the legs directly. □

Example 4.4.2: The FitzHugh-Nagumo(FN) model [36, 100] is a well-known simplified version of the classical Hodgkin-Huxley model [49], the first mathematical model of wave propagation in squid nerve. Originally derived from the Van der Pol oscillator, it is given by

$$\begin{cases} \dot{v} = c(v + w - \frac{1}{3}v^3 + I) & 1 - \frac{2}{3}b < a < 1 \\ \dot{w} = -\frac{1}{c}(v - a + bw) & 0 < b < 1,\ b < c^2 \end{cases}$$

where v is directly related to the membrane potential, w is responsible for accommodation and refractoriness, and I corresponds to stimulating current. Consider a diffusion-coupled network with n identical FitzHugh-Nagumo neurons

$$\begin{cases} \dot{v}_i = c(v_i + w_i - \dfrac{1}{3}v_i^3 + I) + \displaystyle\sum_{j \in \mathcal{N}_i} k_{ji}\ (v_j - v_i) \\ \dot{w}_i = -\frac{1}{c}(v_i - a + bw_i) \qquad\qquad i = 1, \ldots, n \end{cases} \tag{4.10}$$

Defining a transformation matrix $\mathbf{\Theta} = \begin{bmatrix} 1 & 0 \\ 0 & c \end{bmatrix}$, which leaves the coupling gain unchanged, yields the generalized Jacobian of the uncoupled dynamics

$$\mathbf{J}_i = \begin{bmatrix} c(1 - v_i^2) & 1 \\ -1 & -\frac{b}{c} \end{bmatrix}$$

Thus the whole network will synchronize exponentially if the coupling strengths are strong enough that

$$\lambda_2\Big(\sum_{(i,j) \in \mathcal{N}} \mathbf{T}^n_{k_{ij}}\Big) \;=\; \lambda_2(\mathbf{L}_{\bar{\mathbf{K}}}) \;>\; c$$

Note that the model can be generalized using a linear state transformation to the dimensionless system [99]

$$\begin{cases} \dot{v} = v(\alpha - v)(v - 1) - w + I \\ \dot{w} = \beta v - \gamma w \end{cases} \tag{4.11}$$

where α, β, γ are positive constants. The contraction analysis of the coupled network

$$\begin{cases} \dot{v} = v(\alpha - v)(v - 1) - w + I + \displaystyle\sum_{j \in \mathcal{N}_i} k_{ji}\ (v_j - v_i) \\ \dot{w} = \beta v - \gamma w \qquad\qquad i = 1, \ldots, n \end{cases} \tag{4.12}$$

yields a very similar result. We will use both models in the rest of the thesis. They are switchable. □

4.5 Algebraic Connectivity

For a coupled network with given structure, increasing the coupling gain for a link or adding an extra link will both improve the synchronization process. In fact, these two operations are the same in a general understanding by adding an extra term $-\mathbf{T}^n_{\mathbf{K}_{ijs}}$ to the matrix $\mathbf{J}_s$. According to Weyl's Theorem [51], if square matrix $\mathbf{A}$, $\mathbf{B}$ are Hermitian and the eigenvalues $\lambda_i(\mathbf{A})$, $\lambda_i(\mathbf{B})$ and $\lambda_i(\mathbf{A}+\mathbf{B})$ are arranged in increasing order, for each $k = 1, 2, \ldots, n$, we have

$$\lambda_k(\mathbf{A}) + \lambda_1(\mathbf{B}) \leq \lambda_k(\mathbf{A}+\mathbf{B}) \leq \lambda_k(\mathbf{A}) + \lambda_n(\mathbf{B})$$

which means immediately

$$\lambda_k(\mathbf{J}_s - \mathbf{T}^n_{\mathbf{K}_{ijs}}) \leq \lambda_k(\mathbf{J}_s)$$

since $\lambda_{max}(-\mathbf{T}^n_{\mathbf{K}_{ijs}}) = 0$. This result explains the observation from Figure 4-2.

In fact, connecting each node to more neighbors is an effective way for large-size networks to lower the synchronization threshold. To see this in more detail, let us assume that all the links within the network are bidirectional (the corresponding graph is called *undirected graph*) with identical coupling gain $\mathbf{K} = \mathbf{K}^T > 0$. Thus, according to [52]

$$\lambda_{m+1}(\mathbf{L}_\mathbf{K}) \;=\; \lambda_2\, \lambda_{min}(\mathbf{K})$$

where λ_2 is the algebraic connectivity of the standard Laplacian matrix. Denote

$$\bar{\lambda} \;=\; \frac{\max_i \lambda_{max}(\mathbf{J}_{is})}{\lambda_{min}(\mathbf{K})}$$

If both the individual element's uncoupled dynamics and the coupling gains are fixed, the synchronization condition (4.7) can be written as

$$\lambda_2 \;>\; \bar{\lambda} \qquad \text{uniformly}$$

We can further transform this condition to the ones based on more explicit properties in geometry. Given a graph $\mathbf{G}$ of order n, there exist lower bounds on its diameter[1] $d(\mathbf{G})$ and its mean distance[2] $\bar{\rho}(\mathbf{G})$ [97]

$$\begin{aligned} d(\mathbf{G}) \;&\geq\; \frac{4}{n\lambda_2} \\ (n-1)\bar{\rho}(\mathbf{G}) \;&\geq\; \frac{2}{\lambda_2} + \frac{n-2}{2} \end{aligned}$$

(these bounds are most informative when λ_2 is small) which in turn gives us lower

[1] Maximum number of links between two distinct vertices [40]

[2] Average number of links between distinct vertices [97]

bounds on algebraic connectivity

$$\lambda_2 \geq \frac{4}{n \cdot d(\mathbf{G})}$$

$$\lambda_2 \geq \frac{2}{(n-1)\bar{\rho}(\mathbf{G}) - \frac{n-2}{2}}$$

A sufficient condition to guarantee exponential convergence within a coupled network is thus derived as

$$d(\mathbf{G}) < \frac{4}{n\bar{\lambda}}$$

or

$$\bar{\rho}(\mathbf{G}) < \frac{2}{\bar{\lambda}(n-1)} + \frac{n-2}{2(n-1)}$$

These results imply that, different coupling links or nodes may make different contributions to synchronization, because they may play different roles in network structure. In this sense, links between far-separated nodes contribute more than those between close neighbors.

Example 4.5.1: In [65], Kopell and Ermentrout show that closed rings of oscillators will reliably synchronize with nearest-neighbor coupling, while open chains require nearest and next-nearest neighbor coupling. This result can be explained by assuming all gains are identical and expressing the synchronization condition (4.7) as

$$\lambda_{min}(\mathbf{K}) > \frac{\max_i \lambda_{max}(\mathbf{J}_{is})}{\lambda_2} \quad \text{uniformly}$$

Assuming n extremely large, for a graph with two-way-chain structure

$$\lambda_2 = 2\,(\,1 - \cos(\frac{\pi}{n})\,) \approx 2\,(\frac{\pi}{n})^2$$

while for a graph with two-way-ring structure

$$\lambda_2 = 2\,(\,1 - \cos(\frac{2\pi}{n})\,) \approx 8\,(\frac{\pi}{n})^2$$

As illustrated in Figure 4-3, although the number of links only differ by one in these two cases, the effort to synchronize an open chain network is four times of that to a closed one. □

Figure 4-3: Comparison of a chain network and a ring.

Example 4.5.2: As another example, illustrated in Figure 4-4, consider a ring network, a star network and an all-to-all network. With the network size $n \to \infty$, the threshold of

the coupling strength to synchronize the ring network tends to infinite. It tends to 0 for the all-to-all network, and only needs to have order 1 for the star network.

It is much easier to synchronize the star network than to the ring. The reason is that, the central node in the star network performs a global role, which makes the graph diameter keep as constant no matter how big the network size is. Such a star-liked structure is very popular in real world. For instance, internet is composed of many connected subnetworks with star structure. □

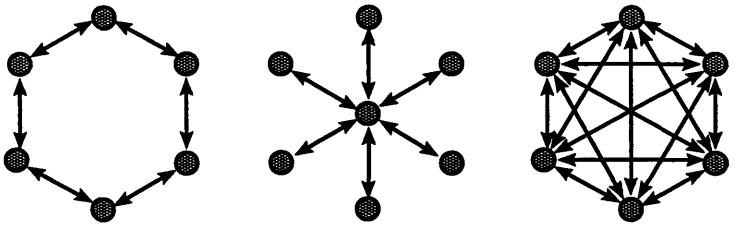

Figure 4-4: Comparison of three different kinds of networks.

The result here is closely related to the Small World problem. Strogatz and Watts showed in [143, 172, 173] that the average distance between nodes decreases with the increasing of the probability of adding short paths to each node. They also conjectured that the synchronizability will be enhanced if the node is endowed with dynamics, which Barahona and Pecora showed numerically in [9].

4.6 Fast Inhibition

The dynamics of a large network of synchronized elements can be completely transformed by the addition of a single inhibitory coupling link. Start for instance with the synchronized network (4.5) and add a single inhibitory link between two arbitrary elements a and b

$$\begin{aligned}\dot{\mathbf{x}}_a &= \mathbf{f}(\mathbf{x}_a, t) + \sum_{j \in \mathcal{N}_a} \mathbf{K}_{ja} \left(\mathbf{x}_j - \mathbf{x}_a\right) + \mathbf{K} \left(-\mathbf{x}_b - \mathbf{x}_a\right) \\ \dot{\mathbf{x}}_b &= \mathbf{f}(\mathbf{x}_b, t) + \sum_{j \in \mathcal{N}_b} \mathbf{K}_{jb} \left(\mathbf{x}_j - \mathbf{x}_b\right) + \mathbf{K} \left(-\mathbf{x}_a - \mathbf{x}_b\right)\end{aligned}$$

The symmetric part of the Jacobian matrix is

$$\mathbf{J}_s = \mathbf{I}^n_{\mathbf{J}_{is}} - \mathbf{L}_{\mathbf{K}} - \bar{\mathbf{T}}^n_{\mathbf{K}}$$

where $\bar{\mathbf{T}}_{\mathbf{K}}^{n}$ is composed of zeroes except for four identical blocks

$$\bar{\mathbf{T}}_{\mathbf{K}}^{n} = \begin{bmatrix} \ddots & \vdots & & \vdots & \\ \cdots & \mathbf{K} & \cdots & \mathbf{K} & \cdots \\ & \vdots & \ddots & \vdots & \\ \cdots & \mathbf{K} & \cdots & \mathbf{K} & \cdots \\ & \vdots & & \vdots & \ddots \end{bmatrix}_{n \times n}$$

The matrix $\mathbf{J}_r^* = -\mathbf{L}_{\mathbf{K}} - \bar{\mathbf{T}}_{\mathbf{K}}^{n}$ is negative definite, since $\forall \mathbf{v} \neq 0$

$$\begin{aligned} \mathbf{v}^T \mathbf{J}_r^* \mathbf{v} &= -\sum_{(i,j)\in\mathcal{N}} (\mathbf{v}_i - \mathbf{v}_j)^T \mathbf{K}_{ijs} (\mathbf{v}_i - \mathbf{v}_j) - (\mathbf{v}_a + \mathbf{v}_b)^T \mathbf{K} (\mathbf{v}_a + \mathbf{v}_b) \\ &< 0 \end{aligned}$$

Thus, the network is contracting for strong enough coupling strengths. Hence, the n elements will be inhibited. If the function $\mathbf{f}$ is autonomous, they will tend to equilibrium points. If the coupling strengths are not very strong, the inhibitory link will still have the ability to destroy the synchrony, and may then generate a desynchronized spiking sequence. Adding more inhibitory couplings preserves the result.

Example 4.6.1: Consider a two-way-ring network of ten coupled FitzHugh-Nagumo neurons (4.10). They synchronize with diffusion couplings. The whole network turns off immediately if we add one extra inhibitory link between any two neurons, and resumes firing if we remove the extra link, as illustrated in Figure 4-5. The parameters are $a = 0.7,\ b = 0.8,\ c = 8,\ I = -0.8$. The coupling gains are identical as $k = 100$, and the initial conditions are set randomly. The inhibitory link is added between the first and fifth neurons at $t = 100$ and removed at $t = 200$. □

Example 4.6.2: Consider a two-way-ring network of twenty coupled FitzHugh-Nagumo neurons with dimensionless form (4.12). The synchrony is destroyed if we add one extra inhibitory link between any two neurons (i.e., between the first one and the tenth one), and resumes if we remove the link, as illustrated in Figure 4-6. The parameters are $\alpha = 5.32, \beta = 3, \gamma = 0.1, I = 60$. The coupling gains are identical with $k = 2$. The inhibitory link is actived at $t = 60$ and removed at $t = 120$. □

Such inhibition properties may be useful in pattern recognition to achieve rapid desynchronization between different objects. They may also be used as simplified models of minimal mechanisms for turning off unwanted synchronization, as e.g. in epileptic seizures or oscillations in internet traffic. In such applications, small and localized inhibition may also allow one to destroy unwanted synchronization while only introducing a small disturbance to the nominal behavior of the system. Cascades of inhibition are common in the brain, in a way perhaps reminiscent of NAND-based logic.

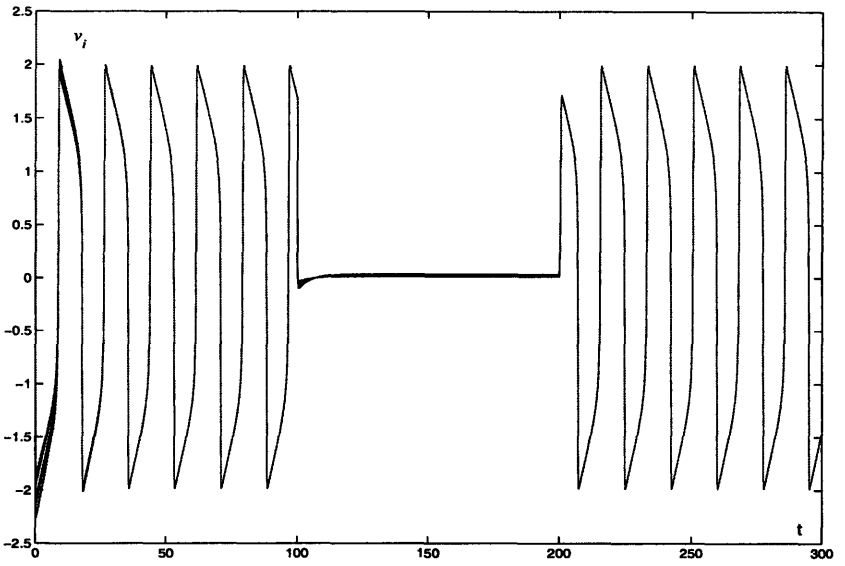

Figure 4-5: Fast inhibition with a single inhibitory link.

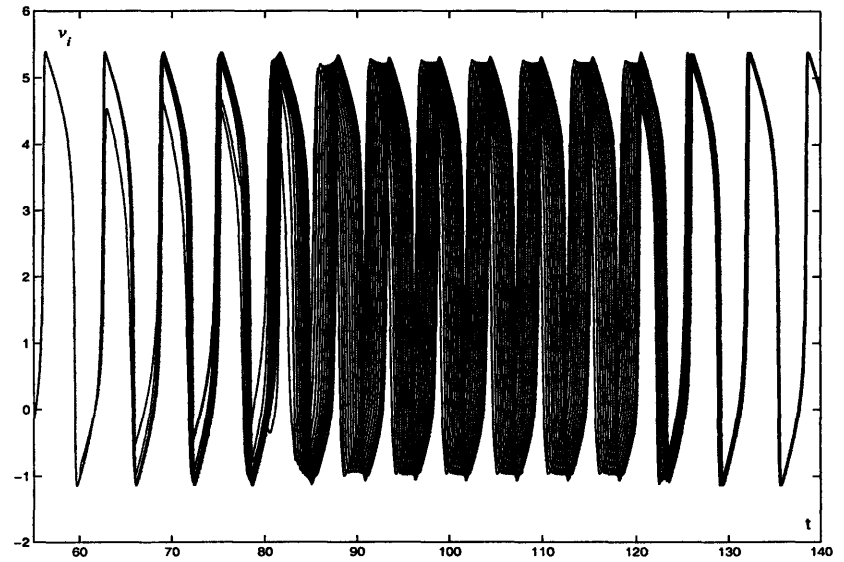

Figure 4-6: A single inhibitory link destroys network synchrony.

Note that the same effect can be achieved if we add self-inhibition to one (or more) arbitrary element. For instance,

$$\dot{\mathbf{x}}_a \;=\; \mathbf{f}(\mathbf{x}_a, t) \;+\; \sum_{j \in \mathcal{N}_a} \mathbf{K}_{ja}\,(\mathbf{x}_j - \mathbf{x}_a) \;-\; \mathbf{K}\,\mathbf{x}_a$$

In this case $\bar{\mathbf{T}}^n_{\mathbf{K}}$ is composed of zeroes except for one diagonal block

$$\bar{\mathbf{T}}^n_{\mathbf{K}} \;=\; \begin{bmatrix} \ddots & & \mathbf{0} \\ & \mathbf{K} & \\ \mathbf{0} & & \ddots \end{bmatrix}_{n \times n}$$

4.7 Appendix: Graph Theory Preliminaries

In this section, we introduce some basic Graph Theory concepts [34, 40, 97].

A graph is denoted as $\mathbf{G} = \mathbf{G}(V, E)$, where V is a non-empty vertex (node) set and E is an edge (link) set. If there is a direction of flow associated with each edge, $\mathbf{G}$ is called a directed graph, otherwise it is undirected. A graph is connected if any two nodes inside are linked by a path. The *adjacency matrix* of a graph is defined as

$$\mathbf{A}(\mathbf{G}) = [a_{ij}] \;\in\; \mathbb{R}^{n \times n}$$

where $a_{ij} = 1$ for all $i \neq j$ if $(i, j) \in E$, otherwise $a_{ij} = 0$. The *valency matrix*

$$\mathbf{V}(\mathbf{G}) = \mathrm{diag}(v_1, \ldots, v_n) \;\in\; \mathbb{R}^{n \times n}$$

is a diagonal matrix with $v_i = \sum_{j=1}^{n} a_{ij}$. The matrix

$$\mathbf{L}(\mathbf{G}) = \mathbf{V} - \mathbf{A}$$

is defined as *Laplacian matrix* of the graph $\mathbf{G}$.

For an undirected graph $\mathbf{G}$ with order n, $\mathbf{L}$ is symmetric and positive semi-definite. Denoting c as the number of connected components of $\mathbf{G}$,

$$\mathrm{rank}(\mathbf{L}) \;=\; n - c$$

Its second minimum eigenvalue $\lambda_2 = \lambda_2(\mathbf{L})$ is called *algebraic connectivity*, which is zero if and only if the graph is not connected. The first eigenvalue is always zero, corresponding to the eigenvector $[1, 1, \ldots, 1]^T$.

Assign an arbitrary orientation σ to an undirected graph $\mathbf{G}$. We get the *incidence matrix*

$$\mathbf{D} = \mathbf{D}(\mathbf{G}^\sigma) = [d_{ij}] \;\in\; \mathbb{R}^{n \times \tau}$$

where τ is the number of the links in E. For each oriented link k which starts from node i and ends at node j, we have $d_{ik} = 1$ and $d_{jk} = -1$. All the other entries of

$\mathbf{D}$ are equal to 0. Moreover,

$$\mathbf{L}(\mathbf{G}) = \mathbf{D}(\mathbf{G}^{\sigma})\ \mathbf{D}^{T}(\mathbf{G}^{\sigma})$$

If the graph is weighted, we have the weighted Laplacian matrix

$$\mathbf{L_K}\ =\ \mathbf{D}\ \mathbf{I}^{\tau}_{\mathbf{K}_{ij}}\ \mathbf{D}^{T}$$

where $\mathbf{I}^{\tau}_{\mathbf{K}_{ij}} \in \mathbb{R}^{\tau \times \tau}$ is a diagonal matrix with the k^{th} diagonal entry $\mathbf{K}_{ij}$ corresponding to the weight of the k^{th} link. If $\mathbf{K}_{ij} \in \mathbb{R}^{m \times m}$ is a matrix, $\mathbf{I}^{\tau}_{\mathbf{K}_{ij}}$ is block diagonal. Similarly $\mathbf{D}$ has block entries $\mathbf{I}$, $-\mathbf{I}$ and $\mathbf{0}$.

Chapter 5

Coupled Network with Switching Topology

Closely related to oscillator synchronization, topics of collective behavior and group cooperation have also been the object of extensive recent research. A fundamental understanding of aggregate motions in the natural world, such as bird flocks, fish schools, animal herds, or bee swarms, for instance, would greatly help in achieving desired collective behaviors of artificial multi-agent systems, such as vehicles with distributed cooperative control rules. In [122], Reynolds published his well-known computer model of "boids", which successfully forms an animation flock using three *local* rules: *collision avoidance*, *velocity matching*, and *flock centering*. Motivated by the growth of colonies of bacteria, Viscek *et al.*[156] proposed a similar discrete-time model which realizes heading matching using information only from neighbors. Viscek's model was later analyzed analytically [57, 150, 151]. Corresponding models in continuous-time [12, 76, 106, 107, 134, 164] and combinations of Reynolds' three rules [73, 108, 110, 145, 146] were also studied. Related questions can also be found e.g. in [15, 64, 70, 126].

In this chapter, we study coupled networks with switching topology. Animal aggregate motions are composed of cooperating moving units. Since each moving unit can only couple to its current neighbors, the network structure may change abruptly and asynchronously.

5.1 Synchronization in Switching Networks

Consider such a network

$$\dot{\mathbf{x}}_i \;=\; \mathbf{f}(\mathbf{x}_i, t) \;+\; \sum_{j \in \mathcal{N}_i(t)} \mathbf{K}_{ji}\,(\mathbf{x}_j - \mathbf{x}_i) \qquad i = 1, \ldots, n$$

where $\mathcal{N}_i(t)$ denotes the set of the active links associated with element i at time t.

Apply partial contraction analysis to each time interval during which the network

structure $\mathcal{N}(t) = \bigcup \mathcal{N}_i(t)$ is fixed. If

$$\lambda_{m+1}(\mathbf{L_K}) > \max_i \lambda_{max}(\mathbf{J}_{is}) \qquad \text{uniformly } \forall \mathcal{N}(t) \ , \tag{5.1}$$

the auxiliary system (4.6) is always contracting, since $\delta\mathbf{z}^T\delta\mathbf{z}$ with $\delta\mathbf{z} = [\delta\mathbf{y}_1, \ldots, \delta\mathbf{y}_n]^T$ is continuous in time and upper bounded by a vanishing exponential (though its time-derivative can be discontinuous at discrete instants). Since the particular solution of the auxiliary system in each time interval is $\mathbf{y}_1 = \cdots = \mathbf{y}_n = \mathbf{y}_\infty$, these n elements will reach synchrony exponentially as they tend to $\mathbf{y}_1 = \cdots = \mathbf{y}_n$ which is a constant region in the state-space. The threshold phenomenon described by inequality (5.1) is also reminiscent of phase transitions in physics [117] and of Bose-Einstein condensation [62] .

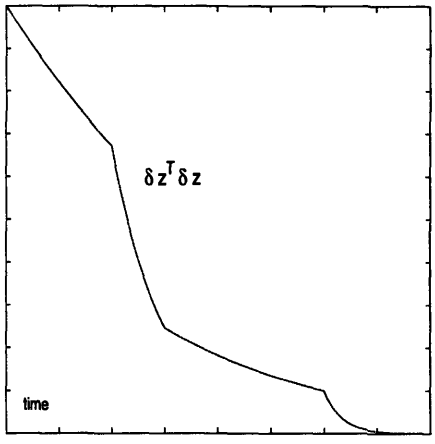

Figure 5-1: Evolution of virtual displacement of a sample switching network.

5.2 A Simple Coupled Model

We now study a simplified model of schooling or flocking in continuous-time with $\mathbf{f} = 0$. Consider such a group

$$\dot{\mathbf{x}}_i \ = \sum_{j \in \mathcal{N}_i(t)} \mathbf{K}_{ji} \ (\mathbf{x}_j - \mathbf{x}_i) \qquad\qquad i = 1, \ldots, n \tag{5.2}$$

where $\mathbf{x}_i \in \mathbb{R}^m$ denotes the states needed to reach agreements such as a vehicle's heading, attitude, velocity, etc. $\mathcal{N}_i(t)$ is defined for instance as the set of the nearest neighbors within a certain distance around element i at current time t, which can change abruptly and asynchronously. The coupling gain $\mathbf{K}_{ji}$ satisfies those assumptions proposed in Section 4.3 and 4.4, i.e., the links are either bidirectional or unidirectional formed in rings. Since $\mathbf{J}_{is} = 0$ here, the condition (5.1) is satisfied if only the network is connected. Therefore $\forall i$, $\mathbf{x}_i$ converges exponentially to a partic-

ular solution, which in this case is a constant value

$$\bar{\mathbf{x}} = \frac{1}{n}\sum_{i=1}^{n}\mathbf{x}_i(0)$$

Note that in the case of heading agreement based on spatial proximity, the issue of chattering is immaterial since switching cannot occur infinitely fast, while in the general case it can be simply avoided by using smooth transitions in time or space.

Moreover, the network (5.2) need not be connected for any $t \geq 0$. A generalized condition can be derived which is the same as that obtained in [57] for a discrete-time model.

Lemma 5.1 *For a coupled network (5.2),* $\sum_{i=1}^{n}||\mathbf{x}_i||^2$ *converges exponentially to its lower limit* $n||\bar{\mathbf{x}}||^2$.

Proof: Letting $\mathbf{x}_i = [x_{i1}, \cdots, x_{im}]^T$, we have $\sum_{i=1}^{n}\dot{\mathbf{x}}_i = 0$ which leads to

$$\sum_{i=1}^{n}\mathbf{x}_i = \sum_{i=1}^{n}\mathbf{x}_i(0) = n\bar{\mathbf{x}} \quad \text{with} \quad \sum_{i=1}^{n}x_{ij} = n\bar{x}_j\ , \quad j = 1, \cdots, m$$

Thus,

$$\begin{aligned}
&\sum_{i=1}^{n}||\mathbf{x}_i - \bar{\mathbf{x}}||^2 \ + \ n\ ||\bar{\mathbf{x}}||^2 && (5.3)\\
=\ &\sum_{i=1}^{n}\sum_{j=1}^{m}(x_{ij} - \bar{x}_j)^2 \ + \ n\ ||\bar{\mathbf{x}}||^2 \\
=\ &\sum_{i=1}^{n}(\sum_{j=1}^{m}x_{ij}^2 \ - \ 2\sum_{j=1}^{m}x_{ij}\bar{x}_j \ + \ \sum_{j=1}^{m}\bar{x}_j^2\ ) \ + \ n\ ||\bar{\mathbf{x}}||^2 \\
=\ &\sum_{i=1}^{n}||\mathbf{x}_i||^2 \ - \ 2\sum_{i=1}^{n}\sum_{j=1}^{m}x_{ij}\bar{x}_j \ + \ 2n\ ||\bar{\mathbf{x}}||^2 && (5.4)\\
=\ &\sum_{i=1}^{n}||\mathbf{x}_i||^2 && (5.5)
\end{aligned}$$

where we used

$$\sum_{i=1}^{n}\sum_{j=1}^{m}x_{ij}\bar{x}_j = \sum_{j=1}^{m}\sum_{i=1}^{n}x_{ij}\bar{x}_j = \sum_{j=1}^{m}(\bar{x}_j\sum_{i=1}^{n}x_{ij}) = \sum_{j=1}^{m}n\bar{x}_j^2 = n\ ||\bar{\mathbf{x}}||^2$$

From partial contraction analysis, we know that any solution of the system (5.2)

converges exponentially to a particular one,

$$\mathbf{x}_1 = \cdots = \mathbf{x}_n = \bar{\mathbf{x}} = \frac{1}{n}\sum_{i=1}^{n}\mathbf{x}_i(0)$$

which implies that $\sum_{i=1}^{n}||\mathbf{x}_i - \bar{\mathbf{x}}||^2$ tends to zero exponentially. Using (5.3) completes the proof. □

With Lemma 5.1, we can now largely generalize the condition to reach group agreement.

Theorem 5.1 *Consider n coupled elements with linear protocol (5.2), the neighborship of which can change abruptly and asynchronously. Separate time into an infinite sequence of bounded intervals starting at $t = 0$. If the network is connected across each such interval*[1]*, the agreement $\mathbf{x}_1 = \cdots = \mathbf{x}_n$ will be reached asymptotically.*

Proof: Assume that at some time t the network is not connected, but instead is composed of k isolated subnetworks, each of which is connected and containing n_j elements with $j = 1, \ldots, k$. Defining $\mathbf{z}_i = \mathbf{x}_i - \bar{\mathbf{x}}$, we get

$$\dot{\mathbf{z}}_i = \sum_{j\in\mathcal{N}_i(t)}\mathbf{K}_{ji}\,(\mathbf{z}_j - \mathbf{z}_i) \qquad\qquad i = 1, \ldots, n$$

and from Lemma 5.1, with $\bar{\mathbf{z}}_j(t) = \frac{1}{n_j}\sum_{i=1}^{n_j}\mathbf{z}_i(t)$,

$$\sum_{i=1}^{n}||\mathbf{z}_i||^2 = \sum_{j=1}^{k}\sum_{i=1}^{n_j}||\mathbf{z}_i||^2 = \sum_{j=1}^{k}(\sum_{i=1}^{n_j}||\mathbf{z}_i - \bar{\mathbf{z}}_j||^2 + n_j\,||\bar{\mathbf{z}}_j||^2)$$

Note that $\bar{\mathbf{z}}_j$ is a local agreement compared to the global one $\bar{\mathbf{x}}$ (corresponding to $\bar{\mathbf{z}} = 0$). $\forall j$, $\bar{\mathbf{z}}_j$ is constant as long as the current network structure keeps unchanged, and according to partial contraction analysis, $\sum_{i=1}^{n_j}||\mathbf{z}_i - \bar{\mathbf{z}}_j||^2$ tends to zero exponentially during this period. Thus $\sum_{i=1}^{n}||\mathbf{z}_i||^2$ is non-increasing.

Furthermore, the condition in Theorem 5.1 guarantees that $\sum_{i=1}^{n}||\mathbf{z}_i||^2$ always decreases across each defined time interval. Hence, it will tend to reach the lower limit zero asymptotically. □

[1] As in [57], being connected across a time interval means that the union of the different graphs accounted along the interval is connected.

Note that the essential fact behind Theorem 5.1 and its proof is that: the closer a subgroup is to the local agreement, the closer it is to the global. This is illustrated in Figure 5-2, where a connected subgroup containing only two elements x_1 and x_2. Point O represents the global agreement and point C the local. The initial position is set at point A and the system trajectory will be along the line ABC.

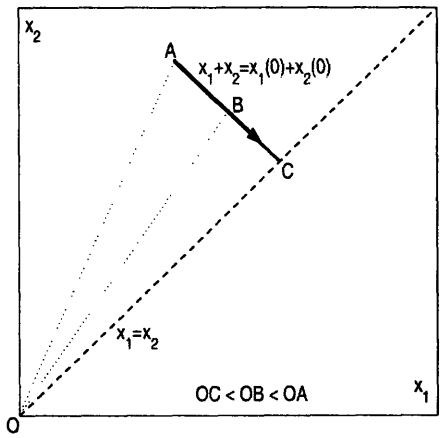

Figure 5-2: Closer to the local agreement, closer to the global.

Chapter 6

Leader-Followers Network

As we have noticed in the previous chapters, for a leaderless network composed of peers, the phase of its collective behavior is hard to predict, since it depends on the initial conditions of all the coupled elements. Thus, in order to let the whole network behave as desired, an additional group leader is necessary. Here the leader is defined as the one whose dynamics is independent and thus followed by all the others. Such a leader-followers network is especially popular in natural aggregate motions, where the leader "tells" the followers "where to go". We name this kind of leader the *power leader*.

There also exists another kind of leader, which we name the *knowledge leader*. In a knowledge-based network, members' dynamics are initially non-identical and mutually coupled. The leader is the one whose dynamics is fixed or changes comparatively slowly. The followers obtain dynamics knowledge from the leader through adaptation. In this sense, a knowledge leader can be understood as the one who indicates "how to go". Different than a power leader, a knowledge leader does not have to be dynamically independent. It may be located at any position in a network.

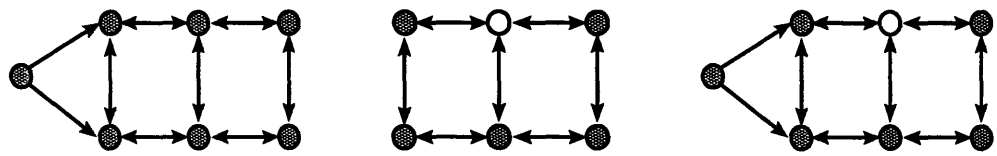

Figure 6-1: Networked systems with (a). a power leader (the most left node); (b). a knowledge leader (the hollow node); (c). both leaders.

6.1 Power Leader

As illustrated in Figure 6-1(a), a power leader is the one whose dynamics is independent in a coupled network.

Consider the dynamics of a coupled network containing one power leader and n power followers

$$\begin{aligned} \dot{\mathbf{x}}_0 &= \mathbf{f}(\mathbf{x}_0, t) \\ \dot{\mathbf{x}}_i &= \mathbf{f}(\mathbf{x}_i, t) + \sum_{j \in \mathcal{N}_i} \mathbf{K}_{ji} \, (\mathbf{x}_j - \mathbf{x}_i) + \gamma_i \, \mathbf{K}_{0i} \, (\mathbf{x}_0 - \mathbf{x}_i) \quad i = 1, \ldots, n \end{aligned} \tag{6.1}$$

where vector $\mathbf{x}_0$ is the state of the leader, and $\mathbf{x}_i$ the state of the ith follower. γ_i is equal to either 0 or 1, representing the connection from the leader to the followers. $\mathcal{N}_i$ denotes the set of peer-neighbors of element i, i.e., it does not include the possible link from $\mathbf{x}_0$ to $\mathbf{x}_i$.

Theorem 6.1 *Regardless of initial conditions, the states of all the followers within a generally coupled network (6.1) will converge exponentially to the state of the leader if*

$$\lambda_{min}(\mathbf{L_K} + \mathbf{I}^n_{\gamma_i \mathbf{K}_{0is}}) > \max_i \lambda_{max}(\mathbf{J}_{is}) \qquad \text{uniformly.} \tag{6.2}$$

Proof: Since the dynamics of $\mathbf{x}_0$ is independent, we can treat it as an external input to the rest of the network, whose Jacobian matrix has the symmetric part

$$\mathbf{J}_s = \mathbf{I}^n_{\mathbf{J}_{is}} - \mathbf{L_K} - \mathbf{I}^n_{\gamma_i \mathbf{K}_{0is}}$$

The matrix $\mathbf{J}^*_r = -\mathbf{L_K} - \mathbf{I}^n_{\gamma_i \mathbf{K}_{0is}}$ is negative definite if the augmented network with $n+1$ elements is connected. In fact, $\forall \mathbf{v} \neq 0$,

$$\mathbf{v}^T \, \mathbf{J}^*_r \, \mathbf{v} = - \sum_{(i,j) \in \mathcal{N}} (\mathbf{v}_i - \mathbf{v}_j)^T \, \mathbf{K}_{ijs} \, (\mathbf{v}_i - \mathbf{v}_j) - \sum_{i=1}^{n} \gamma_i \, (\mathbf{v}_i^T \, \mathbf{K}_{0is} \, \mathbf{v}_i) < 0$$

Thus the system $[\mathbf{x}_1, \ldots, \mathbf{x}_n]^T$ is contracting if the coupling strengths are so strong that the condition (6.2) is true. Therefore, all solutions will converge to the particular one

$$\mathbf{x}_1 = \cdots = \mathbf{x}_n = \mathbf{x}_0$$

exponentially regardless of the initial conditions. This result can be viewed as a generalization of Theorem 3.1. □

A few remarks on Theorem 6.1:

- For nonnegative $\max_i \lambda_{max}(\mathbf{J}_{is})$, a necessary condition to realize leader-following is that the whole network of $n+1$ elements is connected. Thus the n followers $\mathbf{x}_1, \ldots, \mathbf{x}_n$ could be either connected together, or there could be isolated subgroups all connected to the leader. Note that the network structure of a leader-followers group does not have to be fixed during the whole time. Similar to the result in section 5.1, given the dynamics of n followers as

$$\dot{\mathbf{x}}_i = \mathbf{f}(\mathbf{x}_i, t) + \sum_{j \in \mathcal{N}_i(t)} \mathbf{K}_{ji} \, (\mathbf{x}_j - \mathbf{x}_i) + \gamma_i(t) \, \mathbf{K}_{0i} \, (\mathbf{x}_0 - \mathbf{x}_i)$$

a sufficient condition to guarantee exponential following is that (6.2) is true $\forall t \geq 0$.

- Comparing conditions (4.7) and (6.2) shows that, predictably, the existence of an additional leader does not always help the followers' network to reach agreement. But it does so if

$$\lambda_{min}(\mathbf{L_K} + \mathbf{I}^n_{\gamma_i \mathbf{K}_{0is}}) > \lambda_{m+1}(\mathbf{L_K})$$

Example 6.1.1: Consider for instance the case when the leader has identical connections to all other elements, $\forall i,\ \mathbf{K}_{0i} = k\mathbf{I},\ \ k > 0$. Then

$$\lambda_{min}(\mathbf{L_K} + \mathbf{I}^n_{\gamma_i \mathbf{K}_{0is}}) \ = \ \min_{\|\mathbf{v}\|=1} \mathbf{v}^T(\ \mathbf{L_K} + \mathbf{I}^n_{k\mathbf{I}}\ )\mathbf{v} \ = \ k$$

This means the connections between the leader and the followers do promote the convergence within the followers' network if

$$\lambda_{m+1}(\mathbf{L_K}) < k$$

which is more likely to happen in a network with less connectivity. □

- The connectivity of the followers' network helps the following process, which can be seen by applying Weyl's Theorem [51],

$$\lambda_i(\ \mathbf{L_K} + \mathbf{I}^n_{\gamma_i \mathbf{K}_{0is}}\ ) \ \geq \ \lambda_i(\ \mathbf{I}^n_{\gamma_i \mathbf{K}_{0is}}\ ) \quad i = 1, \ldots, mn$$

  This result can be used e.g. to modify the application in Section 9.3.3, by adding couplings between local neighbors according to similarity, so as to react even faster.

- In a generalized understanding, the power leader does not have to be single. It can be a group of leading elements. The leader even does not have to be independent. It can receive feedback from the followers as well. Such an example is synchronization propagation, where the density is not smoothly distributed through the whole network. Since synchronization rate depends on the network connectivity, a high-density region will synchronize very quickly despite disturbances from other parts of the network. The inputs from these leaders then facilitate synchronization in low-density regions, where the elements may not be able to synchronize by themselves. [182] observed a similar phenomenon by setting different interior connection weights inside different subgroups. Note that the leaders group here is very similar to the concept of *core group* in infectious disease dynamics [92], which is a group of the most active individuals. A small change in the core group will make a big difference in whether or not an epidemic can occur in the whole population.

Example 6.1.2: Consider two groups of FitzHugh-Nagumo neurons (Figure 6-2), the first composed of eight neurons coupled all-to-all, and surrounded by a second group of

sixteen neurons coupled as an one-way ring, with every other neuron in the second group connected bilaterally to a distinct neuron of the first group. The system dynamics follows equation (4.10) with coupling gain $k > 0$ identical in the whole network. Figure 6-3 shows simulation results, from which we can observe initially significant phase lag between the two groups. Note that the second group alone would not synchronize without couplings from the first group, as we illustrate in Figure 6-4. In both simulations, the parameters are $a = 0.7,\ b = 0.8,\ c = 8,\ I = -1.4,\ k = 0.5$. Initial conditions are chosen randomly. □

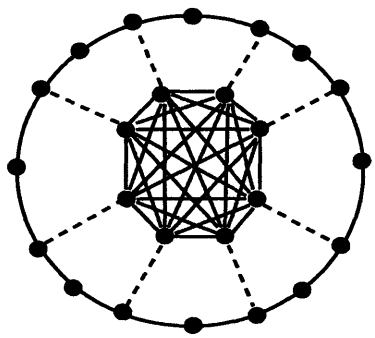

Figure 6-2: Synchronization propagates in a network with non-uniform connectivity.

- Synchronization can be made to propagate from the center outward in a more active way, for instance, through diffusion of a chemical produced by leaders or high-level elements and having the ability to expand the communication channels it passes through, i.e., to increase the gains through diffusion. Such a mechanism represents a hierarchical combination with gain dynamics. By extending the state, the analysis tools provided here can apply more generally to combinations where the gain dynamics are coupled to each other (with arbitrary connectivity) and to the $\mathbf{x}_i$.

- Different leaders $\mathbf{x}_0^j$ of arbitrary dynamics can define different *primitives* which can be combined. Contraction of the followers' dynamics ($i = 1, \ldots, n$)

$$\dot{\mathbf{x}}_i = \mathbf{f}(\mathbf{x}_i, t) \ + \sum_{j \in \mathcal{N}_i} \mathbf{K}_{ji} \, (\mathbf{x}_j - \mathbf{x}_i) \ + \sum_j \alpha_j(t) \, \gamma_i^j \, \mathbf{K}_{0i}^j \, (\mathbf{x}_0^j - \mathbf{x}_i)$$

  is preserved if $\sum_j \alpha_j(t) \geq 1,\ \forall t \geq 0$.

- Besides its dubious moral implications, Theorem 6.1 also means that it is easy to detract a group from its nominal behavior by introducing a "covert" element, with possible applications to group control games, ethology, and animal and plant mimicry.

- Besides orientation, the moving formation with a power leader has other advantages, such as energy saving in aerodynamics [25, 126].

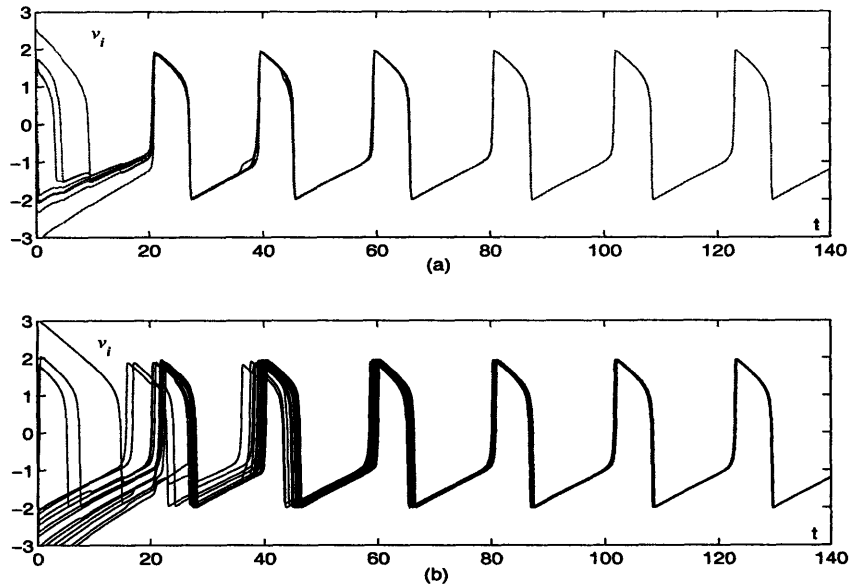

Figure 6-3: v_i of the neurons in (a).the inner group, (b).the outer group with inter-group links.

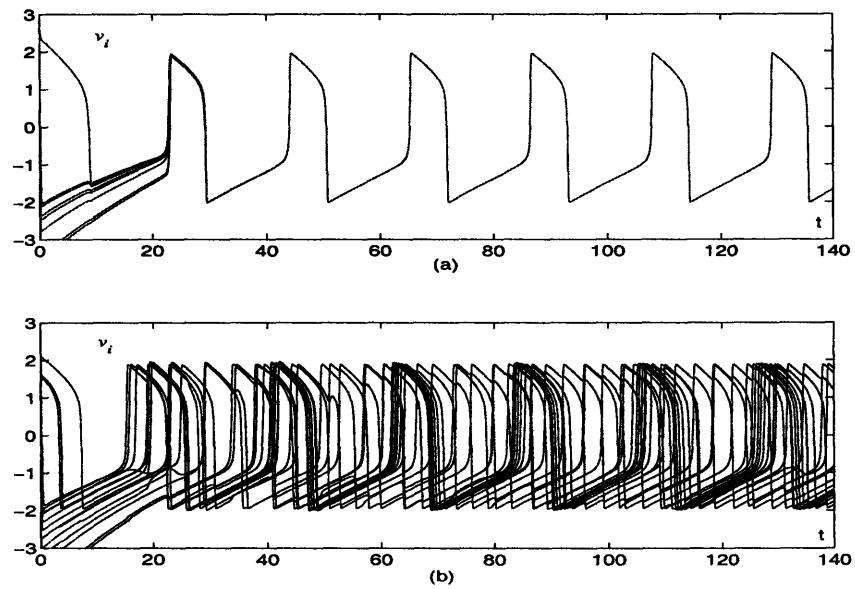

Figure 6-4: v_i of the neurons in (a).the inner group, (b).the outer group without inter-group links.

6.2 Knowledge Leader

A knowledge-based leader-followers network is composed of elements with initially non-identical dynamics. A knowledge leader may be located in any position inside a network as we illustrated in Figure 6-1(b). Its dynamics is fixed or slowly changing, while those of the followers are learned from the leader through adaptation. Synchronization or group agreement can still be achieved in such a network with only local interactions. To show this, we first study a very simple case, which contains only two coupled systems with adaptation.

6.2.1 Two Coupled Systems with Adaptation

Consider two coupled systems as in Theorem 3.2

$$\begin{cases} \dot{\mathbf{x}}_1 &= \mathbf{h}(\mathbf{x}_1, \mathbf{a}, t) \;+\; \mathbf{g}(\mathbf{x}_1, \mathbf{x}_2, t) \\ \dot{\mathbf{x}}_2 &= \mathbf{h}(\mathbf{x}_2, \hat{\mathbf{a}}, t) \;+\; \mathbf{g}(\mathbf{x}_1, \mathbf{x}_2, t) \end{cases} \tag{6.3}$$

Assume that a parameter vector $\mathbf{a}$ is unknown to the second system. To guarantee state convergence, we generate an estimated parameter $\hat{\mathbf{a}}$ through an adaptation mechanism

$$\dot{\hat{\mathbf{a}}} \;=\; \mathbf{P}\,\mathbf{W}^{\mathbf{T}}(\mathbf{x_2}, \mathbf{t})\,\tilde{\mathbf{x}}$$

where $\tilde{\mathbf{x}} = \mathbf{x}_1 - \mathbf{x}_2$, $\mathbf{P} > 0$ is constant symmetric, and $\mathbf{W}(\mathbf{x}_2, t)$ is defined as

$$\mathbf{h}(\mathbf{x}_2, \hat{\mathbf{a}}, t) \;=\; \mathbf{h}(\mathbf{x}_2, \mathbf{a}, t) \;+\; \mathbf{W}(\mathbf{x}_2, t)\tilde{\mathbf{a}}$$

with $\tilde{\mathbf{a}} = \hat{\mathbf{a}} - \mathbf{a}$. A similar adaptive technique was used in [81, 82], but is generalized here in the sense that the couplings could be bidirectional.

Theorem 6.2 *In a coupled system (6.3),* $\tilde{\mathbf{x}}$ *will converge to zero asymptotically if* $\mathbf{x}_1$ *is bounded and* $\mathbf{h}$ *is contracting. Furthermore,* $\tilde{\mathbf{a}}$ *will converge to zero if*

$$\exists\, \alpha > 0, T > 0, \quad \forall t \geq 0 \quad \int_t^{t+T} \mathbf{W}^T(\mathbf{x}_2, t)\mathbf{W}(\mathbf{x}_2, t)dr \;\geq\; \alpha\mathbf{I} \tag{6.4}$$

Proof: Define the Lyapunov function

$$\begin{aligned} V &= \frac{1}{2}\,(\,\tilde{\mathbf{x}}^T\tilde{\mathbf{x}} \;+\; \tilde{\mathbf{a}}^T\mathbf{P}^{-1}\tilde{\mathbf{a}}\,) \;>\; 0 \\ \dot{V} &= \tilde{\mathbf{x}}^T\,(\,\mathbf{h}(\mathbf{x}_1, \mathbf{a}, t) \;-\; \mathbf{h}(\mathbf{x}_2, \mathbf{a}, t)\,) \\ &= \tilde{\mathbf{x}}^T \int_0^1 \frac{\partial \mathbf{h}}{\partial \mathbf{x}}(\mathbf{x}_2 + \chi\tilde{\mathbf{x}})d\chi\;\tilde{\mathbf{x}} \;\leq\; 0 \end{aligned}$$

The boundedness of $\mathbf{x}_1$ implies that of $\mathbf{x}_2$. Assuming all the functions are smoothly differentiable, the boundedness of $\ddot{V}$ can be concluded since all the states including $\mathbf{a}$ are bounded. According to Barbalat's lemma [131], $\dot{V}$ and therefore $\tilde{\mathbf{x}}$ tends to 0 asymptotically.

Note that $\dot{\hat{\mathbf{a}}}$ also tends to 0. Furthermore, since $\ddot{\tilde{\mathbf{x}}}$ is also bounded, we have the asymptotic convergence of $\dot{\tilde{\mathbf{x}}}$ to zero, which leads to the convergence of $\mathbf{W}(\mathbf{x}_2, t)\tilde{\mathbf{a}}$ to zero. In particular [131], if the condition (6.4) is true, $\tilde{\mathbf{a}}$ converges to zero asymptotically. □

The boundedness of $\mathbf{x}_1$ is trivial if $\mathbf{g} = \mathbf{g}(\mathbf{x}_1, t)$, which is a classical observer structure with $\mathbf{x}_1$ dynamics independent. If $\mathbf{g} = \mathbf{g}(\mathbf{x}_1, \mathbf{x}_2, t)$, we have

$$\dot{\mathbf{x}}_1 = \mathbf{h}(\mathbf{x}_1, \mathbf{a}, t) + \mathbf{g}(\mathbf{x}_1, \mathbf{x}_1 - \tilde{\mathbf{x}}, t) = \mathbf{e}(\mathbf{x}_1, \tilde{\mathbf{x}}, t)$$

where $\tilde{\mathbf{x}}$ is bounded. Thus the boundedness of $\mathbf{x}_1$ is determined by the Input-to-State Stability [63] of $\mathbf{e}$.

Example 6.2.1: Consider two coupled FitzHugh-Nagumo neurons

$$\begin{cases} \dot{v}_1 = v_1(\alpha - v_1)(v_1 - 1) - w_1 + I + k(v_2 - v_1) \\ \dot{w}_1 = \beta v_1 - \gamma w_1 \end{cases}$$
$$\begin{cases} \dot{v}_2 = v_2(\hat{\alpha} - v_2)(v_2 - 1) - w_2 + \hat{I} + k(v_1 - v_2) \\ \dot{w}_2 = \hat{\beta} v_2 - \hat{\gamma} w_2 \end{cases}$$

in which case $\mathbf{x}_i = \begin{bmatrix} v_i & w_i \end{bmatrix}^T$, $\mathbf{a} = \begin{bmatrix} \alpha & I & \gamma & \beta \end{bmatrix}^T > 0$ and

$$\mathbf{h}(\mathbf{x}_i, \mathbf{a}, t) = \begin{bmatrix} v_i(\alpha - v_i)(v_i - 1) - w_i + I - 2kv_i \\ \beta v_i - \gamma w_i \end{bmatrix}$$

which is contracting if the coupling gain k is larger than an explicit threshold as we have proved in Example 4.4.2. Thus

$$\mathbf{W} = \begin{bmatrix} v_2^2 - v_2 & 1 & 0 & 0 \\ 0 & 0 & -w_2 & v_2 \end{bmatrix}$$

Note that although the diffusion couplings are only based on variables v_i, full-state feedback is needed for adaptation law in this case. See Appendix 6.4.1 for the boundedness proof. Simulation result is illustrated in Figure 6-5, where the real parameters are $\alpha = 5.32, \beta = 3, \gamma = 0.1$ and $I = 20$. The coupling gain $k = 15$. The matrix $\mathbf{P} = \text{diag}\{0.6, 30, 0.002, 0.4\}$. All initial conditions are chosen arbitrarily. □

6.2.2 Knowledge-Based Leader-Following

Now consider a coupled network containing n elements with a general connectivity

$$\dot{\mathbf{x}}_i = \mathbf{f}(\mathbf{x}_i, \mathbf{a}_i, t) + \sum_{j \in \mathcal{N}_i} \mathbf{K}_{ji}(\mathbf{x}_j - \mathbf{x}_i) \quad i = 1, \ldots, n \tag{6.5}$$

Assume that the uncoupled dynamics $\mathbf{f}(\mathbf{x}_i, \mathbf{a}_i, t)$ contains a parameter set $\mathbf{a}_i$ which has a fixed value $\mathbf{a}$ for all the knowledge leaders. Denote Ω as the set of the followers,

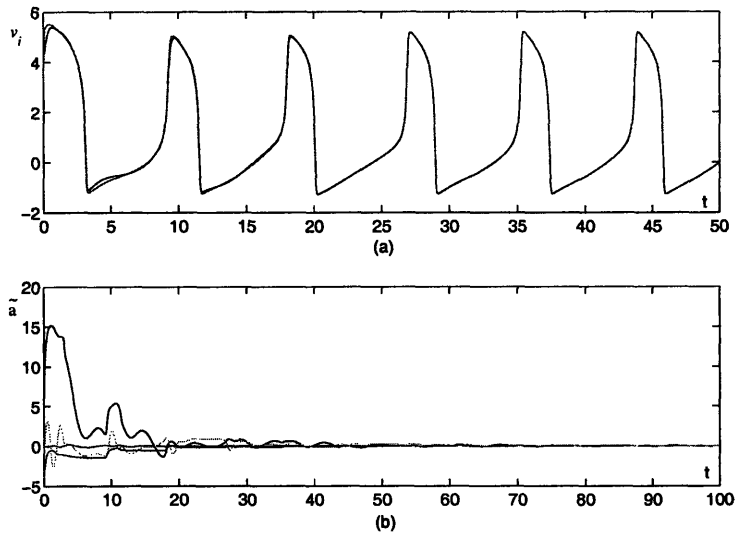

Figure 6-5: Simulation of Example 6.2.1. (a).States v_i $(i = 1, 2)$ versus time; (b).estimator error $\tilde{\mathbf{a}}$ versus time.

whose adaptation laws are based on local interactions

$$\dot{\mathbf{a}}_i \;=\; \mathbf{P}_i \mathbf{W}^T(\mathbf{x}_i, t) \sum_{j \in \mathcal{N}_i} \mathbf{K}_{ji}\,(\mathbf{x}_j - \mathbf{x}_i) \quad \forall\, i \in \mathbf{\Omega} \tag{6.6}$$

where $\mathbf{P}_i > 0$ is constant and symmetric, and $\mathbf{W}(\mathbf{x}_i, t)$ is defined as

$$\mathbf{f}(\mathbf{x}_i, \mathbf{a}_i, t) \;=\; \mathbf{f}(\mathbf{x}_i, \mathbf{a}, t) \;+\; \mathbf{W}(\mathbf{x}_i, t)\tilde{\mathbf{a}}_i$$

with estimation error $\tilde{\mathbf{a}}_i = \mathbf{a}_i - \mathbf{a}$.

To prove convergence, we define a Lyapunov function

$$V = \frac{1}{2}\,(\,\mathbf{x}^T \mathbf{L}_\mathbf{K} \mathbf{x} \;+\; \sum_{i \in \mathbf{\Omega}} \tilde{\mathbf{a}}_i^T \mathbf{P}_i^{-1} \tilde{\mathbf{a}}_i\,)$$

where $\mathbf{x}^T = [\mathbf{x}_1^T, \mathbf{x}_2^T, \ldots, \mathbf{x}_n^T]$. Thus

$$\begin{aligned}
\dot{V} \;&=\; \mathbf{x}^T \mathbf{L}_\mathbf{K} \dot{\mathbf{x}} \;+\; \sum_{i \in \mathbf{\Omega}} \tilde{\mathbf{a}}^T \mathbf{P}_i^{-1} \dot{\mathbf{a}}_i \\
&=\; \mathbf{x}^T \mathbf{L}_\mathbf{K}\,(\,\begin{bmatrix} \mathbf{f}(\mathbf{x}_1, \mathbf{a}, t) \\ \cdots \\ \mathbf{f}(\mathbf{x}_n, \mathbf{a}, t) \end{bmatrix} - \mathbf{L}_\mathbf{K} \mathbf{x}\,) \\
&=\; \mathbf{x}^T\,(\,\mathbf{L}_{\mathbf{K}\mathbf{\Lambda}} - \mathbf{L}_\mathbf{K}^2\,)\,\mathbf{x}
\end{aligned}$$

where matrix $\mathbf{L_{K\Lambda}}$ is symmetric and

$$\mathbf{L_{K\Lambda}} = \mathbf{D}\ (\mathbf{I}^{\tau}_{\mathbf{K}_{ij}}\mathbf{I}^{\tau}_{\Lambda_{ij}})_s\ \mathbf{D}^T = \mathbf{D}\ \mathbf{I}^{\tau}_{(\mathbf{K}\Lambda)_{ijs}}\ \mathbf{D}^T \tag{6.7}$$

Here $\mathbf{I}^{\tau}_{\Lambda_{ij}}$ is a $\tau \times \tau$ block diagonal matrix with the k^{th} diagonal entry

$$\Lambda_{ij} = \int_0^1 \frac{\partial \mathbf{f}}{\partial \mathbf{x}}(\mathbf{x}_j + \chi(\mathbf{x}_i - \mathbf{x}_j), \mathbf{a}, t)\ d\chi$$

corresponding to the k^{th} link which has been assigned an orientation by the incidence matrix $\mathbf{D}$. $\mathbf{I}^{\tau}_{(\mathbf{K}\Lambda)_{ijs}}$ is defined in a similar manner with $(\mathbf{K}\Lambda)_{ijs}$ the symmetric part of $\mathbf{K}_{ij}\Lambda_{ij}$.

To complete the proof, we use the following lemma, which is derived in Appendix 6.4.2.

Lemma 6.1 *Giving any* $\mathbf{x}$, *if*

$$\frac{\lambda^2_{m+1}(\mathbf{L_K})}{\lambda_n(\mathbf{L})} > \max_k \lambda_{max}(\mathbf{K\Lambda})_{ijs} \tag{6.8}$$

$\mathbf{x}^T\ (\ \mathbf{L_{K\Lambda}} - \mathbf{L}^2_{\mathbf{K}}\ )\ \mathbf{x} \leq 0$ *and the equality is true if and only if* $\mathbf{x}_1 = \mathbf{x}_2 = \cdots = \mathbf{x}_n$.

Theorem 6.3 *For a knowledge-based leader-followers network (6.5), the states of all the elements will converge together asymptotically if condition (6.8) is verified and all the states are bounded. Furthermore,* $\forall\ i \in \mathbf{\Omega}$, $\mathbf{a}_i$ *will converge to* $\mathbf{a}$ *if*

$$\exists\ \alpha > 0, T > 0,\quad \forall t \geq 0\quad \int_t^{t+T} \mathbf{W}^T(\mathbf{x}_i, r)\mathbf{W}(\mathbf{x}_i, r)dr\ \geq\ \alpha\mathbf{I} \tag{6.9}$$

Proof: Condition (6.8) means V is non-increasing. Assuming all the functions are smoothly differentiable, the boundedness of $\ddot{V}$ can be concluded if all the states are bounded. According to Barbalat's lemma [131], $\dot{V}$ will then tend to 0 asymptotically, implying that all the states $\mathbf{x}_i$ converge together. Hence, $\mathbf{W}(\mathbf{x}_i, t)\tilde{\mathbf{a}}_i$ will tend to zero, which leads to the convergence of the followers' parameters under condition (6.9). □

Theorem 6.3 implies that new elements can be added into the network without prior knowledge of the individual dynamics, and that elements in an existing network have the ability to recover dynamic information if temporarily lost. Similar knowledge-based leader-followers mechanism may exist in many natural processes. In evolutionary biology, knowledge leaders are essential to keep the evolution processes uninvasible or evolutionary stable [105, 111]. In reproduction, for instance, the leaders could be senior members. The knowledge-based mechanism may also describe evolutionary mutation or disease infection [92], where the leaders are mutants or invaders. Knowledge-based leader-following may also occur in animal aggregate motions or human social activities. In a bird flock, for instance, the knowledge leader can be a junior or injured member whose moving capacity is limited, and which is protected by others through dynamic adaptation.

Note that the adaptive model we described represents a *genotype-phenotype mapping*, where adaptation occurring in genotypic space is based on the interactions of behavioral phenotypes. Due to its complexity, genotype-phenotype mapping remains a big challenge today in evolutionary biology [105].

Additional Remarks:

- Similar as in Theorem 4.2, for condition (6.8) to be true, we need a connected network, an upper bounded $\lambda_{max}(\mathbf{K}\mathbf{\Lambda})_{ijs}$, and strong enough coupling strengths. For an example, if $m = 1$ and all the coupling gains are identical with value κ, condition (6.8) turns to be

$$\kappa > \frac{\lambda_n(\mathbf{L})}{\lambda_2^2(\mathbf{L})} \max \frac{\partial \mathbf{f}}{\partial \mathbf{x}}(\mathbf{x}_i, \mathbf{a}, t)$$

  while the coupling threshold to reach synchronization in condition (4.7) is

$$\kappa > \frac{1}{\lambda_2(\mathbf{L})} \max \frac{\partial \mathbf{f}}{\partial \mathbf{x}}(\mathbf{x}_i, t)$$

  A higher strength threshold is caused partly by the choice of V. A lower value of κ will still work in practice but it may not be able to guarantee non-oscillating convergence of V to zero. To show this, let us consider a network without knowledge-leaders or adaptation. Thus

$$\begin{aligned} V &= \frac{1}{2}\mathbf{x}^T\mathbf{L_K}\mathbf{x} \\ &= \frac{1}{2}(\mathbf{x}-\mathbf{y})^T\mathbf{L_K}(\mathbf{x}-\mathbf{y}) \\ &\leq \frac{1}{2}\lambda_{max}(\mathbf{L_K})\,(\mathbf{x}-\mathbf{y})^T(\mathbf{x}-\mathbf{y}) \end{aligned}$$

  where $\mathbf{y} = [\mathbf{y}_1, \mathbf{y}_2, \ldots, \mathbf{y}_n]^T$ is a particular solution of the auxiliary system and $\mathbf{y}_1 = \mathbf{y}_2 = \cdots = \mathbf{y}_n$ since we assume all the subsystems $\mathbf{y}_i$ have the same initial conditions. The exponential convergence of $(\mathbf{x}-\mathbf{y})^T(\mathbf{x}-\mathbf{y})$ to zero can be proved under the condition (4.7). But it only guarantees convergence, not non-oscillating convergence, of V to zero. We can certainly choose other potential Lyapunov functions, such as $V = \frac{1}{2}\mathbf{x}^T\,\mathbf{L}\,\mathbf{x}$. The result will be slightly different. Note that the analyzing method used in this section provides another analysis tool for synchronization study in network (4.5).

- If the coupling gains are only positive semi-definite, extra restrictions have to be added to the uncoupled system dynamics to guarantee globally stable synchronization, similarly to the fixed-parameters result in Section 4.4.3. See Appendix 6.4.3 for details.

- Leaders holding different knowledges are allowed to exist in the same network, just like a human society may contain experts in different fields. As an ex-

ample, consider (6.5) again. Assume the dynamics $\mathbf{f}$ contains l parameter sets $\mathbf{a}^1, \mathbf{a}^2, \ldots, \mathbf{a}^l$ with

$$\mathbf{f}(\mathbf{x}_i, \mathbf{a}_i^1, \ldots, \mathbf{a}_i^l, t) \;=\; \mathbf{f}(\mathbf{x}_i, \mathbf{a}^1, \ldots, \mathbf{a}^l, t) \;+\; \sum_{k=1}^{l} \mathbf{W}_k(\mathbf{x}_i, t)\tilde{\mathbf{a}}_i^k$$

Denoting by $\Omega^1, \Omega^2, \ldots, \Omega^l$ the followers sets corresponding to different knowledges, the adaptation laws are, for $k = 1, 2, \ldots, l$,

$$\dot{\mathbf{a}}_i^k \;=\; \mathbf{P}_i^k \mathbf{W}_k^T(\mathbf{x}_i, t) \sum_{j \in \mathcal{N}_i} \mathbf{K}_{ji}\,(\mathbf{x}_j - \mathbf{x}_i) \qquad \forall\, i \in \Omega^k$$

States and parameters will converge under the same conditions as those given in Theorem 6.3.

- The adaptation law we used corresponds to inserting an integrator in the feedback loop [131]. Such an integrator can be replaced by any operator which preserves the passivity of the mapping from measurement error to parameter error. For instance, the adaptation law (6.6) may be refined as

$$\hat{\mathbf{a}}_i = \mathbf{a}_i + \mathbf{Q}_i \mathbf{W}^T(\mathbf{x}_i, t) \sum_{j \in \mathcal{N}_i} \mathbf{K}_{ji}\,(\mathbf{x}_j - \mathbf{x}_i)$$

where $\mathbf{Q}_i > 0$ is constant and symmetric, and $\mathbf{a}_i$ is defined by (6.6). Note that in the theoretical analysis we should use a modified Lyapunov function

$$V = \frac{1}{2}\,(\,\mathbf{x}^T \mathbf{L}_\mathbf{K} \mathbf{x} \;+\; \sum_{i \in \Omega} \tilde{\mathbf{a}}_i^T \mathbf{P}_i^{-1} \tilde{\mathbf{a}}_i\,) \;+\; \sum_{i \in \Omega} \int_0^t \mathbf{z}_i^T \mathbf{Q}_i \mathbf{z}_i dt$$

where $\tilde{\mathbf{a}}_i \;=\; \mathbf{a}_i - \mathbf{a}$ and $\mathbf{z}_i \;=\; \mathbf{W}^T(\mathbf{x}_i, t) \sum_{j \in \mathcal{N}_i} \mathbf{K}_{ji}\,(\mathbf{x}_j - \mathbf{x}_i)$. Using estimated parameter $\hat{\mathbf{a}}_i$ in the followers' dynamics corresponds to putting an PI block in feedback loop, which improves the convergence rate as compared to having only the I operator.

- The number of leaders in a knowledge-based network can be arbitrary. At the limit all elements could be adaptive, i.e., there is no leader at all, in which case they may converge to any odd parameter set depending on initial conditions. While all states will still converge together, the desired individual behaviors (such as oscillations) may not be preserved.

- Theorem 6.3 requires the states to be bounded, which can be shown following the same steps as we did in Section 6.2.1. In fact, since $\dot{V} \leq 0$, we know that $\forall i \in \Omega$, $\mathbf{a}_i$ and $\forall$ neighbored i, j, $\mathbf{x}_i - \mathbf{x}_j$ are bounded. Thus the boundedness of the states are simply determined by the Input-to-State Stability of the system $\dot{\mathbf{y}} = \mathbf{f}(\mathbf{y}, \mathbf{a}, t) + \mathbf{u}$ where the input $\mathbf{u}$ is bounded.

- The condition (6.9) is true if the stable system behaviors are sufficiently rich or persistently exciting. This is the case, for instance, when the individual elements are oscillators, where the possibilities that any component of $\mathbf{x}_i$ converges to zero can be excluded by dynamic analysis showing that zero is an unstable state.

- Both power leaders and knowledge leaders could be virtual, which is common in animal aggregate motions. For instance, a landmark may be used as a virtual power leader. Similarly, when hunting, an escaping prey could specify both the where and the how of the movement.

Example 6.2.2: Consider six FitzHugh-Nagumo neurons (4.12), connected as in Figure 6-1(b). Assume that the parameter set $\mathbf{a} = [\alpha, I, \gamma, \beta]^T$ is fixed to the only knowledge leader with the same values as in Example 6.2.1, and those of the others change according to the adaptation law (6.6). Simulation results are plotted in Figure 6-6. □

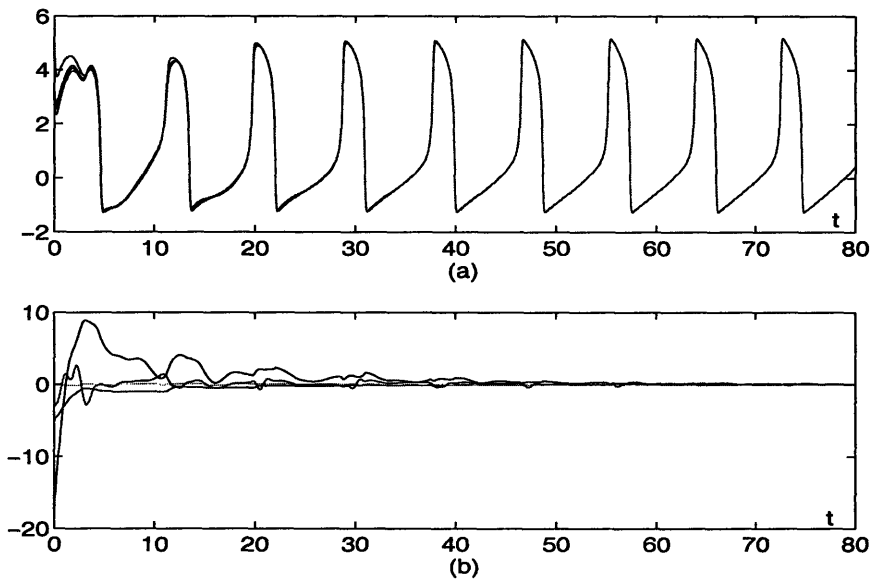

Figure 6-6: Simulation of Example 6.2.2. (a).States v_i $(i = 1, \ldots, 6)$ versus time; (b).estimation error $\tilde{\mathbf{a}}_i$ of one follower versus time.

6.3 Pacific Coexistence

Different types of leaders can co-exist in the same network. A power leader could be also a knowledge leader, or conversely, as we illustrated in Figure 6-1(c), a power leader guiding the direction may use state measurements from its neighbors to adapt its parameters to the values of the knowledge leaders.

Consider the power-based leader-followers network (6.1) again, assuming the dynamics $\mathbf{f}$ contains a parameter set $\mathbf{a}$. There are knowledge leaders holding the fixed

value $\mathbf{a}$ and knowledge followers using adaptation to learn. If $0 \in \Omega$, the set of the knowledge followers, we have

$$\dot{\mathbf{a}}_0 \;=\; \mathbf{P}_0 \mathbf{W}^T(\mathbf{x}_0, t) \sum_{i=1}^{n} \gamma_i \; \mathbf{K}_{0i} \; (\mathbf{x}_i - \mathbf{x}_0)$$

while if $i \in \Omega$ with $i = 1, \ldots, n$,

$$\dot{\mathbf{a}}_i \;=\; \mathbf{P}_i \mathbf{W}^T(\mathbf{x}_i, t) (\sum_{j \in \mathcal{N}_i} \mathbf{K}_{ji} \; (\mathbf{x}_j - \mathbf{x}_i) + \gamma_i \; \mathbf{K}_{0i} \; (\mathbf{x}_0 - \mathbf{x}_i) \;)$$

To prove state convergence, first we define several Laplacian matrices for a power-based network structure:

- $\mathbf{L_K}$, the weighted Laplacian of the followers network.
- $\vec{\mathbf{L}}_\mathbf{K}$, the weighted Laplacian of the whole network, which is non-symmetric since we have uni-directional links between the leader and the followers. Thus,

$$\vec{\mathbf{L}}_\mathbf{K} = \begin{bmatrix} \mathbf{0} & \mathbf{0} \\ -\mathbf{b} & \mathbf{C} \end{bmatrix} \quad \text{where} \quad \mathbf{b} = \begin{bmatrix} \vdots \\ \gamma_i \; \mathbf{K}_{0i} \\ \vdots \end{bmatrix}, \quad \mathbf{C} = \mathbf{L_K} + \mathbf{I}^n_{\gamma_i \mathbf{K}_{0i}}$$

  $\mathbf{C}$ is positive definite if the whole network is connected.

- $\bar{\mathbf{L}}_\mathbf{K}$, the weighted Laplacian of the whole network which we consider as an undirected graph. Thus,

$$\bar{\mathbf{L}}_\mathbf{K} = \vec{\mathbf{L}}_\mathbf{K}^T + \begin{bmatrix} \sum_{i=1}^{n} \gamma_i \mathbf{K}_{0i} & \mathbf{0} \\ -\mathbf{b} & \mathbf{0} \end{bmatrix}$$

Define the Lyapunov function

$$V = \frac{1}{2} \; (\; \mathbf{x}^T \bar{\mathbf{L}}_\mathbf{K} \mathbf{x} \; + \; \sum_{i \in \Omega} \tilde{\mathbf{a}}_i^T \mathbf{P}_i^{-1} \tilde{\mathbf{a}}_i \;)$$

We can show that

$$\begin{aligned} \dot{V} \;&=\; \mathbf{x}^T \bar{\mathbf{L}}_\mathbf{K} \; (\begin{bmatrix} \mathbf{f}(\mathbf{x}_1, \mathbf{a}, t) \\ \cdots \\ \mathbf{f}(\mathbf{x}_n, \mathbf{a}, t) \end{bmatrix} - \vec{\mathbf{L}}_\mathbf{K} \mathbf{x} \;) \\ &=\; \mathbf{x}^T \; (\; \bar{\mathbf{L}}_{\mathbf{K}\Lambda} - \vec{\mathbf{L}}_\mathbf{K}^T \; \vec{\mathbf{L}}_\mathbf{K} \;) \; \mathbf{x} \end{aligned}$$

where $\bar{\mathbf{L}}_{\mathbf{K}\Lambda}$ is defined similar as (6.7), except that here the incidence matrix is based on the whole network which we consider as an undirected graph. See Appendix 6.4.4

for the condition for $\bar{\mathbf{L}}_{\mathbf{K}\mathbf{\Lambda}} - \vec{\mathbf{L}}_{\mathbf{K}}^T \vec{\mathbf{L}}_{\mathbf{K}}$ to be negative semi-definite. Following the same proofs as those in Sections 6.2, this then implies that all the states $\mathbf{x}_i$, $i = 0, 1, \ldots, n$ will converge together asymptotically. Parameter convergence conditions are also the same.

6.4 Appendices

6.4.1 Boundedness of Coupled FN Neurons

For notation simplicity, define $u = I + k(v_2 - v_1)$ and $\bar{w} = \frac{w}{\sqrt{\beta}}$. The dynamics of the first neuron changes to

$$\begin{cases} \dot{v}_1 = v_1(\alpha - v_1)(v_1 - 1) - \sqrt{\beta}\bar{w}_1 + u \\ \dot{\bar{w}}_1 = \sqrt{\beta}v_1 - \gamma\bar{w}_1 \end{cases} \tag{6.10}$$

Define $U = \frac{1}{2}\ (\ v_1^2\ +\ \bar{w}_1^2\ )$. Then

$$\dot{U} = -(v_1 - \alpha)(v_1 - 1)v_1^2\ -\ \gamma\bar{w}_1^2\ +\ uv_1$$

Since u is bounded, there must exist a large but bounded number $v_0 > 0$, $\forall\ |v_1| > v_0$, $\dot{U} < 0$. We denote the region $|v_1| \leq v_0$ as Ω.

If the system (6.10) starts inside Ω, since the dynamics of $\bar{w}_1$ is linear and strictly stable, v_1 and $\bar{w}_1$ are always bounded as long as the system stays inside Ω. In fact,

$$\begin{aligned} |\bar{w}_1(t)| &= |(\ \bar{w}_1(0) + \int_0^t \sqrt{\beta}v_1(t)e^{\gamma t}dt\ )\ e^{-\gamma t}| \\ &\leq |\bar{w}_1(0)|e^{-\gamma t}\ +\ v_0\frac{\sqrt{\beta}}{\gamma}(1 - e^{-\gamma t}) \end{aligned}$$

Thus, for any initial condition $|\bar{w}_1(0)| > v_0\frac{\sqrt{\beta}}{\gamma}$, we have $|\bar{w}_1(t)| \leq |\bar{w}_1(0)|$, which implies that the bound of $|\bar{w}_1(t)|$ inside Ω is $\max(v_0\frac{\sqrt{\beta}}{\gamma}, |\bar{w}_1(0)|)$.

Suppose that at some moment, the system leaves Ω through point $(v_0\ \bar{w}_{out})$. Since $\dot{U} < 0$ outside Ω, $v_1^2(t)$ and $\bar{w}_1^2(t)$ will be both bounded by $v_0^2 + \bar{w}_{out}^2$ until the system trajectory re-enters Ω, at which moment we should have $|\bar{w}_{in}| < |\bar{w}_{out}|$. See Figure 6-7 for an illustration. The proof is similar if the system starts outside Ω.

Thus, $\mathbf{x}_1 = [\ v_1\ \ w_1\ ]^T$ is always bounded, which leads to asymptotic convergence of $\tilde{\mathbf{x}}$ to 0 according to Theorem 6.2. Moreover, since the two FN neurons synchronize along a limit cycle, the convergence of $\mathbf{W}(\mathbf{x}_2, t)\tilde{\mathbf{a}}$ to zero implies that of $\tilde{\mathbf{a}}$.

6.4.2 Proof of Lemma 6.1

For notational simplicity, we first show the derivations for the case $m = 1$.

Since

$$\mathbf{L}_{\mathbf{K}\mathbf{\Lambda}} - \mathbf{L}_{\mathbf{K}}^2\ =\ \mathbf{D}\ (\ (\mathbf{I}_{\mathbf{K}_{ij}}^r\mathbf{I}_{\mathbf{\Lambda}_{ij}}^r)_s\ -\ \mathbf{I}_{\mathbf{K}_{ij}}^r\mathbf{D}^T\mathbf{D}\mathbf{I}_{\mathbf{K}_{ij}}^r\ )\ \mathbf{D}^T$$

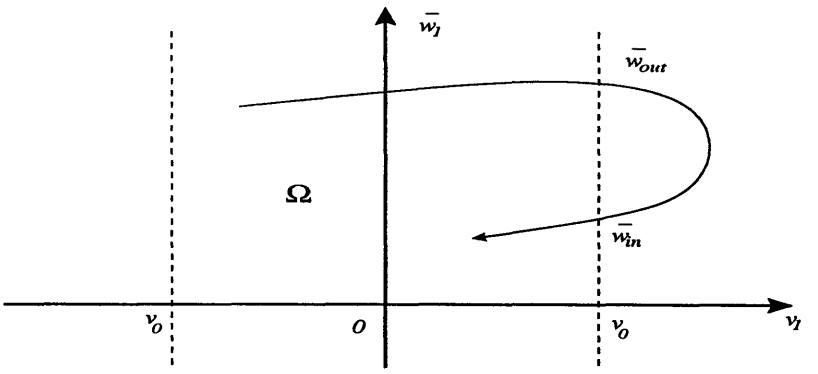

Figure 6-7: A solution trajectory of system (6.10) leaves and re-enters the region $\Omega: \ |v_1| \leq v_0$.

we know that 0 is always one of the eigenvalues of $\mathbf{L_{K\Lambda}} - \mathbf{L_K^2}$, with one corresponding eigenvector $\mathbf{v} = [1, 1, \ldots, 1]^T$. Assume all the eigenvalues λ_i are arranged in increasing order for $i = 1, 2, \ldots, n$. According to Weyl's Theorem [51], for two Hermitian matrix $\mathbf{A}$ and $\mathbf{B}$,

$$\lambda_k(\mathbf{A}) + \lambda_1(\mathbf{B}) \ \leq \ \lambda_k(\mathbf{A}+\mathbf{B}) \ \leq \ \lambda_k(\mathbf{A}) + \lambda_n(\mathbf{B})$$

for each $k = 1, 2, \ldots, n$. Thus, we have

$$\lambda_{n-k+1}(\mathbf{L_{K\Lambda}} - \mathbf{L_K^2}) \ \leq \ \lambda_n(\mathbf{L_{K\Lambda}}) - \lambda_k(\mathbf{L_K^2})$$

which implies that, $\forall k > 1$, $\lambda_{n-k+1}(\mathbf{L_{K\Lambda}} - \mathbf{L_K^2}) < 0$ if

$$\lambda_n(\mathbf{L_{K\Lambda}}) \ < \ \lambda_2(\mathbf{L_K^2}) \tag{6.11}$$

Therefore, $\lambda_n(\mathbf{L_{K\Lambda}} - \mathbf{L_K^2}) = 0$, i.e., $\mathbf{L_{K\Lambda}} - \mathbf{L_K^2}$ is negative semi-definite.

Denote $\max_k \lambda_{max}(\mathbf{K\Lambda})_{ijs} = \bar{\lambda}$. If $\bar{\lambda} \leq 0$, we have $\lambda_n(\mathbf{L_{K\Lambda}}) \leq 0$ and both the conditions (6.11) and (6.8) are always true; if $\bar{\lambda} > 0$,

$$\lambda_n(\mathbf{L_{K\Lambda}}) \ \leq \ \bar{\lambda} \, \lambda_n(\mathbf{L})$$

where $\mathbf{L}$ is the graph Laplacian matrix. Considering the fact that $\lambda_2(\mathbf{L_K^2}) = \lambda_2^2(\mathbf{L_K})$, condition (6.8) is sufficient to guarantee (6.11).

For a real symmetric matrix, the state space has an orthogonal basis consisting of all eigenvectors. Without loss generality, we assume there is such an orthogonal eigenvector set, $\{\mathbf{v}_1, \mathbf{v}_2, \ldots, \mathbf{v}_n\}$, of $\mathbf{L_{K\Lambda}} - \mathbf{L_K^2}$, where $\mathbf{v}_n = [1, 1, \ldots, 1]^T$ is the only

zero eigenvector. For any $\mathbf{x}$, we have $\mathbf{x} = \sum_{i=1}^{n} k_i \mathbf{v}_i$ and

$$\begin{aligned}
\mathbf{x}^T \left(\mathbf{L}_{\mathbf{K}\mathbf{\Lambda}} - \mathbf{L}_{\mathbf{K}}^2 \right) \mathbf{x} &= \sum_{i=1}^{n} k_i \mathbf{v}_i^T \left(\mathbf{L}_{\mathbf{K}\mathbf{\Lambda}} - \mathbf{L}_{\mathbf{K}}^2 \right) \sum_{i=1}^{n} k_i \mathbf{v}_i \\
&= \sum_{i=1}^{n-1} k_i \mathbf{v}_i^T \left(\mathbf{L}_{\mathbf{K}\mathbf{\Lambda}} - \mathbf{L}_{\mathbf{K}}^2 \right) \sum_{i=1}^{n-1} k_i \mathbf{v}_i \\
&= \sum_{i=1}^{n-1} \lambda_i k_i^2 \mathbf{v}_i^T \mathbf{v}_i
\end{aligned}$$

Since the eigenvalue $\lambda_i < 0 \; \forall i < n$, $\mathbf{x}^T \left(\mathbf{L}_{\mathbf{K}\mathbf{\Lambda}} - \mathbf{L}_{\mathbf{K}}^2 \right) \mathbf{x} = 0$ if and only if $\mathbf{x} = k_n \mathbf{v}_n$, that is, $\mathbf{x}_1 = \mathbf{x}_2 = \cdots = \mathbf{x}_n$.

In case $m > 1$, we can follow the same proof except that zero eigenvalue here has m multiplicity, and the corresponding eigenvectors $\{\mathbf{v}_1, \mathbf{v}_2, \ldots, \mathbf{v}_m\}$ are linear combinations of the orthogonal set $[\mathbf{I}, \mathbf{I}, \ldots, \mathbf{I}]^T$ where $\mathbf{I} \in \mathbb{R}^{m \times m}$ is identity matrix.

6.4.3 Positive Semi-Definite Couplings

Assume the coupling gain of the k^{th} link (between nodes i and j) is

$$\mathbf{K}_k = \begin{bmatrix} \mathbf{K}_1 & 0 \\ 0 & 0 \end{bmatrix}_k$$

where $\mathbf{K}_{1k}$ is symmetric positive definite and has a common dimension to all links. We divide the uncoupled dynamics $\mathbf{J}$, and in turn the block diagonal entry of $\mathbf{\Lambda}$ into the form

$$[\mathbf{\Lambda}]_k = \frac{\partial \mathbf{f}}{\partial \mathbf{x}}(\bar{\mathbf{x}}_k, \mathbf{a}, t) = \mathbf{J}(\bar{\mathbf{x}}_k, t) = \begin{bmatrix} \mathbf{J}_{11} & \mathbf{J}_{12} \\ \mathbf{J}_{21} & \mathbf{J}_{22} \end{bmatrix}_k$$

where $\bar{\mathbf{x}}$ is a value between the states of two neighboring nodes $\mathbf{x}_i$ and $\mathbf{x}_j$, and each component of $\mathbf{J}_k$ has the same dimension as that of the corresponding part in $\mathbf{K}_k$. Re-define the function V as

$$V = \frac{1}{2} \left(\mathbf{x}^T \mathbf{L}_{\mathbf{K}} \mathbf{x} + \mathbf{x}^T \mathbf{L}_{\mathbf{Y}} \mathbf{x} + \sum_{i \in \mathbf{\Omega}} \tilde{\mathbf{a}}_i^T \mathbf{P}^{-1} \tilde{\mathbf{a}}_i \right)$$

where

$$\mathbf{L}_{\mathbf{Y}} = \mathbf{D} \, \mathbf{I}_{\mathbf{Y}_{ij}}^{\tau} \, \mathbf{D}^T$$

is a weighted Laplacian based on the same graph as $\mathbf{L}_{\mathbf{K}}$ but different weights

$$\mathbf{Y}_{ij} = \mathbf{Y}_k = \begin{bmatrix} 0 & 0 \\ 0 & \mathbf{K}_2 \end{bmatrix}_k$$

and $\mathbf{K}_{2k}$ is a constant symmetric matrix acting as an additional part of the coupling gain. Using a modified adaptive law

$$\dot{\mathbf{a}}_i \;=\; \mathbf{P}_i \mathbf{W}^T(\mathbf{x}_i, t) \sum_{j \in \mathcal{N}_i} (\mathbf{K} + \mathbf{Y})_{ji} \, (\mathbf{x}_j - \mathbf{x}_i) \quad \forall \, i \in \mathbf{\Omega}$$

we can show that

$$\begin{aligned} \dot{V} &= \mathbf{x}^T \left(\mathbf{L}_{(\mathbf{K}+\mathbf{Y})\mathbf{\Lambda}} - \mathbf{L}_{\mathbf{K}}^2 \right) \mathbf{x} \\ &= \mathbf{x}^T \, \mathbf{L}_{(\mathbf{K}+\mathbf{Y})(\mathbf{\Lambda}-\bar{\mathbf{\Lambda}})} \, \mathbf{x} \;+\; \mathbf{x}^T \left(\mathbf{L}_{\mathbf{K}\bar{\mathbf{\Lambda}}} - \mathbf{L}_{\mathbf{K}}^2 \right) \mathbf{x} \end{aligned}$$

where we define the diagonal entry $[\bar{\mathbf{\Lambda}}]_k \;=\; \begin{bmatrix} \bar{\mathbf{J}}_{11} & 0 \\ 0 & 0 \end{bmatrix}_k$ so that

$$\begin{aligned} \left[\mathbf{I}_{\mathbf{K}_{ij}}^T \mathbf{I}_{\bar{\Lambda}_{ij}}^T \right]_k &= \begin{bmatrix} \mathbf{K}_1 \bar{\mathbf{J}}_{11} & 0 \\ 0 & 0 \end{bmatrix}_k \\ \left[\mathbf{I}_{(\mathbf{K}+\mathbf{Y})_{ij}}^T \mathbf{I}_{(\mathbf{\Lambda}-\bar{\mathbf{\Lambda}})_{ij}}^T \right]_k &= \begin{bmatrix} \mathbf{K}_1(\mathbf{J}_{11} - \bar{\mathbf{J}}_{11}) & \mathbf{K}_1 \mathbf{J}_{12} \\ \mathbf{K}_2 \mathbf{J}_{21} & \mathbf{K}_2 \mathbf{J}_{22} \end{bmatrix}_k \end{aligned}$$

A non-positive $\dot{V}$ can be guaranteed if

- $\mathbf{L}_{\mathbf{K}\bar{\mathbf{\Lambda}}} - \mathbf{L}_{\mathbf{K}}^2 \;\leq 0$, which can be satisfied under a similar condition as (6.8);
- $\mathbf{L}_{(\mathbf{K}+\mathbf{Y})(\mathbf{\Lambda}-\bar{\mathbf{\Lambda}})} \leq 0$, which is true if $\forall k \left[\mathbf{I}_{(\mathbf{K}+\mathbf{Y})_{ij}}^T \mathbf{I}_{(\mathbf{\Lambda}-\bar{\mathbf{\Lambda}})_{ij}}^T \right]_k \leq 0$, i.e., the symmetric parts of $\mathbf{K}_1(\mathbf{J}_{11} - \bar{\mathbf{J}}_{11})$ and $\mathbf{K}_2 \mathbf{J}_{22}$ are both negative definite, and $\sigma_{max}(\mathbf{K}_1 \mathbf{J}_{12} + \mathbf{J}_{21}^T \mathbf{K}_2^T)$ is bounded, an explicit condition derived from feedback combination condition (2.4).

The rest of the convergence proof are the same as that of positive definite couplings.

6.4.4 Network with Both Leaders

For notational simplicity, we only show the case $m = 1$. The proof is similar if $m > 1$.

Similarly to the proof in 6.4.2, $\bar{\mathbf{L}}_{\mathbf{K}\mathbf{\Lambda}} - \vec{\mathbf{L}}_{\mathbf{K}}^T \, \vec{\mathbf{L}}_{\mathbf{K}}$ is negative semi-definite if

$$\lambda_{n+1}(\bar{\mathbf{L}}_{\mathbf{K}\mathbf{\Lambda}}) \;<\; \lambda_2(\vec{\mathbf{L}}_{\mathbf{K}}^T \, \vec{\mathbf{L}}_{\mathbf{K}})$$

and its only eigendirection for the zero eigenvalue is thus $\mathbf{v} = [1, 1, \ldots, 1]^T$. Since

$$\vec{\mathbf{L}}_{\mathbf{K}}^T \, \vec{\mathbf{L}}_{\mathbf{K}} = \begin{bmatrix} \mathbf{b}^T \mathbf{b} & -\mathbf{b}^T \mathbf{C} \\ -\mathbf{C}\mathbf{b} & \mathbf{C}^2 \end{bmatrix}$$

we have

$$\lambda_2(\vec{\mathbf{L}}_{\mathbf{K}}^T \, \vec{\mathbf{L}}_{\mathbf{K}}) \geq \lambda_1(\mathbf{C}^2) = \lambda_1^2(\mathbf{C})$$

according to the Interlacing Eigenvalues Theorem for bordered matrices [51]. Thus a sufficient condition to guarantee negative semi-definite is

$$\lambda_1^2(\mathbf{C}) > \lambda_{n+1}(\bar{\mathbf{L}}_{\mathbf{K}\mathbf{\Lambda}}) \tag{6.12}$$

This condition is similar to the one we derived in Theorem 6.1 for synchronization of pure power-based leader-followers network. Assuming all the coupling strengths are identical with value κ, condition (6.12) becomes

$$\kappa \; > \; \frac{\lambda_{n+1}(\bar{\mathbf{L}})}{\lambda_1^2(\mathbf{L} + \mathbf{I}_{\gamma_i}^n)} \; \max \frac{\partial \mathbf{f}}{\partial \mathbf{x}}(\mathbf{x}_i, \mathbf{a}, t)$$

Chapter 7

Contraction Analysis of Time-Delayed Communications

In many engineering applications, communications delays between subsystems cannot be neglected. Such an example is bilateral teleoperation, where signals can experience significant transmission delays between local and remote sites. Throughout the last decade, the both internet and wireless technologies have vastly extended practical communication distances. Information exchange and cooperation can in principle occur in very widely distributed systems, making the effect of time delays even more central.

In the context of telerobotics, [2] proposed a control law for force-reflecting teleoperators which preserves passivity, and thus overcomes the instability caused by time delays. The idea was reformulated in [102], which led to the introduction of wave variables. Transmission of wave variables across communication channels ensures stability without knowledge of the time delay. Further extensions to internet-based applications were developed [104, 103, 18], in which the communication delays are variable.

Recently, [83] extended the application of wave variables to a more general context by performing a nonlinear contraction analysis [81] of the effect of time-delayed communications between contracting systems. This paper modifies the design of the wave variables proposed in [83]. One simplified form provides an efficient analysis tool for interacted nonlinear systems with time-delayed feedback communications. Contraction as a generalized stability property preserves regardless of the delay values. The result also explains the well-known fact in teleoperation, that even small time-delays in feedback PD controllers may create stability problems for coupled second-order systems, which motivated approaches based on passivity and wave variables. The approach is then applied to study the group cooperation problem where the communications are delayed. We show that synchronization is robust to time delays and network connectivity if the protocol is linear. In a leaderless network, all the coupled elements tend to reach a common state which varies according to the initial conditions and the time delays, while in a leader-followers network, this group agreement point is fixed by the leader. The approach is suitable to study both continuous and discrete-time models. At last, we construct and analyze the model of a large pop-

ulation composed of loosely-tied groups, where synchronization in different groups disturb by each other and the signals being transmitted contain only information on group synchronization status. Its analogs exist widely, e.g., in human psychology and macro-economics.

7.1 Contraction Analysis of Time-Delayed Communications

Inspired by the use of passivity [2] and wave variables [102] in force-reflecting teleoperation, [83] performed a contraction analysis of the effect of time-delayed communications. In fact, as we will discuss in this section, the form of the transmitted variables in [83] can be simplified, which then provides us a more powerful tool. It can be applied to analyze time-delayed feedback communications, and also to realize teleoperation in a more straightforward manner.

7.1.1 Wave Variables

Wave variables [102] are used in bilateral teleoperation systems to guarantee the passivity [2] of the time-delayed transmissions. The idea was generalized in [83] by conducting a contraction analysis on time-delayed transmission channels. As illustrated in Figure 7-1, [83] considers two interacting systems of possibly different dimensions in $\mathbf{x}_1$ and $\mathbf{x}_2$,

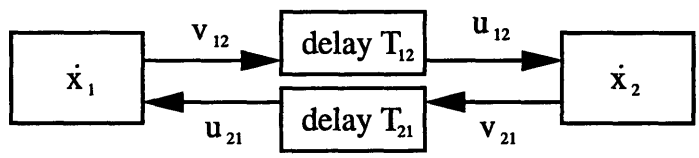

Figure 7-1: Two interacting systems with delayed communications

$$\begin{cases} \dot{\mathbf{x}}_1 &= \mathbf{f}_1(\mathbf{x}_1, t) + \mathbf{G}_{21}\tau_{21} \\ \dot{\mathbf{x}}_2 &= \mathbf{f}_2(\mathbf{x}_2, t) + \mathbf{G}_{12}\tau_{12} \end{cases} \tag{7.1}$$

where $\mathbf{G}_{12}$, $\mathbf{G}_{21}$ are constant matrices and τ_{12}, τ_{21} have the same dimension. The intermediate variables are defined as

$$\begin{aligned} \mathbf{u}_{21} &= \mathbf{G}_{21}^T\mathbf{x}_1 + \tau_{21} & \qquad \mathbf{v}_{12} &= \mathbf{G}_{21}^T\mathbf{x}_1 - \tau_{21} \\ \mathbf{u}_{12} &= \mathbf{G}_{12}^T\mathbf{x}_2 + \tau_{12} & \qquad \mathbf{v}_{21} &= \mathbf{G}_{12}^T\mathbf{x}_2 - \tau_{12} \end{aligned}$$

Because of time-delays, one has

$$\mathbf{u}_{12}(t) = \mathbf{v}_{12}(t - T_{12}) \qquad \mathbf{u}_{21}(t) = \mathbf{v}_{21}(t - T_{21})$$

where T_{12} and T_{21} are two possibly different constants. It can be proved that, if both $\mathbf{f}_1$ and $\mathbf{f}_2$ are contracting, the overall system is asymptotically contracting independently of the time delays.

Note that the subscripts containing two numbers indicate the communication direction. For instance, subscript 12 means the associated communication is from node 1 to 2. Such a definition is helpful to make the notation clear in Section 7.2, where our result will be extended to a group of interacted subsystems.

7.1.2 Time-Delayed Feedback Communications

Let us now consider modified choices of the transmitted variables above. Specifically, for interacting systems (7.1), define now the transmitted variables as

$$\begin{aligned} \mathbf{u}_{21} &= \mathbf{G}_{21}^T \mathbf{x}_1 + k_{21}\tau_{21} & \mathbf{v}_{12} &= \mathbf{G}_{21}^T \mathbf{x}_1 \\ \mathbf{u}_{12} &= \mathbf{G}_{12}^T \mathbf{x}_2 + k_{12}\tau_{12} & \mathbf{v}_{21} &= \mathbf{G}_{12}^T \mathbf{x}_2 \end{aligned} \tag{7.2}$$

where k_{12} and k_{21} are two strictly positive constants. Consider, similarly to [83, 132], the differential length

$$V = \frac{k_{21}}{2}\,\delta\mathbf{x}_1^T\delta\mathbf{x}_1 + \frac{k_{12}}{2}\,\delta\mathbf{x}_2^T\delta\mathbf{x}_2 + \frac{1}{2}\,V_{1,2}$$

where

$$V_{1,2} = \int_{t-T_{12}}^{t} \delta\mathbf{v}_{12}^T\delta\mathbf{v}_{12}\,d\epsilon + \int_{t-T_{21}}^{t} \delta\mathbf{v}_{21}^T\delta\mathbf{v}_{21}\,d\epsilon - \int_{-T_{12}}^{0} \delta\mathbf{v}_{12}^T\delta\mathbf{v}_{12}\,d\epsilon - \int_{-T_{21}}^{0} \delta\mathbf{v}_{21}^T\delta\mathbf{v}_{21}\,d\epsilon$$

Note that

$$\begin{aligned} V_{1,2} &= \int_0^t (\,\delta\mathbf{v}_{12}^T\delta\mathbf{v}_{12}(\epsilon) - \delta\mathbf{v}_{12}^T\delta\mathbf{v}_{12}(\epsilon - T_{12}) + \delta\mathbf{v}_{21}^T\delta\mathbf{v}_{21}(\epsilon) - \delta\mathbf{v}_{21}^T\delta\mathbf{v}_{21}(\epsilon - T_{21})\,)\,d\epsilon \\ &= \int_0^t (\,\delta\mathbf{v}_{12}^T\delta\mathbf{v}_{12}(\epsilon) - \delta\mathbf{u}_{12}^T\delta\mathbf{u}_{12}(\epsilon) + \delta\mathbf{v}_{21}^T\delta\mathbf{v}_{21}(\epsilon) - \delta\mathbf{u}_{21}^T\delta\mathbf{u}_{21}(\epsilon)\,)\,d\epsilon \\ &= -2\int_0^t (\,k_{21}\delta\mathbf{x}_1^T\mathbf{G}_{21}\delta\tau_{21} + k_{12}\delta\mathbf{x}_2^T\mathbf{G}_{12}\delta\tau_{12})\,d\epsilon - \int_0^t (\,k_{21}^2\delta\tau_{21}^T\delta\tau_{21} + k_{12}^2\delta\tau_{12}^T\delta\tau_{12})\,d\epsilon \end{aligned}$$

This yields

$$\dot{V} = k_{21}\delta\mathbf{x}_1^T\frac{\partial\mathbf{f}_1}{\partial\mathbf{x}_1}\,\delta\mathbf{x}_1 + k_{12}\delta\mathbf{x}_2^T\frac{\partial\mathbf{f}_2}{\partial\mathbf{x}_2}\,\delta\mathbf{x}_2 - \frac{k_{21}^2}{2}\,\delta\tau_{21}^T\delta\tau_{21} - \frac{k_{12}^2}{2}\,\delta\tau_{12}^T\delta\tau_{12}$$

If $\mathbf{f}_1$ and $\mathbf{f}_2$ are both contracting with identity metrics (i.e., if $\frac{\partial\mathbf{f}_1}{\partial\mathbf{x}_1}$ and $\frac{\partial\mathbf{f}_2}{\partial\mathbf{x}_2}$ are both uniformly negative definite), then $\dot{V} \leq 0$, and V is bounded and tends to a limit. Applying Barbalat's lemma [131] in turn shows that, if $\ddot{V}$ is bounded, then $\dot{V}$ tends to zero asymptotically, which implies that $\delta\mathbf{x}_1$, $\delta\mathbf{x}_2$, $\delta\tau_{12}$ and $\delta\tau_{21}$ all tend to zero. Regardless of the values of the delays, all solutions of system (7.1) converge to a single

trajectory, independently of the initial conditions. In the sequel we shall assume that $\ddot{V}$ can indeed be bounded as a consequence of the boundedness of V.

This result has a useful interpretation. Expanding system dynamics (7.1) using (7.2) yields

$$\begin{cases} \dot{\mathbf{x}}_1 = \mathbf{f}_1(\mathbf{x}_1, t) + \frac{1}{k_{21}} \mathbf{G}_{21} \left(\mathbf{G}_{12}^T \mathbf{x}_2(t - T_{21}) - \mathbf{G}_{21}^T \mathbf{x}_1(t) \right) \\ \dot{\mathbf{x}}_2 = \mathbf{f}_2(\mathbf{x}_2, t) + \frac{1}{k_{12}} \mathbf{G}_{12} \left(\mathbf{G}_{21}^T \mathbf{x}_1(t - T_{12}) - \mathbf{G}_{12}^T \mathbf{x}_2(t) \right) \end{cases}$$

so that the above communications in fact correspond to simple feedback interactions. If we assume further that $\mathbf{x}_1$ and $\mathbf{x}_2$ have the same dimension, and choose $\mathbf{G}_{12} = \mathbf{G}_{21} = \mathbf{G}$, the whole system is actually equivalent to two diffusively coupled subsystems

$$\begin{cases} \dot{\mathbf{x}}_1 = \mathbf{f}_1(\mathbf{x}_1, t) + \frac{1}{k_{21}} \mathbf{G}\mathbf{G}^T \left(\mathbf{x}_2(t - T_{21}) - \mathbf{x}_1(t) \right) \\ \dot{\mathbf{x}}_2 = \mathbf{f}_2(\mathbf{x}_2, t) + \frac{1}{k_{12}} \mathbf{G}\mathbf{G}^T \left(\mathbf{x}_1(t - T_{12}) - \mathbf{x}_2(t) \right) \end{cases} \tag{7.3}$$

Note that constants k_{12} and k_{21} and thus coupling gains along different diffusion directions can be different. We can thus state

Theorem 7.1 *Consider two subsystems, both contracting with identity metrics, and interacting through time-delayed diffusion-like couplings (7.3). Then the overall system is asymptotically contracting.*

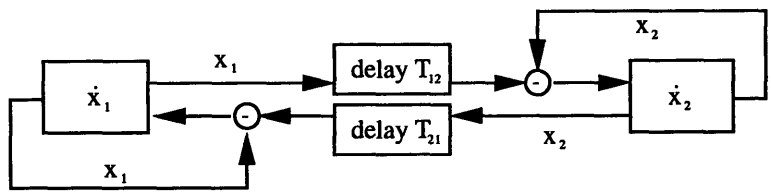

Figure 7-2: Two interacting systems with time-delayed diffusion couplings

Remarks

- Theorem 7.1 does not contradict the well-known fact in teleoperation, that even small time-delays in bilateral PD controllers may create stability problems for coupled second-order systems [2, 102, 103, 18], which motivates approaches based on passivity and wave variables. In fact, a key condition for contraction to be preserved is that the diffusion-like coupling gains be symmetric positive semi-definite *in the same metric* as the subsystems, as we shall illustrate later in this section.

- If there are no delays, i.e., $T_{12} = T_{21} = 0$, then $V_{1,2} = 0$. Thus, the analysis of

the differential length yields that

$$\begin{aligned}\dot{V} &= \frac{1}{2}\frac{d}{dt}(\, k_{21}\delta\mathbf{x}_1^T\delta\mathbf{x}_1 \,+\, k_{12}\delta\mathbf{x}_2^T\delta\mathbf{x}_2 \,) \,\leq\, k_{21}\delta\mathbf{x}_1^T\frac{\partial\mathbf{f}_1}{\partial\mathbf{x}_1}\delta\mathbf{x}_1 \,+\, k_{12}\delta\mathbf{x}_2^T\frac{\partial\mathbf{f}_2}{\partial\mathbf{x}_2}\delta\mathbf{x}_2 \\ &\leq \lambda_{max}\,(\, k_{21}\delta\mathbf{x}_1^T\delta\mathbf{x}_1 \,+\, k_{12}\delta\mathbf{x}_2^T\delta\mathbf{x}_2 \,)\end{aligned}$$

where

$$\lambda_{max} \,=\, \max(\, \lambda_{max}(\frac{\partial\mathbf{f}_1}{\partial\mathbf{x}_1})_s,\; \lambda_{max}(\frac{\partial\mathbf{f}_2}{\partial\mathbf{x}_2})_s \,)$$

This implies that $\delta\mathbf{x}_1$ and $\delta\mathbf{x}_2$ tend to zero exponentially for contracting dynamics $\mathbf{f}_1$ and $\mathbf{f}_2$, i.e., the overall system is exponentially contracting.

- If $\mathbf{f}_1$ and $\mathbf{f}_2$ are both contracting and time-invariant, all solutions of system (7.3) converge to a unique equilibrium point, whose value is independent of the time delays and the initial conditions. Indeed, in a globally contracting autonomous system, all trajectories converge to a unique equilibrium point [81, 133], which implies that if $\mathbf{f}_1$ and $\mathbf{f}_2$ are both contracting and time-invariant, an equilibrium point must exist for system (7.3) when $T_{12} = T_{21} = 0$. In turn, this point remains an equilibrium point for arbitrary non-zero T_{12} and T_{21}. Since the delayed system (7.3) also preserves contraction, all solutions will converge to this point independently of the initial conditions and the explicit values of the delays.

- Theorem 7.1 can be extended directly to study more general connections between groups, such as bidirectional meshes or webs of arbitrary size, and parallel unidirectional rings of arbitrary length, both of which will be illustrated through Section 7.2. Inputs to the overall system can be provided through any of the subgroup dynamics.

Example 7.1.1: Consider two identical second-order systems coupled through time-delayed feedback PD controllers

$$\begin{cases} \ddot{x}_1 + b\dot{x}_1 + \omega^2 x_1 \;=\; k_d(\dot{x}_2(t-T_{21}) - \dot{x}_1(t)) + k_p(x_2(t-T_{21}) - x_1(t)) \\ \ddot{x}_2 + b\dot{x}_2 + \omega^2 x_2 \;=\; k_d(\dot{x}_1(t-T_{12}) - \dot{x}_2(t)) + k_p(x_1(t-T_{12}) - x_2(t)) \end{cases}$$

with $b > 0$, $\omega > 0$. If $T_{12} = T_{21} = 0$, partial contraction analysis [134, 164] shows that x_1 and x_2 converge together exponentially regardless of initial conditions, which makes the origin a stable equilibrium point. If $T_{12}, T_{21} > 0$, a simple coordinate transformation yields

$$\begin{aligned}\begin{bmatrix} \dot{x}_1 \\ \dot{y}_1 \end{bmatrix} &= \begin{bmatrix} \omega y_1 - b x_1 \\ -\omega x_1 \end{bmatrix} + \mathbf{K}(\begin{bmatrix} x_2(t-T_{21}) \\ y_2(t-T_{21}) \end{bmatrix} - \begin{bmatrix} x_1(t) \\ y_1(t) \end{bmatrix}) \\ \begin{bmatrix} \dot{x}_2 \\ \dot{y}_2 \end{bmatrix} &= \begin{bmatrix} \omega y_2 - b x_2 \\ -\omega x_2 \end{bmatrix} + \mathbf{K}(\begin{bmatrix} x_1(t-T_{12}) \\ y_1(t-T_{12}) \end{bmatrix} - \begin{bmatrix} x_2(t) \\ y_2(t) \end{bmatrix})\end{aligned}$$

where

$$\mathbf{f}_1 = \begin{bmatrix} \omega y_1 - b x_1 \\ -\omega x_1 \end{bmatrix} \qquad \text{and} \qquad \mathbf{f}_2 = \begin{bmatrix} \omega y_2 - b x_2 \\ -\omega x_2 \end{bmatrix}$$

are both contracting with identity metric [164]. However, the transformed coupling gain

$$\mathbf{K} = \begin{bmatrix} k_d & 0 \\ \frac{k_p}{\omega} & 0 \end{bmatrix}$$

is neither symmetric nor positive semi-definite for any $k_p \neq 0$. Contraction cannot be preserved in this case, and the coupled systems turn out to be unstable for large enough delays as the simulation result in Figure 7-3(a) illustrates. In Figure 7-3(b) we set $k_p = 0$ so that the overall system is contracting according to Theorem 7.1. □

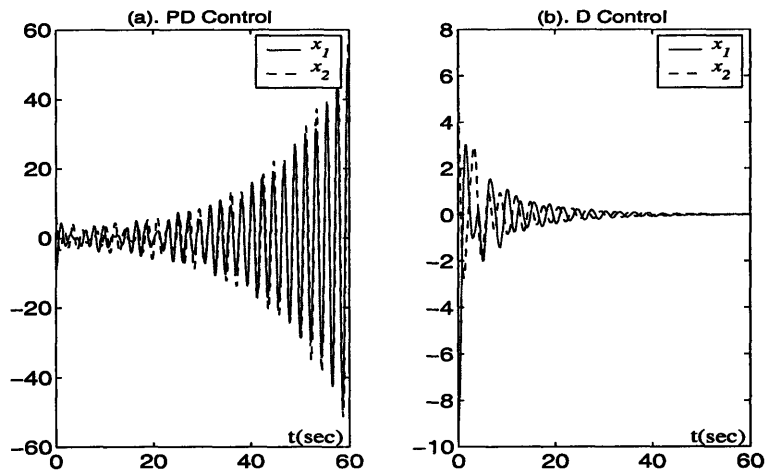

Figure 7-3: Simulation results of two coupled mass-spring-damper systems with (a) PD control and (b) D control. Parameters are $b = 0.5$, $\omega^2 = 5$, $T_{12} = 2s$, $T_{21} = 4s$, $k_d = 1$, $k_p = 5$ in (a) and $k_p = 0$ in (b). Initial conditions, chosen randomly, are identical for the two plots.

The instability mechanism in the above example is actually very similar to that of the classical Smale model [136, 164] of spontaneous oscillation, in which two or more identical biological cells, inert by themselves, tend to self-excited oscillations through diffusion interactions. In both cases, the instability is caused by a non-identity metric, which makes the transformed coupling gains lose positive semi-definiteness. Note that the relative simplicity with which both phenomena can be analyzed makes fundamental use of the notion of a metric, central to contraction theory.

7.1.3 Other Simplified Forms of Wave-Variables

Different simplifications of the original wave-variable design can be made based on the same choice of V, yielding different qualitative properties. For instance, the transmitted signals can be defined as

$$\begin{aligned} \mathbf{u}_{21} &= \mathbf{G}_{21}^T \mathbf{x}_1 + k_{21}\tau_{21} & \mathbf{v}_{12} &= -k_{21}\tau_{21} \\ \mathbf{u}_{12} &= \mathbf{G}_{12}^T \mathbf{x}_2 + k_{12}\tau_{12} & \mathbf{v}_{21} &= -k_{12}\tau_{12} \end{aligned}$$

which leads to

$$\begin{aligned}\dot{V} &= k_{21}\delta\mathbf{x}_1^T\frac{\partial \mathbf{f}_1}{\partial \mathbf{x}_1}\delta\mathbf{x}_1 + k_{12}\delta\mathbf{x}_2^T\frac{\partial \mathbf{f}_2}{\partial \mathbf{x}_2}\delta\mathbf{x}_2 - \frac{1}{2}\delta\mathbf{x}_1^T\mathbf{G}_{21}\mathbf{G}_{21}^T\delta\mathbf{x}_1 - \frac{1}{2}\delta\mathbf{x}_2^T\mathbf{G}_{12}\mathbf{G}_{12}^T\delta\mathbf{x}_2 \\ &= \delta\mathbf{x}_1^T\Big(k_{21}\frac{\partial \mathbf{f}_1}{\partial \mathbf{x}_1} - \frac{1}{2}\mathbf{G}_{21}\mathbf{G}_{21}^T\Big)\delta\mathbf{x}_1 + \delta\mathbf{x}_2^T\Big(k_{12}\frac{\partial \mathbf{f}_2}{\partial \mathbf{x}_2} - \frac{1}{2}\mathbf{G}_{12}\mathbf{G}_{12}^T\Big)\delta\mathbf{x}_2 \qquad (7.4)\end{aligned}$$

and thus also preserves contraction through time-delayed communications. Similarly to the previous section, if both $\mathbf{f}_1$ and $\mathbf{f}_2$ are contracting and time-invariant, the whole system tends towards a unique equilibrium point, regardless of the delay values. At this steady state, $\mathbf{u}_{12}(\infty) = \mathbf{v}_{12}(\infty)$ and $\mathbf{u}_{21}(\infty) = \mathbf{v}_{21}(\infty)$, which immediately implies that

$$\mathbf{G}_{21}^T\,\mathbf{x}_1(\infty) = \mathbf{G}_{12}^T\,\mathbf{x}_2(\infty)$$

and, if $\mathbf{G}_{12} = \mathbf{G}_{21} = \mathbf{G}$ with $\mathbf{G}$ of full rank, that

$$\mathbf{x}_1(\infty) = \mathbf{x}_2(\infty)$$

Thus, contrary to the case (7.2) of diffusion-like couplings, the remote tracking ability of wave variables is preserved.

Example 7.1.2: Consider the example of two second-order systems

$$\begin{cases}\ddot{x}_1 + b_1\dot{x}_1 + \omega_1^2 x_1 = F_{21} + F_e \\ \ddot{x}_2 + b_2\dot{x}_2 + \omega_2^2 x_2 = F_{12}\end{cases}$$

where F_e is an external force, and F_{21}, F_{12} are internal forces undergoing time delays. Performing a coordinate transformation, we get new equations

$$\begin{bmatrix}\dot{x}_1 \\ \dot{y}_1\end{bmatrix} = \begin{bmatrix}\omega_1 y_1 - b_1 x_1 \\ -\omega_1 x_1 + \frac{F_e}{\omega_1}\end{bmatrix} + \begin{bmatrix}0 \\ \frac{F_{21}}{\omega_1}\end{bmatrix}$$

$$\begin{bmatrix}\dot{x}_2 \\ \dot{y}_2\end{bmatrix} = \begin{bmatrix}\omega_2 y_2 - b_2 x_2 \\ -\omega_2 x_2\end{bmatrix} + \begin{bmatrix}0 \\ \frac{F_{12}}{\omega_2}\end{bmatrix}$$

The signals being transmitted are defined as simplified wave variables

$$u_{21} = y_1 + \frac{k_{21}}{\omega_1}F_{21} \qquad v_{12} = -\frac{k_{21}}{\omega_1}F_{21}$$

$$u_{12} = y_2 + \frac{k_{12}}{\omega_2}F_{12} \qquad v_{21} = -\frac{k_{12}}{\omega_2}F_{12}$$

Note that here $\mathbf{G}_{12} = \mathbf{G}_{21} = \begin{bmatrix}0 & 0 \\ 0 & 1\end{bmatrix}$, and that although the variables y_1 and y_2 are virtual, their values can be calculated based on x_1, $\dot{x}_1$ and x_2, $\dot{x}_2$. According to the result we derived above, the whole system will tend to reach an equilibrium point asymptotically. This point is independent to the time delays and satisfies $y_1(\infty) = y_2(\infty)$, i.e.,

$$\frac{b_1}{\omega_1}x_1(\infty) = \frac{b_2}{\omega_2}x_2(\infty)$$

□

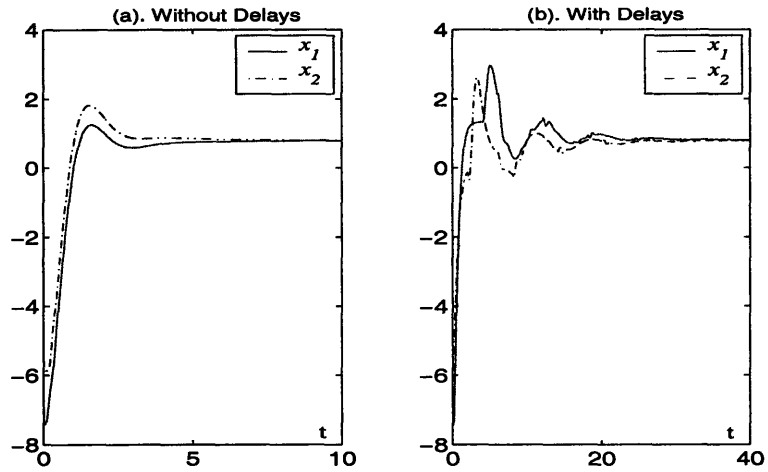

Figure 7-4: Simulation results of Example 7.1.2 with (a). $T_{12} = T_{21} = 0$ and with (b). $T_{12} = 2s$, $T_{21} = 4s$. The parameters are $b_1 = b_2 = 0.5$, $\omega_1^2 = \omega_2^2 = 5$, $k_{12} = k_{21} = 0.2$, and $F_e = 10$. Initial conditions, chosen randomly, are identical for the two plots. Convergence to a common equilibrium point independent to the time delays is achieved in both cases.

Finally note that even if the subsystems are not contracting but have upper bounded Jacobian, for instance, as limit-cycle oscillators, the overall system still can be contracting by choosing appropriate gains such that

$$\mathbf{G}_{21}\mathbf{G}_{21}^T > 2k_{21}(\frac{\partial \mathbf{f}_1}{\partial \mathbf{x}_1})_s \qquad \text{and} \qquad \mathbf{G}_{12}\mathbf{G}_{12}^T > 2k_{12}(\frac{\partial \mathbf{f}_2}{\partial \mathbf{x}_2})_s$$

Here the transmission of wave variables performs a stabilizing role.

There are also other simplified forms of wave variables. For instance, we can define the transmitted signals as

$$\begin{aligned} \mathbf{u}_{21} &= \mathbf{G}_{21}^T\mathbf{x}_1 + k_{21}\tau_{21} & \mathbf{v}_{12} &= k_{21}\tau_{21} \\ \mathbf{u}_{12} &= \mathbf{G}_{12}^T\mathbf{x}_2 + k_{12}\tau_{12} & \mathbf{v}_{21} &= k_{12}\tau_{12} \end{aligned}$$

If both $\mathbf{f}_1$ and $\mathbf{f}_2$ are contracting and time-invariant, and if $\mathbf{G}_{12} = \mathbf{G}_{21} = \mathbf{G}$ with $\mathbf{G}$ of full rank, the whole system tends towards a unique equilibrium point such that $\mathbf{x}_1(\infty) = -\mathbf{x}_2(\infty)$.

7.2 Group Cooperation with Time-Delayed Communications

Recently, synchronization or group agreement has been the object of extensive literature [12, 57, 73, 106, 117, 122, 133, 144, 146, 156]. Understanding natural aggregate motions as in bird flocks, fish schools, or animal herds may help achieve desired collective behaviors in artificial multi-agent systems. In our previous work [134, 164], a synchronization condition was obtained for a group of coupled nonlinear systems, where the number of the elements can be arbitrary and the network structure can be very general. In this section, we study a simplified continuous-time model of schooling or flocking with time-delayed communications, and generalize recent results in the literature [109, 98]. In particular, we show that synchronization is robust to time delays both for the leaderless case and for the leader-followers case, without requiring the delays to be known or equal in all links. Similar results are then derived for discrete-time models.

7.2.1 Leaderless Group

We first investigate a flocking model without group leader, whose non-time-delayed version has been studied in Section 5.2. The dynamics of the ith element is given as

$$\dot{\mathbf{x}}_i = \sum_{j \in \mathcal{N}_i} \mathbf{K}_{ji} (\mathbf{x}_j - \mathbf{x}_i) \qquad i = 1, \ldots, n \tag{7.5}$$

where $\mathbf{x}_i \in \mathbb{R}^m$ denotes the states needed to reach agreements such as a vehicle's heading, attitude, velocity, etc. $\mathcal{N}_i$ denotes the set of the active neighbors of element i, which for instance can be defined as the set of the nearest neighbors within a certain distance around i. $\mathbf{K}_{ji}$ is the coupling gain, which is assumed to be symmetric and positive definite.

Theorem 7.2 *Consider n coupled elements with linear protocol (7.5). The whole system will tend to reach a group agreement*

$$\mathbf{x}_1(t) = \cdots = \mathbf{x}_n(t) = \frac{1}{n}(\mathbf{x}_1(0) + \cdots + \mathbf{x}_n(0))$$

exponentially if the network is connected, and the coupling links are either bidirectional with $\mathbf{K}_{ji} = \mathbf{K}_{ij}$, or unidirectional but formed in closed rings with identical gains.

Theorem 7.2 can be proved by using partial contraction analysis. In Section 5.2, we illustrated the proof by studying switching networks ($\mathcal{N}_i = \mathcal{N}_i(t)$) with looser connectivity conditions. The result can be further extended to study time-varying couplings ($\mathbf{K}_{ji} = \mathbf{K}_{ji}(t)$),

Assume now that time delays are non-negligible in communications. The dynamics of the ith element then turns to be

$$\dot{\mathbf{x}}_i = \sum_{j \in \mathcal{N}_i} \mathbf{K}_{ji} \left(\mathbf{x}_j(t - T_{ji}) - \mathbf{x}_i(t) \right) \tag{7.6}$$

Theorem 7.3 *Consider n coupled elements (7.6) with time-delayed communications. Regardless of the explicit values of the delays, the whole system will tend to reach a group agreement $\mathbf{x}_1(t) = \cdots = \mathbf{x}_n(t)$ asymptotically if the network is connected, and the coupling links are either bidirectional with $\mathbf{K}_{ji} = \mathbf{K}_{ij}$, or unidirectional but formed in closed rings with identical gains.*

Proof: For notational simplicity, we first assume that all the links are bidirectional with $\mathbf{K}_{ji} = \mathbf{K}_{ij}$, but the time delays could be different along the opposite directions, i.e., $T_{ji} \neq T_{ij}$. Thus, Equation (7.6) can be transformed to

$$\dot{\mathbf{x}}_i = \sum_{j \in \mathcal{N}_i} \mathbf{G}_{ji} \tau_{ji}$$

where τ_{ji} and correspondingly τ_{ij} are defined as

$$\begin{aligned} \mathbf{u}_{ji} &= \mathbf{G}_{ji}^T \mathbf{x}_i + \tau_{ji} & \mathbf{v}_{ij} &= \mathbf{G}_{ji}^T \mathbf{x}_i \\ \mathbf{u}_{ij} &= \mathbf{G}_{ij}^T \mathbf{x}_j + \tau_{ij} & \mathbf{v}_{ji} &= \mathbf{G}_{ij}^T \mathbf{x}_j \end{aligned} \tag{7.7}$$

with $\mathbf{G}_{ij} = \mathbf{G}_{ji} > 0$ and $\mathbf{K}_{ji} = \mathbf{K}_{ij} = \mathbf{G}_{ij}\mathbf{G}_{ij}^T$. Define

$$V = \frac{1}{2} \sum_{i=1}^{n} \delta \mathbf{x}_i^T \delta \mathbf{x}_i + \frac{1}{2} \sum_{(i,j) \in \mathcal{N}} V_{i,j} \tag{7.8}$$

where $\mathcal{N} = \cup_{i=1}^{n} \mathcal{N}_i$ denotes the set of all active links, and $V_{i,j}$ is defined as in Section 7.1.2 for each link connecting two nodes i and j. Therefore

$$\dot{V} = -\frac{1}{2} \sum_{(i,j) \in \mathcal{N}} (\delta \tau_{ji}^T \delta \tau_{ji} + \delta \tau_{ij}^T \delta \tau_{ij})$$

One easily shows that $\ddot{V}$ is bounded. Thus according to Barbalat's lemma, $\dot{V}$ will tend to zero asymptotically, which implies that, $\forall (i,j) \in \mathcal{N}$, $\delta \tau_{ji}$ and $\delta \tau_{ij}$ tend to zero asymptotically. Thus, we know that $\forall i$, $\delta \dot{\mathbf{x}}_i$ tends to zero. In standard calculus, a vanishing $\delta \dot{\mathbf{x}}_i$ does not necessarily mean that $\delta \mathbf{x}_i$ is convergent. But it does in this case because otherwise it will conflict with the fact that $\delta \mathbf{x}_i$ tends to be periodic with a constant period $T_{ji} + T_{ij}$, which can be shown since

$$\begin{aligned} \delta \mathbf{u}_{ji}(t) &= \mathbf{G}_{ji}^T \delta \mathbf{x}_i(t) + \delta \tau_{ji}(t) = \mathbf{G}_{ij}^T \delta \mathbf{x}_j(t - T_{ji}) \\ \delta \mathbf{u}_{ij}(t) &= \mathbf{G}_{ij}^T \delta \mathbf{x}_j(t) + \delta \tau_{ij}(t) = \mathbf{G}_{ji}^T \delta \mathbf{x}_i(t - T_{ij}) \end{aligned} \tag{7.9}$$

From (7.9) we can also conclude that, if $\forall i$ $\delta \mathbf{x}_i$ is convergent, they will tend to a steady state

$$\delta \mathbf{x}_1(t) = \cdots = \delta \mathbf{x}_n(t) = \mathbf{c}$$

where $\mathbf{c}$ is a constant vector whose value dependents on the specific trajectories we analyze. Moreover, we notice that, in the state-space, any point inside the region $\mathbf{x}_1 = \cdots = \mathbf{x}_n$ is invariant to (7.6). By path integration, this implies immediately that, regardless of the delay values or the initial conditions, all solutions of the system (7.6) will tend to reach a group agreement $\mathbf{x}_1 = \cdots = \mathbf{x}_n$ asymptotically.

In case that coupling links are unidirectional but formed in closed rings with coupling gains identical in each ring, we set

$$\begin{aligned} V &= \frac{1}{2}\sum_{i=1}^{n} \delta \mathbf{x}_i^T \delta \mathbf{x}_i + \frac{1}{2}\sum_{(j\to i)\in\mathcal{N}} \left(\int_{t-T_{ji}}^{t} \delta \mathbf{v}_{ji}^T \delta \mathbf{v}_{ji} d\epsilon - \int_{-T_{ji}}^{0} \delta \mathbf{v}_{ji}^T \delta \mathbf{v}_{ji}\, d\epsilon \right) \\ &= \frac{1}{2}\sum_{i=1}^{n} \delta \mathbf{x}_i^T \delta \mathbf{x}_i + \frac{1}{2}\sum_{(j\to i)\in\mathcal{N}} \int_{0}^{t} \left(\delta \mathbf{v}_{ji}^T \delta \mathbf{v}_{ji}(\epsilon) - \delta \mathbf{v}_{ji}^T \delta \mathbf{v}_{ji}(\epsilon - T_{ji}) \right) d\epsilon \end{aligned}$$

and the rest of the proof is the same. The case when both types of links are involved is similar. □

Example 7.2.1: Compared to Theorem 7.2, the group agreement point in Theorem 7.3 generally does not equal the average value of the initial conditions, but depends on the values of the time delays.

Consider the cooperative group (7.6) with one-dimensional $\mathbf{x}_i$, $n = 6$, and a two-way chain structure

$$1 \longleftrightarrow 2 \longleftrightarrow 3 \longleftrightarrow 4 \longleftrightarrow 5 \longleftrightarrow 6$$

The coupling gains are set to be identical with value $k = 5$. The delay values are different, and each is chosen randomly around 0.5 second. Simulation results are plotted in Figure 7-5. □

Remarks

- The conditions on coupling gains can be relaxed. For instance, if the links are bidirectional, we do not have to ask $\mathbf{K}_{ij} = \mathbf{K}_{ji}$. Instead, the dynamics of the ith element could be

$$\dot{\mathbf{x}}_i = \mathbf{K}_i \sum_{j\in\mathcal{N}_i} \left(\mathbf{x}_j(t - T_{ji}) - \mathbf{x}_i(t) \right)$$

  where $\mathbf{K}_i = \frac{1}{k_i}\mathbf{G}\mathbf{G}^T$ and $\mathbf{G}$ is unique through the whole network. The proof is the same except that we incorporate k_i into the wave variables and the function V. Such a design brings more flexibility to cooperation-law design. The discrete-time model studied in Section 7.2.3 in in this spirit. A similar condition was derived in [19] for a swarm model in the no-delay case.

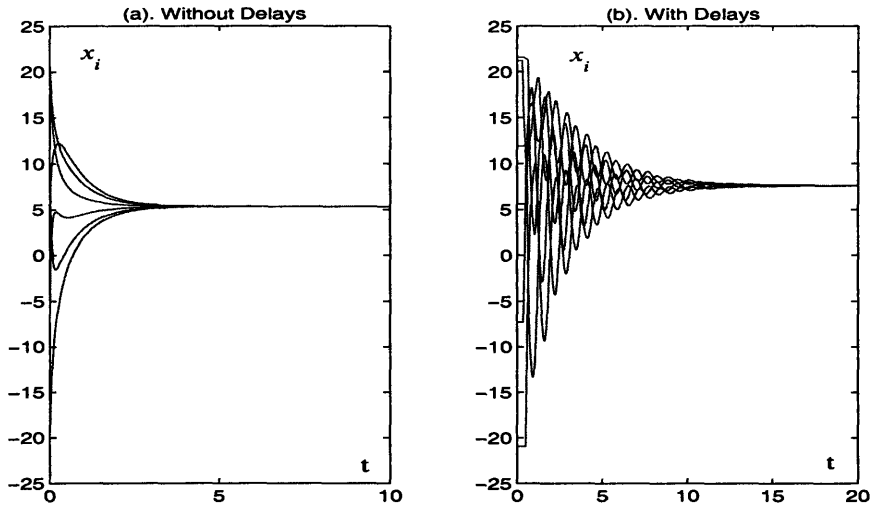

Figure 7-5: Simulation results of Example 7.2.1 without delays and with delays. Initial conditions, chosen randomly, are the same for each simulation. Group agreement is reached in both cases, although the agreement value is different.

- Model (7.5) with delayed communications was also studied in [109], but the result is limited by the assumptions that communication delays are equal in all links and that the self-response part in each coupling uses the same time-delay. Recently, [98] independently analyzed the system (7.6) in the scalar case with the same assumption that delays are equal in all links.

7.2.2 Leader-Followers Group

Similar analysis can be applied to study coupled networks with group leaders. Consider such a model

$$\dot{\mathbf{x}}_i = \sum_{j \in \mathcal{N}_i} \mathbf{K}_{ji} \left(\mathbf{x}_j(t - T_{ji}) - \mathbf{x}_i(t)\right) + \gamma_i \, \mathbf{K}_{0i} \left(\mathbf{x}_0 - \mathbf{x}_i\right) \qquad i = 1, \ldots, n \qquad (7.10)$$

where $\mathbf{x}_0$ is the state of the leader, which we first assume to be a constant. $\forall i$, $\mathbf{x}_i$ are the states of the followers; $\mathcal{N}_i$ indicate the neighborship among the followers, where time-delays are non-negligible in communications; $\gamma_i = 0$ or 1 represent the unidirectional links from the leader to the corresponding followers. For each non-zero γ_i, the coupling gain $\mathbf{K}_{0i}$ is positive definite.

Theorem 7.4 *Consider a leader-followers network (7.10) with time-delayed communications. Regardless of the explicit values of the delays, the whole system will tend to reach a group agreement*

$$\mathbf{x}_1(t) = \cdots = \mathbf{x}_n(t) = \mathbf{x}_0$$

asymptotically if the whole network is connected, and the coupling links among the followers are either bidirectional with $\mathbf{K}_{ji} = \mathbf{K}_{ij}$, *or unidirectional but formed in closed rings with identical gains.*

Proof: Exponential convergence of the leader-followers network (7.10) without delays has been shown in [134, 164] using contraction theory. If the communication delays are non-negligible, and assuming that all the links among the followers are bidirectional, we can transform the equation (7.10) to

$$\dot{\mathbf{x}}_i \;=\; \sum_{j\in\mathcal{N}_i} \mathbf{G}_{ji}\tau_{ji} + \gamma_i\, \mathbf{K}_{0i}\, (\mathbf{x}_0 - \mathbf{x}_i)$$

where τ_{ji} and correspondingly τ_{ij} are defined as the same as those in (7.7). Considering the same Lyapunov function V as (7.8), we get

$$\dot{V} \;=\; -\sum_{i=1}^{n} \gamma_i \delta\mathbf{x}_i^T \mathbf{K}_{0i} \delta\mathbf{x}_i \;-\; \frac{1}{2} \sum_{(i,j)\in\mathcal{N}} (\delta\tau_{ji}^T \delta\tau_{ji} + \delta\tau_{ij}^T \delta\tau_{ij})$$

where $\mathcal{N} = \cup_{i=1}^{n} \mathcal{N}_i$ denotes the set of all active links among the followers. Applying Barbalat's lemma shows that, $\dot{V}$ will tend to zero asymptotically. It implies that, $\forall i$ if $\gamma_i = 1$, $\delta\mathbf{x}_i$ will tend to zero, as well as $\delta\tau_{ji}$ and $\delta\tau_{ij}$ $\forall (i,j) \in \mathcal{N}$. Moreover, since

$$\delta\tau_{ji}(t) \;=\; \mathbf{G}_{ji}^T(\; \delta\mathbf{x}_j(t - T_{ji}) \;-\; \delta\mathbf{x}_i(t)\;)$$

we can conclude that, if the whole leader-followers network is connected, the virtual dynamics will converge to

$$\delta\mathbf{x}_1(t) = \cdots = \delta\mathbf{x}_n(t) = 0$$

regardless of the initial conditions or the delay values. In other words, the whole system is asymptotically contracting. All solutions will converge to a particular one, which in this case is the point $\mathbf{x}_1(t) = \cdots = \mathbf{x}_n(t) = \mathbf{x}_0$. The proof is similar if there are unidirectional links formed in closed rings. □

Example 7.2.2: Consider a leader-followers network (7.10) with one-dimensional $\mathbf{x}_i$, $n = 6$, and structured as

$$0 \longrightarrow 1 \longleftrightarrow 2 \longleftrightarrow 3 \longleftrightarrow 4 \longleftrightarrow 5 \longleftrightarrow 6$$

The state of the leader is constant with value $\mathbf{x}_0 = 10$. All the coupling gains are set to be identical with value $k = 5$. The delay values are not equal, each of which is chosen randomly around 0.5 second. Simulation results are plotted in Figure 7-6. □

Note that even if $\mathbf{x}_0$ is not a constant, i.e., the dynamics of the ith element is given as

$$\dot{\mathbf{x}}_i = \sum_{j\in\mathcal{N}_i} \mathbf{K}_{ji}\, (\mathbf{x}_j(t - T_{ji}) - \mathbf{x}_i(t)) + \gamma_i\, \mathbf{K}_{0i}\, (\mathbf{x}_0(t - T_{0i}) - \mathbf{x}_i(t))$$

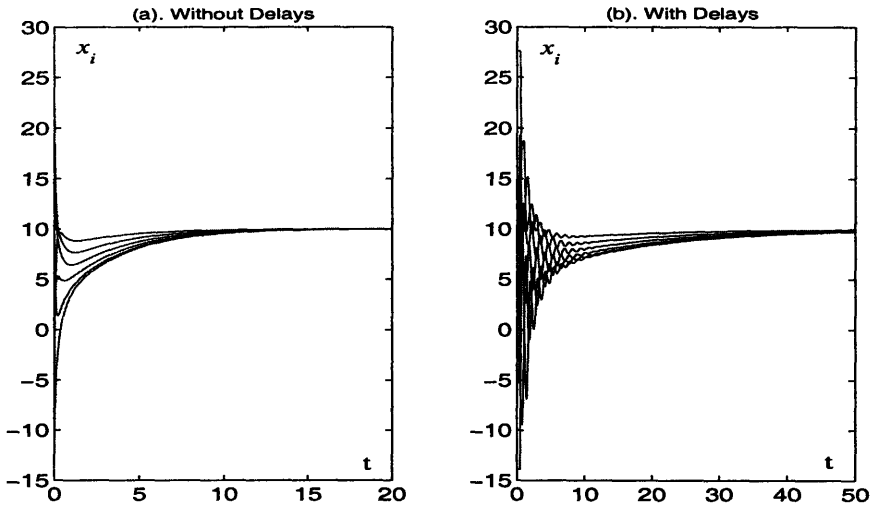

Figure 7-6: Simulation results of Example 7.2.2 without delays and with delays. Initial conditions, chosen randomly, are the same for each simulation. In both cases, group agreement to the leader value $\mathbf{x}_0$ is reached.

the whole system is still asymptotically contracting according to exactly the same proof. Regardless of the initial conditions, all solutions will converge to a particular one, which in this case depends on the dynamics of $\mathbf{x}_0$ and the explicit values of the delays. Moreover, if $\mathbf{x}_0$ is periodic, as one of the main properties of contraction [81], all the followers' state $\mathbf{x}_i$ will tend to be periodic with the same period as $\mathbf{x}_0$.

Example 7.2.3: Consider the leader-followers network in Example 7.2.2 again. We set everything the same except that the leader's states is not constant. Instead, we choose

$$\mathbf{x}_0 = 10 \ \sin(\frac{t}{2})$$

The whole system is still asymptotically contracting regardless of the delays. Simulation results are plotted in Figure 7-7. □

7.2.3 Discrete-Time Model

Simplified wave variables can also be applied to study time-delayed communications in discrete-time models. Consider the model of flocking or schooling studied in [57, 156], where each element's state is updated according to the discrete-time law that computes the average of its neighbors' states plus its own state, i.e.,

$$x_i(t+1) \ = \ \frac{1}{1+n_i} \ (\ x_i(t) \ + \ \sum_{j \in \mathcal{N}_i} x_j(t) \ ) \qquad\qquad i = 1, \ldots, n \qquad (7.11)$$

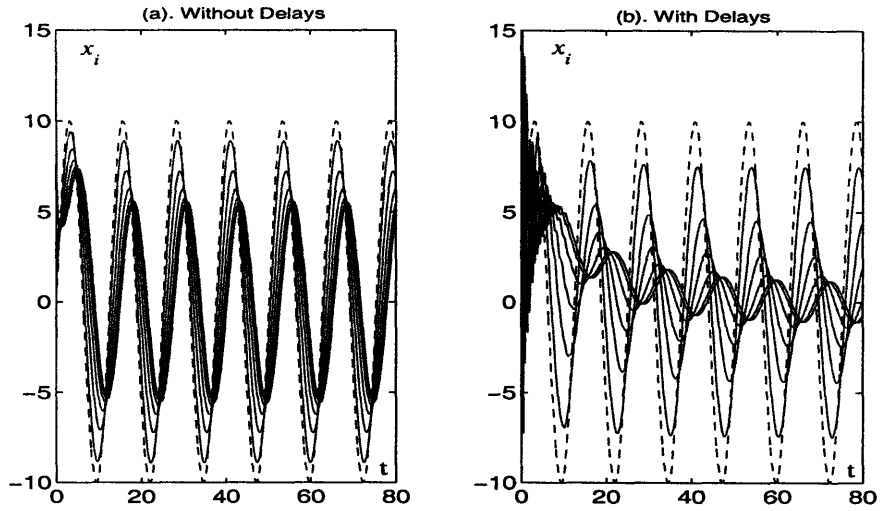

Figure 7-7: Simulation results of Example 7.2.3 without delays and with delays. In both plots, the dashed curve is the state of the leader while the solid ones are the states of the followers, which converge to a periodic solution in both cases regardless of the initial conditions.

or, in an equivalent form

$$x_i(t+1) \;=\; x_i(t) \;+\; \frac{1}{1+n_i} \sum_{j \in \mathcal{N}_i} \left(x_j(t) \;-\; x_i(t) \right)$$

In fact, in equation (7.11), there is no difference if x_i is a scalar or a vector. For notation simplicity we set x_i as a scalar, but our analysis can be extended directly to the vector case. In equation (7.11), t is the index of the updating steps, so that its value is always an integer. $\mathcal{N}_i$ denotes the set of the active neighbors of element i, which for instance can be defined as the set of the nearest neighbors within a certain distance r around i. n_i equals to the number of the neighbors of element i. As proved in [57], the whole system (7.11) will tend to reach a group agreement if the network is connected in a very loose sense.

Assume now that time delays are non-negligible in communications. The updating law of the ith element changes to

$$x_i(t+1) \;=\; x_i(t) \;+\; \frac{1}{1+n_i} \sum_{j \in \mathcal{N}_i} \left(x_j(t - T_{ji}) \;-\; x_i(t) \right) \qquad (7.12)$$

where the delay value T_{ji} is an integer based on the number of updating steps. As in previous sections, T_{ji} could be different for different communication links, or even different along opposite directions on the same link. For our later analysis, here we make a few assumptions: all elements update their states synchronously, and the time interval between any two updating steps is a constant; the network structure is fixed

and always connected, which implies that $\forall i$, n_i is a positive integer; the value of neighborship radius r is unique through the whole network, which leads to the fact that all interactions are bidirectional.

Theorem 7.5 *Consider n coupled elements (7.12) with time-delayed communications. Regardless of the explicit values of the delays, the whole system will tend to reach a group agreement $x_1(t) = \cdots = x_n(t)$ asymptotically.*

Proof: Equation (7.12) can be transformed to

$$x_i(t+1) \;=\; x_i(t) \;+\; \sum_{j\in\mathcal{N}_i} \tau_{ji}(t)$$

where the wave variables are defined as

$$u_{ji} = x_i \;+\; k_i\tau_{ji} \qquad\qquad v_{ij} = x_i$$

and $k_i = 1 + n_i$. Note that compared to (7.7), here we have $\mathbf{G}_{ij} = \mathbf{G}_{ji} = 1$. The cooperation law could be extended to a more general form otherwise. Define

$$V(t) \;=\; \sum_{i=1}^{n} k_i\delta x_i^2(t) \;+\; \sum_{(i,j)\in\mathcal{N}} V_{ij}(t)$$

where $\forall(i,j) \in \mathcal{N} = \cup_{i=1}^{n}\mathcal{N}_i$

$$V_{ij}(t) \;=\; \sum_{\epsilon=t-1-T_{ij}}^{t-1} \delta v_{ij}^2(\epsilon) \;+\; \sum_{\epsilon=t-1-T_{ji}}^{t-1} \delta v_{ji}^2(\epsilon) \;-\; \sum_{\epsilon=-T_{ij}}^{0} \delta v_{ij}^2(\epsilon) \;-\; \sum_{\epsilon=-T_{ji}}^{0} \delta v_{ji}^2(\epsilon)$$

and therefore

$$\begin{aligned} V_{ij}(t) \;&=\; \sum_{\epsilon=0}^{t-1}(\; \delta v_{ij}^2(\epsilon) \;-\; \delta u_{ji}^2(\epsilon) \;+\; \delta v_{ji}^2(\epsilon) \;-\; \delta u_{ij}^2(\epsilon)\;) \\ &=\; -\sum_{\epsilon=0}^{t-1}(\; 2k_i\delta x_i\delta\tau_{ji}(\epsilon) \;+\; k_i^2\delta\tau_{ji}^2(\epsilon) \;+\; 2k_j\delta x_j\delta\tau_{ij}(\epsilon) \;+\; k_j^2\delta\tau_{ij}^2(\epsilon)\;) \end{aligned}$$

Since

$$\begin{aligned} &\sum_{(i,j)\in\mathcal{N}} V_{ij}(t+1) \;-\; \sum_{(i,j)\in\mathcal{N}} V_{ij}(t) \\ =\; &-\sum_{(i,j)\in\mathcal{N}} (\; 2k_i\delta x_i\delta\tau_{ji}(t) \;+\; k_i^2\delta\tau_{ji}^2(t) \;+\; 2k_j\delta x_j\delta\tau_{ij}(t) \;+\; k_j^2\delta\tau_{ij}^2(t)\;) \\ =\; &-\sum_{i=1}^{n} (\; 2k_i \sum_{j\in\mathcal{N}_i} \delta x_i\delta\tau_{ji}(t) \;+\; k_i^2 \sum_{j\in\mathcal{N}_i} \delta\tau_{ji}^2(t)\;) \end{aligned}$$

one has

$$\begin{aligned} V(t+1) &= \sum_{i=1}^{n} k_i(\delta x_i(t) + \sum_{j\in\mathcal{N}_i} \delta\tau_{ji}(t))^2 + \sum_{(i,j)\in\mathcal{N}} V_{ij}(t+1) \\ &= V(t) + \sum_{i=1}^{n} k_i ((\sum_{j\in\mathcal{N}_i} \delta\tau_{ji}(t))^2 - k_i \sum_{j\in\mathcal{N}_i} \delta\tau_{ji}^2(t)) \end{aligned}$$

Note that

$$\begin{aligned} (\sum_{j\in\mathcal{N}_i} \delta\tau_{ji})^2 - k_i \sum_{j\in\mathcal{N}_i} \delta\tau_{ji}^2 &= \delta\Gamma_i^T \begin{bmatrix} 1 & \cdots & 1 \\ \vdots & \ddots & \vdots \\ 1 & \cdots & 1 \end{bmatrix} \delta\Gamma_i - k_i \delta\Gamma_i^T \delta\Gamma_i \\ &= \delta\Gamma_i^T \begin{bmatrix} -n_i & 1 & \cdots & 1 \\ 1 & -n_i & \cdots & 1 \\ \vdots & \vdots & \ddots & \vdots \\ 1 & 1 & \cdots & -n_i \end{bmatrix} \delta\Gamma_i \\ &\leq - \delta\Gamma_i^T \delta\Gamma_i = - \sum_{j\in\mathcal{N}_i} \delta\tau_{ji}^2 \end{aligned}$$

where $\delta\Gamma_i = [\cdots, \delta\tau_{ji}, \cdots]^T \in \mathbb{R}^{n_i}$. Thus, we conclude that

$$V(t+1) \leq V(t) - \sum_{i=1}^{n} k_i \sum_{j\in\mathcal{N}_i} \delta\tau_{ji}^2(t)$$

A lower bounded V guarantees that it converges, that is, $\forall(i,j) \in \mathcal{N}$, $\delta\tau_{ji}$ tends to zero as t tends to infinity. This implies that $\forall i$, δx_i converges. The rest of the proof is then similar to that of Theorem 7.3. □

Consider the discrete-time model of a cooperating group with a leader-followers structure, where the dynamics of the ith follower is given as

$$\begin{aligned} x_i(t+1) &= \frac{1}{1+n_i+\gamma_i} (x_i(t) + \sum_{j\in\mathcal{N}_i} x_j(t - T_{ji}) + \gamma_i x_0) \\ &= \frac{1+n_i}{1+n_i+\gamma_i} x_i(t) + \sum_{j\in\mathcal{N}_i} \tau_{ji}(t) + \frac{\gamma_i}{1+n_i+\gamma_i} x_0 \end{aligned}$$

and τ_{ji} is defined as the same as (7.2.3) with $k_i = 1+n_i+\gamma_i$ and $\gamma_i = 0$ or 1. One easily shows that a very similar analysis leads to the same result as that of Theorem 7.4.

7.3 Mutual Perturbation

In a large population, interacted groups may not communicate tightly. For instance, the signals between groups may not contain explicit state information, but only in-

formation on group synchronization. In this section, we construct such a model and investigate its dynamics behavior.

7.3.1 Synchronization of Coupled Nonlinear Systems

As the background, we first review our basic result on the analysis of coupled nonlinear systems [134, 164]. Consider a leaderless network with all links bidirectional. Given the dynamics of the ith element

$$\dot{\mathbf{x}}_i \;=\; \mathbf{f}(\mathbf{x}_i, t) + \sum_{j \in \mathcal{N}_i} \mathbf{K}_{ji}\,(\mathbf{x}_j - \mathbf{x}_i) \qquad i = 1, \ldots, n$$

the whole network will synchronize exponentially if

$$\lambda_{m+1}(\mathbf{L_K}) > \max_{i=1}^{n} \lambda_{max}(\frac{\partial \mathbf{f}}{\partial \mathbf{x}}(\mathbf{x}_i, t))_s \qquad \text{uniformly}$$

where m is the dimension of $\mathbf{x}_i$, and $\mathbf{L_K}$ denotes the weighted Laplacian matrix [40] with

$$\mathbf{L_K} \;=\; \mathbf{D}\,\mathbf{I}^{\tau}_{\mathbf{K}_{ij}}\,\mathbf{D}^T$$

Assuming the network has τ inner links, the $n \times \tau$ block matrix $\mathbf{D}$ is a generalized incidence matrix by replacing each number 1 or -1 in the incidence matrix [40] with identity matrix $\mathbf{I} \in \mathbb{R}^{m \times m}$ or $-\mathbf{I}$. Note that the incidence matrix is defined by assigning an arbitrary orientation to the undirected graph. $\mathbf{I}^{\tau}_{\mathbf{K}_{ij}}$ is a $\tau \times \tau$ block diagonal matrix with the k^{th} diagonal entry $\mathbf{K}_{ij}$ corresponding to the weight of the k^{th} link which connects the nodes i and j.

While the result (4.7) is based on partial contraction analysis, a very similar condition [167] can be derived by defining $\mathbf{x} = [\mathbf{x}_1^T, \ldots, \mathbf{x}_n^T]^T$ and

$$V \;=\; \frac{1}{2}\,\mathbf{x}^T \mathbf{L_K} \mathbf{x}$$

which leads to

$$\dot{V} \;=\; \mathbf{x}^T \mathbf{L_K}\,\Big(\begin{bmatrix} \mathbf{f}(\mathbf{x}_1,,t) \\ \cdots \\ \mathbf{f}(\mathbf{x}_n,,t) \end{bmatrix} - \mathbf{L_K}\mathbf{x}\Big) \;=\; \mathbf{x}^T\,(\,\mathbf{L_{K\Lambda}} - \mathbf{L}_{\mathbf{K}}^2\,)\,\mathbf{x}$$

with

$$\mathbf{L_{K\Lambda}} \;=\; \mathbf{D}\,\mathbf{I}^{\tau}_{(\mathbf{K}_{ij}\Lambda_{ij})_s}\,\mathbf{D}^T$$

Here $\mathbf{I}^{\tau}_{(\mathbf{K}_{ij}\Lambda_{ij})_s}$ is a $\tau \times \tau$ block diagonal matrix where the k^{th} diagonal entry is the symmetric part of $\mathbf{K}_{ij}\Lambda_{ij}$ and

$$\Lambda_{ij} = \int_0^1 \frac{\partial \mathbf{f}}{\partial \mathbf{x}}(\mathbf{x}_j + \chi(\mathbf{x}_i - \mathbf{x}_j), t)\; d\chi$$

corresponds to the k^{th} link. It can be shown that [167], if

$$\frac{\lambda_{m+1}^2(\mathbf{L_K})}{\lambda_n(\mathbf{L})} > \max_k \lambda_{max}(\mathbf{K}_{ij}\mathbf{\Lambda}_{ij})_s \tag{7.13}$$

$\dot{V}$ is negative semi-definite, which implies that all the states $\mathbf{x}_i$ will synchronize. Here $\mathbf{L}$ is the standard Laplacian matrix. Note that both synchronization conditions (4.7) and (7.13) need the network to be connected and the coupling strengths to be strong. Assuming $m = 1$ and all the coupling gains are identical with value κ, (4.7) turns to be $\kappa > \frac{1}{\lambda_2(\mathbf{L})} \max \frac{\partial \mathbf{f}}{\partial \mathbf{x}}(\mathbf{x}_i, t)$ while (7.13) represents a higher threshold $\kappa > \frac{\lambda_n(\mathbf{L})}{\lambda_2^2(\mathbf{L})} \max \frac{\partial \mathbf{f}}{\partial \mathbf{x}}(\mathbf{x}_i, t)$. Note that for the synchronization conditions to be true, $\frac{\partial \mathbf{f}}{\partial \mathbf{x}}(\mathbf{x}_i, t)$ needs to be upper bounded, which can be satisfied if the coupled systems are for instance oscillators.

7.3.2 Mutual Perturbation Between Synchronized Groups

Consider now two groups of coupled systems

$$\begin{aligned}
\dot{\mathbf{x}}_i &= \mathbf{f}(\mathbf{x}_i, t) + \sum_{j \in \mathcal{N}_i} \mathbf{K}_{ji} \, (\mathbf{x}_j - \mathbf{x}_i) \qquad i = 1, \ldots, n \\
\dot{\mathbf{y}}_i &= \mathbf{g}(\mathbf{y}_i, t) + \sum_{j \in \mathcal{M}_i} \mathbf{H}_{ji} \, (\mathbf{y}_j - \mathbf{y}_i) \qquad i = 1, \ldots, m
\end{aligned}$$

with possibly different dimensions in $\mathbf{x}_i$ and $\mathbf{y}_i$. Communications are allowed between the nodes in different groups, which transmits only information on group synchronization and may undergo time delays. As a simple example, assume $\mathbf{x}_1$ and $\mathbf{y}_1$ are the only pair of such inter-connected nodes, whose dynamics change to

$$\begin{aligned}
\dot{\mathbf{x}}_1 &= \mathbf{f}(\mathbf{x}_1, t) + \sum_{j \in \mathcal{N}_1} \mathbf{K}_{j1} \, (\mathbf{x}_j - \mathbf{x}_1) + \mathbf{G}_{yx}(\, \mathbf{G}_{xy}^T \mathbf{p}_y(t - T_{yx}) - \mathbf{G}_{yx}^T \mathbf{p}_x(t) \,) \\
\dot{\mathbf{y}}_1 &= \mathbf{g}(\mathbf{y}_1, t) + \sum_{j \in \mathcal{M}_1} \mathbf{H}_{j1} \, (\mathbf{y}_j - \mathbf{y}_1) + \mathbf{G}_{xy}(\, \mathbf{G}_{yx}^T \mathbf{p}_x(t - T_{xy}) - \mathbf{G}_{xy}^T \mathbf{p}_y(t) \,)
\end{aligned}$$

where $\mathbf{p}_x$, $\mathbf{p}_y$ represent synchronization error in each group, as seen from its node 1,

$$\begin{aligned}
\mathbf{p}_x &= \sum_{j \in \mathcal{N}_1} \mathbf{K}_{j1} \, (\mathbf{x}_j - \mathbf{x}_1) \\
\mathbf{p}_y &= \sum_{j \in \mathcal{M}_1} \mathbf{H}_{j1} \, (\mathbf{y}_j - \mathbf{y}_1)
\end{aligned}$$

Theorem 7.6 *Consider loosely-tied groups described above. Synchronization in each group is robust to mutual perturbation as well as to the time delays attached. However, a small disturbance in a single group may cause big uncertainty in the entire population and take a long time to finally settle down.*

Proof: Again, we use simplified wave-variables and define

$$V = \frac{1}{2}\mathbf{x}^T\mathbf{L_K}\mathbf{x} + \frac{1}{2}\mathbf{y}^T\mathbf{L_H}\mathbf{y} + \frac{1}{2}\left(\int_{t-T_{xy}}^{t} \mathbf{v}_{xy}^T\mathbf{v}_{xy}d\epsilon + \int_{t-T_{yx}}^{t} \mathbf{v}_{yx}^T\mathbf{v}_{yx}d\epsilon - \int_{-T_{xy}}^{0} \mathbf{v}_{xy}^T\mathbf{v}_{xy}d\epsilon - \int_{-T_{yx}}^{0} \mathbf{v}_{yx}^T\mathbf{v}_{yx}d\epsilon \right)$$

where $\mathbf{x} = [\mathbf{x}_1^T, \ldots, \mathbf{x}_n^T]^T$, $\mathbf{y} = [\mathbf{y}_1^T, \ldots, \mathbf{y}_m^T]^T$, $\mathbf{L_K}$ and $\mathbf{L_H}$ are the weighted Laplacian matrices in $\mathbf{x}$ and $\mathbf{y}$ groups, respectively, and the corresponding wave-variables are defined as the same as those in (7.7) except that here we use $\mathbf{p}_x$, $\mathbf{p}_y$ replace otherwise $\mathbf{x}_1$, $\mathbf{y}_1$. For instance,

$$\begin{aligned} \tau_{yx} &= \mathbf{G}_{xy}^T\mathbf{p}_y(t - T_{yx}) - \mathbf{G}_{yx}^T\mathbf{p}_x(t) \\ \tau_{xy} &= \mathbf{G}_{yx}^T\mathbf{p}_x(t - T_{xy}) - \mathbf{G}_{xy}^T\mathbf{p}_y(t) \end{aligned}$$

Therefore

$$\dot{V} = \mathbf{x}^T \left(\mathbf{L_{K\Lambda}} - \mathbf{L_K^2} \right) \mathbf{x} + \mathbf{y}^T \left(\mathbf{L_{H\Lambda}} - \mathbf{L_H^2} \right) \mathbf{y} - \frac{1}{2}\tau_{yx}^T\tau_{yx} - \frac{1}{2}\tau_{xy}^T\tau_{xy}$$

and it is negative semi-definite if both groups satisfy the synchronization condition (7.13). This implies that, synchronization ability in each group preserves after we add time-delayed mutual perturbation, which, however, makes the entire population easier to be disturbed and the transition period much longer. □

Note that the result can be extended directly to study more complex populations, which may contain multiple groups and more general inter-connections. Similar phenomena can be found e.g. in human psychology and macro-economics.

Chapter 8

A General Study of Time-Delayed Nonlinear Systems

In this chapter, we study nonlinear systems involving time delays in very general dynamics equations. The method is again based on contraction analysis. We show that, by satisfying some simple relations between time-delayed terms and non-delayed terms, contraction property can be preserved regardless of the explicit value or changing rate of the delays. Especially, if the system dynamics is autonomous, all solutions will converge to the same equilibrium point regardless of the delays. Such a property is very useful to reach performance robustness in a distributed working environment, for instance.

In Chapter 7, we developed contraction analysis methods for time-delayed communications using simplified wave-variables. Simplified wave-variables are very powerful to study diffusive communications, in a sense the effects of time-delays in different directions within the same communication channel are cancelled by each other. But they are difficult to be applied to study other kinds of delayed terms. Although not as strong as simplified wave-variables in analyzing diffusion couplings, the method developed here has no limitation on application areas.

8.1 Time-Delayed Continuous Systems

8.1.1 Time-Delayed Continuous Systems

Consider a nonlinear system whose dynamics at time t depends on the current state $\mathbf{x} = \mathbf{x}(t)$ and on the delayed state $\mathbf{x}_T = \mathbf{x}(t - T)$,

$$\dot{\mathbf{x}} = \mathbf{f}(\mathbf{x}, \mathbf{x}_T, t) \tag{8.1}$$

The delay $T \geq 0$ can be *time-varying*, although we assume that the time-ordering of the data is preserved in the transmission, i.e., that

$$\dot{T} < 1$$

Since the virtual dynamics is

$$\delta\dot{\mathbf{x}} \;=\; \mathbf{J}(t)\;\delta\mathbf{x} \;+\; \mathbf{B}(t)\;\delta\mathbf{x}_T$$

where

$$\mathbf{J}(t) \;=\; \frac{\partial \mathbf{f}}{\partial \mathbf{x}} \qquad\qquad \mathbf{B}(t) \;=\; \frac{\partial \mathbf{f}}{\partial \mathbf{x}_T} \tag{8.2}$$

consider the differential length

$$V \;=\; \frac{1}{2}\,\delta\mathbf{x}^T\delta\mathbf{x} \;+\; k\int_{t-T}^{t} \delta\mathbf{x}^T\delta\mathbf{x}(\epsilon)\;d\epsilon$$

with k a positive constant, yielding

$$\begin{aligned}
\dot{V} \;&=\; \delta\mathbf{x}^T\delta\dot{\mathbf{x}} \;+\; k\;(\;\delta\mathbf{x}^T\delta\mathbf{x} \;-\; (1-\dot{T})\;\delta\mathbf{x}_T^T\delta\mathbf{x}_T\;) \\
&=\; \delta\mathbf{x}^T(\;\mathbf{J}+k\mathbf{I}\;)\delta\mathbf{x} + \delta\mathbf{x}^T\;\mathbf{B}\;\delta\mathbf{x}_T \;-\; k(1-\dot{T})\;\delta\mathbf{x}_T^T\delta\mathbf{x}_T \\
&=\; \delta\mathbf{y}^T(t)\begin{bmatrix} \mathbf{J}+k\mathbf{I} & \mathbf{B} \\ \mathbf{0} & -k(1-\dot{T})\mathbf{I} \end{bmatrix}\delta\mathbf{y}(t)
\end{aligned}$$

with $\delta\mathbf{y}^T \;=\; [\delta\mathbf{x}^T, \delta\mathbf{x}_T^T]$. Thus, $\dot{V} \leq 0$ if

$$\begin{bmatrix} \mathbf{J}+k\mathbf{I} & \mathbf{B} \\ \mathbf{0} & -k(1-\dot{T})\mathbf{I} \end{bmatrix} \;<\; 0 \tag{8.3}$$

In the sequel, we shall assume that $\ddot{V}$ is bounded as a a consequence of the boundedness of V for the systems of interest. Then, Barbalat's lemma [131] shows that (8.3) implies that $\dot{V}$ tends to zero asymptotically, and hence that $\delta\mathbf{x}(t)$ tends to zero, i.e., that the system (8.1) is asymptotically contracting regardless of the explicit value of T. This result may be considered as a generalization of the stability analysis of linear switching systems in [179, 180].

Theorem 8.1 *A nonlinear time-delayed continuous system (8.1) is asymptotically contracting if*

$$\sigma_{max}(\mathbf{B}) \;<\; -\;\lambda_{max}(\mathbf{J}_s)\;\sqrt{1-\dot{T}} \tag{8.4}$$

where $\mathbf{J}_s$ *is the symmetric part of* $\frac{\partial \mathbf{f}}{\partial \mathbf{x}}$, $\lambda_{max}(\mathbf{J}_s)$ *is the largest eigenvalue of* $\mathbf{J}_s$ *and* $\sigma_{max}(\mathbf{B})$ *is a constant upper bound on the largest singular value of* $\mathbf{B}$.

Proof: Contraction condition (8.3) can be written

$$\begin{bmatrix} \mathbf{J}_s+k\mathbf{I} & \frac{1}{2}\mathbf{B} \\ \frac{1}{2}\mathbf{B}^T & -k(1-\dot{T})\mathbf{I} \end{bmatrix} \;<\; 0$$

Since k is positive, a necessary and sufficient condition for the above inequality to be true is [51]

$$\mathbf{J}_s + k\mathbf{I} \;<\; \frac{1}{4}\;\mathbf{B}(\;-k(1-\dot{T})\mathbf{I}\;)^{-1}\mathbf{B}^T$$

Thus, a sufficient condition is

$$-\lambda_{max}(\mathbf{J}_s) > k + \frac{1}{4k(1-\dot{T})}\sigma^2_{max}(\mathbf{B})$$

The value k which minimizes the right-hand side of the above inequality is

$$k = \frac{1}{2\sqrt{1-\dot{T}}}\sigma_{max}(\mathbf{B})$$

yielding (8.4). □

Theorem 8.1 guarantees that asymptotic contraction is preserved by arbitrarily time-delayed feedback as long as the control gain is limited by the system's contraction rate. Note the Doppler-like time in $\dot{T}$.

Example 8.1.1: Consider a system with time-delayed feedback

$$\dot{\mathbf{x}} = \mathbf{f}(\mathbf{x},t) + \mathbf{u}(\mathbf{x}_T,t)$$

where $\mathbf{u}(\mathbf{x}_T,t)$ is a term containing the control input and based on time-delayed feedback. One thus has the contraction condition

$$\sigma_{max}(\frac{\partial \mathbf{u}}{\partial \mathbf{x}_T}) < -\frac{1}{2}\lambda_{max}(\frac{\partial \mathbf{f}}{\partial \mathbf{x}} + \frac{\partial \mathbf{f}}{\partial \mathbf{x}}^T)\sqrt{1-\dot{T}}$$

Since an autonomous contracting system contains a globally stable equilibrium point [81, 133], we now know that, the stability property of this equilibrium point is independent to the value of time delay if the condition above is satisfied. □

Example 8.1.2: The property that an equilibrium point could be stable independent to the value of the time delay may help to realize robust performance in parallel computation or distributed computation. For instance, to implement [133]

$$\dot{\mathbf{x}} = -\text{grad}(V(\mathbf{x}))$$

we can let part of the task computed parellelly. If time delay is significant, we have

$$\dot{\mathbf{x}} = -\text{grad}(V_1(\mathbf{x})) - \text{grad}(V_2(\mathbf{x}_T))$$

Regardless of the time delay, the whole computation will always converge to a unique steady state if

$$\sigma_{max}(\frac{\partial^2 V_2}{\partial \mathbf{x}_T^2}) < -\lambda_{min}(\frac{\partial^2 V_1}{\partial \mathbf{x}^2} + \frac{\partial^2 V_1}{\partial \mathbf{x}^2}^T)\sqrt{1-\dot{T}}$$

The task can be further separated according to the extension result derived below. □

8.1.2 Two Extensions

The result can be extended to nonlinear systems with multiple time delays,

$$\dot{\mathbf{x}} = \mathbf{f}(\mathbf{x}, \mathbf{x}_{T_1}, \ldots, \mathbf{x}_{T_l}, t) \tag{8.5}$$

where $\mathbf{x}_{T_i} = \mathbf{x}(t - T_i)$. The virtual dynamics is now

$$\delta\dot{\mathbf{x}} \;=\; \mathbf{J}(t)\;\delta\mathbf{x} \;+\; \sum_{i=1}^{l} \mathbf{B}_i(t)\;\delta\mathbf{x}_{T_i}$$

where

$$\mathbf{B}_i(t) \;=\; \frac{\partial \mathbf{f}}{\partial \mathbf{x}_{T_i}}$$

Define

$$V \;=\; \frac{1}{2}\,\delta\mathbf{x}^T\delta\mathbf{x}(t) \;+\; \sum_{i=1}^{l} k_i \int_{t-T_i}^{t} \delta\mathbf{x}^T\delta\mathbf{x}\; d\epsilon$$

where the k_i are positive constants, yielding

$$\begin{aligned}\dot{V} \;&=\; \delta\mathbf{x}^T\delta\dot{\mathbf{x}}(t) \;+\; \sum_{i=1}^{l} k_i\;(\;\delta\mathbf{x}^T\delta\mathbf{x}(t) \;-\; (1-\dot{T}_i)\delta\mathbf{x}^T\delta\mathbf{x}(t-T_i)\;) \\ &=\; \delta\mathbf{y}^T \begin{bmatrix} \mathbf{J}(t) + \sum_i k_i\mathbf{I} & \mathbf{B}_1(t) & \cdots & \mathbf{B}_l(t) \\ \mathbf{0} & -k_1(1-\dot{T}_1)\mathbf{I} & \cdots & \mathbf{0} \\ \cdots & \cdots & \cdots & \cdots \\ \mathbf{0} & \mathbf{0} & \cdots & -k_l(1-\dot{T}_l)\mathbf{I} \end{bmatrix} \delta\mathbf{y}\end{aligned}$$

with $\delta\mathbf{y}^T \;=\; [\delta\mathbf{x}^T(t), \delta\mathbf{x}^T(t-T_1), \ldots, \delta\mathbf{x}^T(t-T_l)]$. Similarly, if $\dot{V} < 0$ and $\ddot{V}$ is bounded, $\dot{V}$ will tend to zero asymptotically, which implies that the overall system is asymptotically contracting regardless of the explicit values of the T_i's.

Proposition 1 *A nonlinear system with multiple time delays (8.5) is asymptotically contracting if*

$$\sum_i \frac{\sigma_{max}(\mathbf{B}_i)}{\sqrt{1-\dot{T}_i}} \;<\; -\,\lambda_{max}(\mathbf{J}_s) \quad \text{uniformly}$$

where the notations are the same as in Theorem 8.1,

Proof: For notation simplicity, we set $\forall i\ \dot{T}_i = 0$. (The proof is the same if $\dot{T}_i \neq 0$.) Assume that $\lambda_{max}(\mathbf{J}_s) \;\leq\; -\sum_i \sigma_{max}(\mathbf{B}_i) - \delta$ with $\delta > 0$ a constant. This implies

$$\mathbf{J}_s \;<\; (-\sum_i \sigma_{max}(\mathbf{B}_i) - \delta)\;\mathbf{I}$$

Letting $k_i = \frac{1}{2}\sigma_{max}(\mathbf{B}_i)$ in (8.1.2), we have

$$\dot{V} \;\leq\; \delta\mathbf{y}^T \begin{bmatrix} -(\delta + \frac{1}{2}\sum_i \sigma_{max}(\mathbf{B}_i))\mathbf{I} & \frac{1}{2}\mathbf{B}_1 & \cdots & \frac{1}{2}\mathbf{B}_l \\ \frac{1}{2}\mathbf{B}_1^T & -\frac{1}{2}\sigma_{max}(\mathbf{B}_1)\mathbf{I} & \cdots & \mathbf{0} \\ \cdots & \cdots & \cdots & \cdots \\ \frac{1}{2}\mathbf{B}_l^T & \mathbf{0} & \cdots & -\frac{1}{2}\sigma_{max}(\mathbf{B}_l)\mathbf{I} \end{bmatrix} \delta\mathbf{y} \;\leq\; 0$$

Indeed, the matrix above is a sum of symmetric negative semi-definite matrices, since for each i

$$\begin{bmatrix} -(\frac{1}{2}\sigma_{max}(\mathbf{B}_i) + \frac{\delta}{l})\mathbf{I} & \frac{1}{2}\mathbf{B}_i \\ \frac{1}{2}\mathbf{B}_i^T & -\frac{1}{2}\sigma_{max}(\mathbf{B}_i)\mathbf{I} \end{bmatrix} < 0 \qquad \square$$

In fact, Proposition 1 can be considered as a generalization of the feedback combination of contracting systems [164].

Example 8.1.3: Consider coupled two systems with time-delayed feedback

$$\begin{cases} \dot{\mathbf{x}}_1 &= \mathbf{f}_1(\mathbf{x}_1, t) + \mathbf{u}_2(\mathbf{x}_{2T_2}, t) \\ \dot{\mathbf{x}}_2 &= \mathbf{f}_2(\mathbf{x}_2, t) + \mathbf{u}_1(\mathbf{x}_{1T_1}, t) \end{cases}$$

where $\mathbf{x}_{iT_i} = \mathbf{x}_i(t - T_i)$, $i = 1, 2$. According Proposition 1, the contraction condition is thus

$$\sum_{i=1,2} \frac{1}{\sqrt{1 - \dot{T}_i}} \sigma_{max}(\frac{\partial \mathbf{u}_i}{\partial \mathbf{x}_{iT_i}}) < - \max_{i=1,2} \lambda_{max}(\frac{\partial \mathbf{f}_i}{\partial \mathbf{x}_i} + \frac{\partial \mathbf{f}_i}{\partial \mathbf{x}_i}^T)$$

Note that here $\mathbf{B}_1 = \begin{bmatrix} \mathbf{0} & \mathbf{0} \\ \frac{\partial \mathbf{u}_1}{\partial \mathbf{x}_{1T_1}} & \mathbf{0} \end{bmatrix}$ and similar is $\mathbf{B}_2$.

Readers can compare this result with those in our recent paper [168], where our analysis is also based on Contraction Theory, but using a different methodology which we call *simplified wave-variables*. Simplified wave-variables are very powerful to study diffusive communications, in a sense the effects of time-delays in different directions within the same communication channel are cancelled by each other. The contraction property of two (or more) coupled subsystems are always preserved regardless of the coupling gains or time delays. The result derived in this paper is weaker in diffusion case, but more general since there is no limitation on the types of the couplings. $\square$

The proposition below extends the result to the model where the open loop system is contracting in a general metric.

Proposition 2 *In system (8.5), if the open-loop function* $\mathbf{f}$ *is contracting with metric* $\mathbf{\Theta}^T\mathbf{\Theta}$*, contraction is preserved for the overall system if*

$$\sum_i \frac{\sigma_{max}(\mathbf{B}_i)}{\sqrt{1 - \dot{T}_i}} < - \lambda_{max}(\mathbf{F}_s) \quad \text{uniformly}$$

where $\mathbf{F}$ *is the generalized Jacobian defined in (2.3) and* $\mathbf{B}_i$ *is re-defined in the proof below.*

Proof: Given a coordinate transformation (2.2), the virtual dynamics is now

$$\delta\dot{\mathbf{z}} = \mathbf{F}(t)\ \delta\mathbf{z} + \sum_{i=1}^{l} \mathbf{B}_i(t)\ \delta\mathbf{z}_{T_i}$$

where $\mathbf{F}$ is generalized Jacobian defined in (2.3) and

$$\mathbf{B}_i(t) = \mathbf{\Theta}(t) \frac{\partial \mathbf{f}}{\partial \mathbf{x}_{T_i}} \mathbf{\Theta}^{-1}(t - T_i)$$

Define

$$V \;=\; \frac{1}{2}\,\delta\mathbf{z}^T\delta\mathbf{z}(t) \;+\; \sum_i k_i \int_{t-T_i}^{t} \delta\mathbf{z}^T\delta\mathbf{z}\; d\epsilon$$

yielding

$$\dot{V} \;=\; \delta\mathbf{y}^T \begin{bmatrix} \mathbf{F}(t)+\sum_i k_i\mathbf{I} & \mathbf{B}_1(t) & \cdots & \mathbf{B}_l(t) \\ \mathbf{0} & -k_1(1-\dot{T}_1)\mathbf{I} & \cdots & \mathbf{0} \\ \cdots & \cdots & \cdots & \cdots \\ \mathbf{0} & \mathbf{0} & \cdots & -k_l(1-\dot{T}_l)\mathbf{I} \end{bmatrix} \delta\mathbf{y}$$

with $\delta\mathbf{y}^T = [\delta\mathbf{z}^T(t), \delta\mathbf{z}^T(t-T_1), \ldots, \delta\mathbf{z}^T(t-T_l)]$. The rest of the proof is the same as that for Proposition 1. □

8.2 Time-Delayed Discrete-Time Systems

Consider a nonlinear discrete-time system with part of its dynamics relying on a delayed state

$$\mathbf{x}(t+1) \;=\; \mathbf{f}(\mathbf{x}, \mathbf{x}_T, t) \tag{8.6}$$

where $\mathbf{x} = \mathbf{x}(t)$, $\mathbf{x}_T = \mathbf{x}(t-T)$, and T is a constant integer. The virtual dynamics is then

$$\delta\mathbf{x}(t+1) \;=\; \mathbf{J}(t)\;\delta\mathbf{x} \;+\; \mathbf{B}(t)\;\delta\mathbf{x}_T$$

where $\mathbf{J}$ and $\mathbf{B}$ are defined as in (8.2). Now consider the differential length

$$V(t) \;=\; \delta\mathbf{x}^T\delta\mathbf{x}(t) \;+\; k\sum_{\epsilon=t-T}^{t-1} \delta\mathbf{x}^T\delta\mathbf{x}(\epsilon)$$

with k a positive constant, yielding

$$V(t+1) - V(t) \;=\; \delta\mathbf{y}^T(t) \begin{bmatrix} \mathbf{J}^T\mathbf{J}(t) + k\mathbf{I} - \mathbf{I} & \mathbf{J}^T\mathbf{B}(t) \\ \mathbf{B}^T\mathbf{J}(t) & \mathbf{B}^T\mathbf{B}(t) - k\mathbf{I} \end{bmatrix} \delta\mathbf{y}(t) \tag{8.7}$$

where $\delta\mathbf{y}^T = [\delta\mathbf{x}^T, \delta\mathbf{x}_T^T]$. Thus, if uniformly

$$\begin{bmatrix} \mathbf{J}^T\mathbf{J}(t) + k\mathbf{I} - \mathbf{I} & \mathbf{J}^T\mathbf{B}(t) \\ \mathbf{B}^T\mathbf{J}(t) & \mathbf{B}^T\mathbf{B}(t) - k\mathbf{I} \end{bmatrix} \;<\; 0 \tag{8.8}$$

$V(t)$ will converge to a limit asymptotically, which implies that $V(t+1) - V(t)$ tends to zero. From (8.7) this implies that $\delta\mathbf{x}$ tends to zero, i.e., that the system (8.6) is asymptotically contracting regardless of the explicit value of T.

Theorem 8.2 *A nonlinear time-delayed discrete-time system (8.6) is asymptotically contracting if*

$$\sigma_{max}(\mathbf{J}) \;+\; \sigma_{max}(\mathbf{B}) \;<\; 1 \tag{8.9}$$

where $\sigma_{max}(\mathbf{J})$ *and* $\sigma_{max}(\mathbf{B})$ *are constant upper bounds on the largest singular value of* $\mathbf{J}$ *and* $\mathbf{B}$*, respectively.*

Proof: For condition (8.8) to be true, we need

$$\mathbf{B}^T\mathbf{B} \;<\; k\mathbf{I} \tag{8.10}$$

$$\mathbf{J}^T\mathbf{J} - (1-k)\mathbf{I} \;<\; \mathbf{J}^T\mathbf{B}\,(\mathbf{B}^T\mathbf{B} - k\mathbf{I})^{-1}\,\mathbf{B}^T\mathbf{J} \tag{8.11}$$

Assuming $k = a\sigma^2_{max}(\mathbf{B})$ and $a > 1$, (8.10) is verified. One then has

$$\mathbf{B}^T\mathbf{B} - k\mathbf{I} \;<\; -(a-1)\sigma^2_{max}(\mathbf{B})\mathbf{I} \;<\; 0$$

Therefore

$$(\mathbf{B}^T\mathbf{B} - k\mathbf{I})^{-1} \;>\; -\frac{1}{(a-1)\sigma^2_{max}(\mathbf{B})}\mathbf{I}$$

and

$$\mathbf{J}^T\mathbf{B}\,(\mathbf{B}^T\mathbf{B} - k\mathbf{I})^{-1}\,\mathbf{B}^T\mathbf{J} \;>\; -\frac{1}{(a-1)\sigma^2_{max}(\mathbf{B})}\,\mathbf{J}^T\mathbf{B}\mathbf{B}^T\mathbf{J} \;>\; -\frac{1}{a-1}\,\mathbf{J}^T\mathbf{J}$$

Thus, (8.11) will be satisfied if

$$\mathbf{J}^T\mathbf{J} - (1 - a\;\sigma^2_{max}(\mathbf{B}))\mathbf{I} \;<\; -\frac{1}{a-1}\,\mathbf{J}^T\mathbf{J}$$

that is, if

$$\frac{a}{a-1}\,\mathbf{J}^T\mathbf{J} \;+\; a\;\sigma^2_{max}(\mathbf{B})\mathbf{I} \;<\; \mathbf{I}$$

or, more sufficiently, if

$$\frac{a}{a-1}\,\sigma^2_{max}(\mathbf{J}) \;+\; a\;\sigma^2_{max}(\mathbf{B}) \;<\; 1$$

The value a which minimizes the right-hand side of the above inequality is

$$a \;=\; \frac{\sigma_{max}(\mathbf{J})}{\sigma_{max}(\mathbf{B})} \;+\; 1$$

which then yields (8.9). □

Similar extensions as those in Section 8.1.2 can be made on discrete-time systems, too.

Chapter 9

Fast Computation With Neural Oscillators

Recent research has explored the notion that artificial spike-based computation, inspired by models of computations in the central nervous system, may present significant advantages for specific types of large scale problems [14, 29, 38, 44, 50, 56, 59, 61, 72, 77, 87, 129, 148, 149, 160, 163]. This intuition is motivated in part by the fact that while neurons in the brain are enormously "slower" than silicon based elements (about six orders of magnitude in both elementary computation time and signal transmission speed), their performance in networks often compares very favorably with their artificial counterparts even when reaction speed is concerned. In a sense, evolution may have been forced to develop extremely efficient computational schemes given available hardware limitations.

In this chapter, we study new models for two common instances of such computation, winner-take-all (and k-winner-take-all) and coincidence detection. In both cases, very fast convergence is achieved and network complexity is linear in the number of inputs. Fully distributed structures are further derived by replacing the single global neuron with a group of interneurons synchronized by fast diffusion mechanisms. Such mechanisms could be provided by electrical synapses, which are ubiquitous in the brain [11, 27, 23, 39], for instance in the form of gap junction-mediated connections.

We first present a simple network of FitzHugh-Nagumo (FN) neurons for winner-take-all computation, as well as for k-winner-take-all and soft-winner-take-all. In contrast to most existing studies, the network's initial state can be arbitrary, and its convergence is guaranteed in at most two spiking periods, making it particularly suitable to track time-varying inputs. If several neurons receive the same largest input, they all spike as a group.

Using a very similar architecture, but replacing global inhibition by global excitation, we obtain an FN network for fast coincidence detection, in a spirit similar to [14, 50]. Again the system's response is practically immediate, regardless of the number of inputs.

9.1 The FitzHugh-Nagumo Model

As we have introduced, the FitzHugh-Nagumo(FN) model [36, 100] is a well-known simplified version of the classical Hodgkin-Huxley model [49], the first mathematical model of wave propagation in squid nerve. Originally derived from the Van der Pol oscillator [131, 141], it can be generalized using a linear state transformation to the dimensionless system [99]

$$\begin{cases} \dot{v} = v(\alpha - v)(v - 1) - w + I \\ \dot{w} = \beta v - \gamma w \end{cases} \tag{9.1}$$

where α, β, γ are positive constants, v models membrane potential, w accommodation and refractoriness, and I stimulating current.

Simple properties of the FN model can be exploited for neural computations. For appropriate parameter choices, there exists a unique equilibrium point for any given value of I, which is stable except for a finite range $I_l \leq I \leq I_h$ where the system tends to a limit cycle. The steady-state value of v at the stable equilibrium point increases with I. Moreover, the FN model inherits Hodgkin-Huxley's excitability feature, in that a small perturbation from the equilibrium point may cause a large excursion to return. We can see this clearly in Figure 9-1(a), where the cubic curves are the null clines corresponding to $\dot{v} = 0$, and the straight lines corresponding to $\dot{w} = 0$. A small perturbation (point A) from the equilibrium point (point B) causes a large excursion to return.

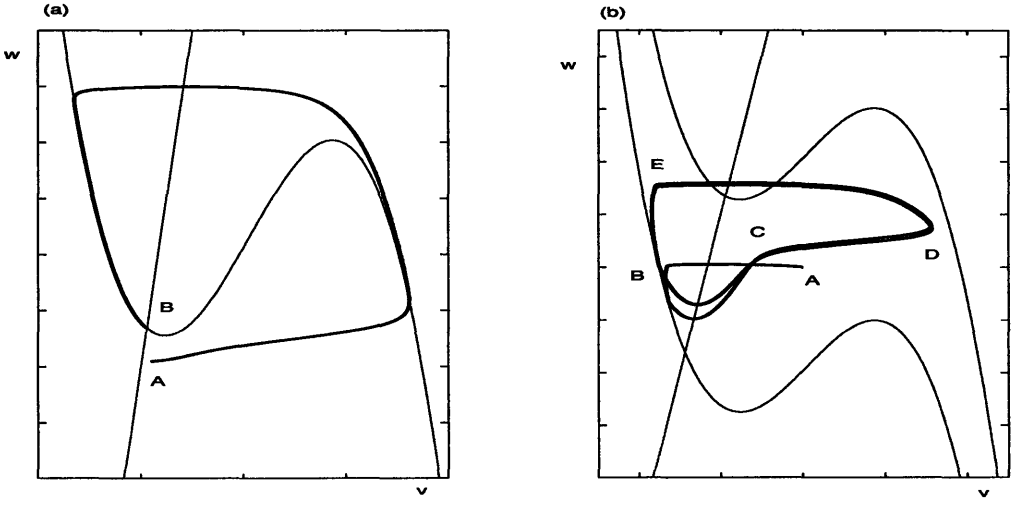

Figure 9-1: The FN model (9.1) in the state space. (a) Illustration of the excitability feature; (b) illustration of the WTA computation.

9.2 Winner-Take-All Network

Winner-take-all (WTA) networks, which pick the largest element from a collection of inputs, are ubiquitous in models of neural computation, and have been used extensively in the contexts of competitive learning, pattern recognition, selective visual attention, and decision making [4, 1, 31, 32, 45, 46, 55, 161, 184]. Furthermore, Maass [85, 86] showed that WTA represents a powerful computational primitive as compared to standard neural network models based on threshold or sigmoidal gates.

The architectures of most existing WTA models are based on inhibitory interactive networks, implemented either by a global inhibitory unit or by mutual inhibitory connections. Many studies, such as [33, 183], require the system dynamics to be initiated from a particular state, which may be unrealistic biologically and also prevents effective tracking of time-varying inputs. Starting with [72], many WTA implementations in analog VLSI circuits have been proposed. While they do guarantee a unique global minimum, dynamic analysis is difficult and computation resolution limited. Studies of spike-based WTA computation, as in [59], are comparatively recent. In this section, we describe a very simple network of FN neurons for fast winner-take-all computation, whose complexity is linear in the number of inputs. The network's initial state can be arbitrary, and its convergence is guaranteed in at most two spiking periods, making it particularly suitable to track time-varying inputs. If several neurons receive the same largest input, they all spike as a group of winners.

9.2.1 Basic structure

The basic network consists of n FN neurons. Each neuron receives a stimulating input I_i and a common inhibition current z from a global inhibitory neuron (Figure 9-2). The dynamics of the FN neurons ($i = 1, \ldots, n$) are

$$\begin{cases} \dot{v}_i = v_i(\alpha - v_i)(v_i - 1) - w_i + I_i - z \\ \dot{w}_i = \beta v_i - \gamma w_i \end{cases}$$

Note that the coupling term z can be replaced by a more general form, for instance, a nonlinear function of z.

The global inhibition neuron receives synaptic inputs from the FN neurons. It spikes whenever any FN neuron spikes, after which it slowly converges to a rest steady state. The specific dynamics of the global neuron can be very general. As an example, we assume that it is composed of a charging mode and a discharging mode. Specifically, charging starts if there is any FN neuron spiking in the network, i.e. when v_i exceeds a given threshold value v_0. It switches to discharging if the state is saturated (close to the saturation value in simulation) and stays in this mode until a FN neuron spikes next. For simplicity, we define

$$\dot{z} = \begin{cases} -k_c\ (z - z_0) & \text{charging mode} \\ -k_d\ z & \text{discharging mode} \end{cases} \tag{9.2}$$

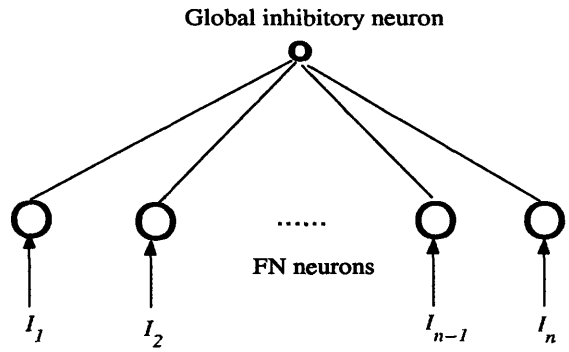

Figure 9-2: Basic WTA network structure

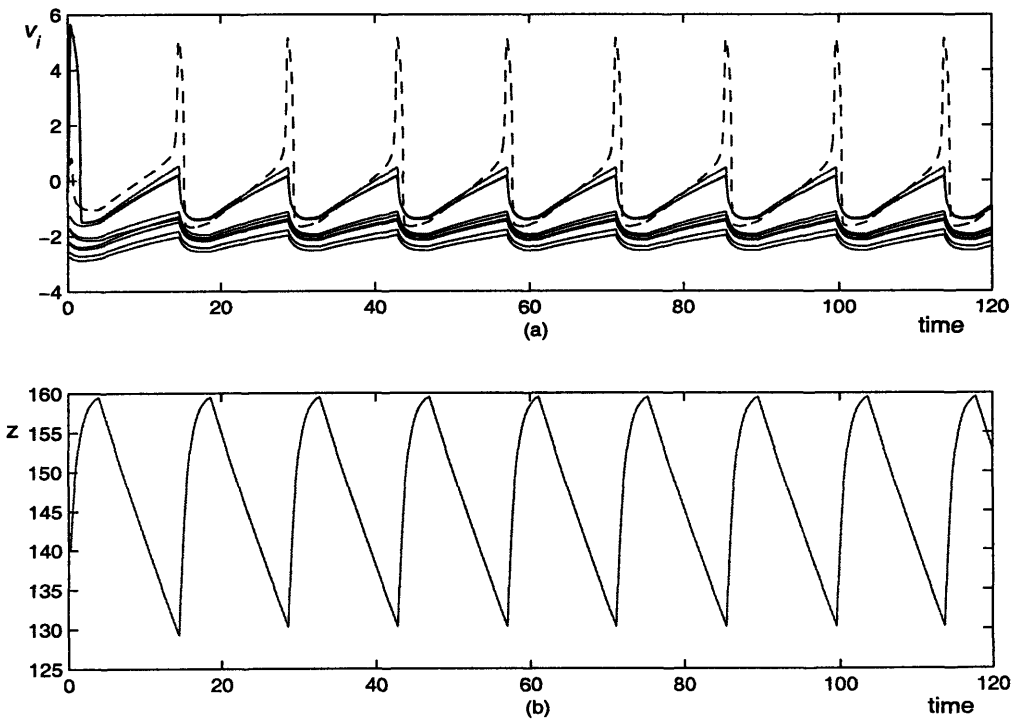

Figure 9-3: Simulation of WTA computation with $n = 10$. (a) States v_i versus time (the dashed curve represents the state of the neuron receiving the largest input); (b) state z versus time.

where z_0 is a constant saturation value, and k_c and k_d are the charging rate and discharging rate.

To perform WTA computation, we set k_c to be large while k_d to be small. As illustrated in Figure 9-1(b) (where we only draw the curve ABCDEC as the trajectory of the FN neuron receiving the largest input. It spikes within two periods. The two cubic null clines correspond to a full-valued inhibition, the lower one, and a discharged inhibition, the upper one.), if there is any FN neuron spiking, the strength of the inhibition current increases to its saturation value rapidly, leaving no chance for other neurons to spike. Therefore, the potential value of all FN neurons drops sharply (from point A to B), and then converges to a varying equilibrium point smoothly (from B to C). The inhibition current discharges slowly after spiking, leading the FN neurons approaching the oscillation region slowly. The first neuron entering the oscillation region will be the one with the largest input. Because of the excitability feature we explained in Section 9.1, this neuron actually spikes (from C to D) before it enters the oscillation region, and its spiking ignites a repeating period (from D to E and then to C again). Thus, the winner is identified within two periods. Note that, since the FN neurons converge to varying equilibrium points with the inhibition slowly discharging, and the potential values v_i at equilibrium points are ranked by the inputs I_i, the neuron with the larger input will soon occupy the higher position as we can see in Figure 9-3. This property also helps the winner to spike first (otherwise the neuron entering the oscillation region later may reach the spiking value first).

Given the parameters of the FN neurons, the frequency of the result depends on the global neuron's saturation value, its charging and discharging rates, and the value of the largest input. If we fix the global neuron's dynamics, the frequency increases with the value of the largest input. A simulation result is shown in Figure 9-3 with $n = 10$. The parameters of the FN neurons are set as $\alpha = 5.32, \beta = 3, \gamma = 0.1$, with spiking threshold $v_0 = 5$. The inputs I_i are chosen randomly from 20 to 125. The parameters of the global neuron are $z_0 = 160, k_c = 1, k_d = 1/50$. All the initial conditions are chosen arbitrarily.

9.2.2 Distributed Version

The linear complexity of the WTA network makes it possible to replace the single global inhibitory neuron with a group of interneurons, each of which only inhibits a set of local FN neurons (as illustrated in Figure 9-4). In this distributed version, synchronization of the interneurons can be guaranteed by the general nonlinear synchronization mechanisms derived in previous chapters. As an example, assume that the interneurons are only coupled to nearest neighbors, and each of them spikes if there is any local FN neurons spiking or if there is any neighboring interneuron spiking. The specific form of the dynamics is given, for instance, as

$$\dot{z}_i = f(z_i) + \sum_{j \in \mathcal{N}_i} \gamma_{ji}(z_j - z_i)$$

where $\mathcal{N}_i$ is the set of the neighbors of interneuron i, f represents the dynamics defined in (9.2), and γ_{ji} is equal to a constant positive value γ if neurons i and j are in the same mode, otherwise it is 0. Such a coupling is based on both proximity and similarity, and is achieved with electrical synapses. Note that electrical synapses, such as gap junction-mediated connections, appear to play a central role in generating widespread synchronous inhibitory activities in neocortex [11, 27, 23, 39], for instance.

Figure 9-5 illustrates a simulation result with four interneurons connected as a chain. Each interneuron inhibits five FN neurons. The parameters are the same as those in Figure 9-3, except that $k_c = 10$ and $\gamma = 1$. The initial conditions and the inputs are chosen randomly. Note that increasing interneuron connectivity would lead to faster synchronization.

9.2.3 Discussion

In the following, while we refer for simplicity to the global mechanism of section 3.1, the results apply as well to the distributed version of section 3.2.

- **Initial conditions and computation speed**
  The mechanism described above guarantees that initial conditions can be set arbitrarily, which cannot be realized by most of the previous WTA models. With appropriate parameters, the computation can be completed at most in two periods. The first spiking neuron is chosen partly by initial conditions, while the second one will be the one with the largest input, and it remains spiking until the inputs change. Actually, if the initial inhibition is set large enough so that all the FN neurons are depressed in the beginning, the neuron with the largest input will spike within the first period.

- **Varying inputs and noise**
  Since initial conditions do not matter in our model, the network can easily track time-varying inputs. Figure 9-6 illustrates such an example, where three inputs switch winning positions several times. The parameters are all equal to those in Figure 9-3. The state in plot (a) corresponds to the input in plot (b) with the same color and style. Although the inputs change continuously, the spiking neuron always tracks the largest input. Note that the computation is robust to signal noise as well.

- **Multiple winners**
  Decreasing the global neuron's discharging rate k_d extends the waiting time before the winner spikes. This is helpful if there exist several neurons receiving the same largest input and we expect them all spike as a group of winners. Enlarging the time neurons stay in the stable region allows these neurons with the same input converge to each other, and to enter the oscillation region and spike simultaneously. Figure 9-7 shows a simulation result, where the parameters are the same as in Figure 9-3 except that $k_c = 5$, $k_d = 1/80$. The inputs are $I_1 = \cdots = I_9 = 120, I_{10} = 119.5$. The first plot shows states v_i versus time. The dashed (red) line represents v_{10} and the solid (blue) lines the other

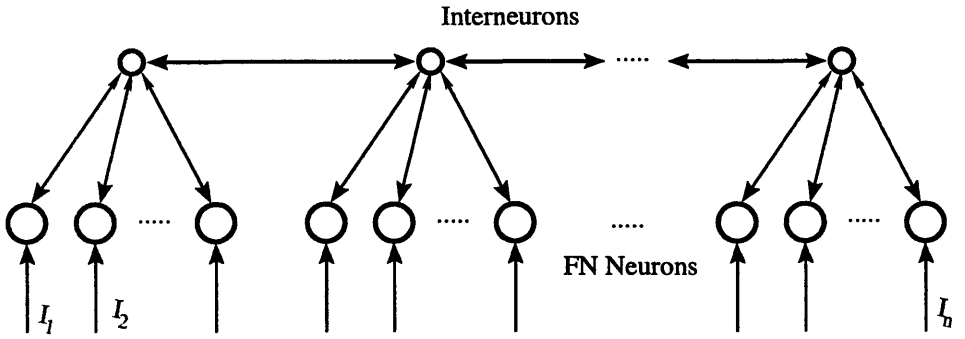

Figure 9-4: A distributed WTA network structure.

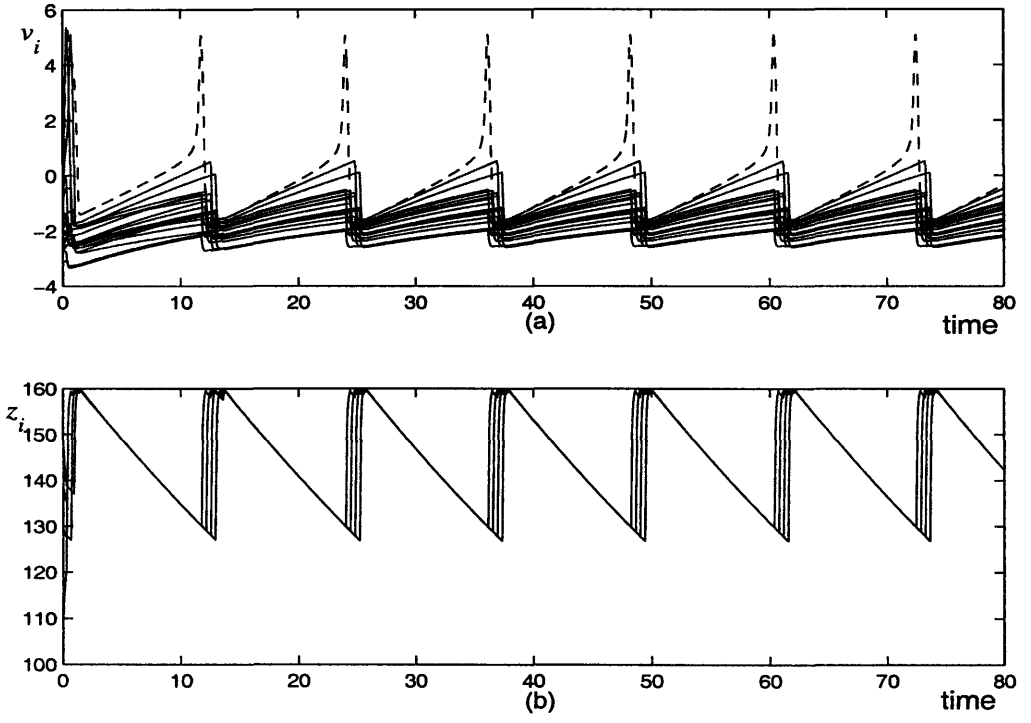

Figure 9-5: Simulation of distributed WTA computation. (a) States v_i versus time; (b) inhibitions z_i versus time.

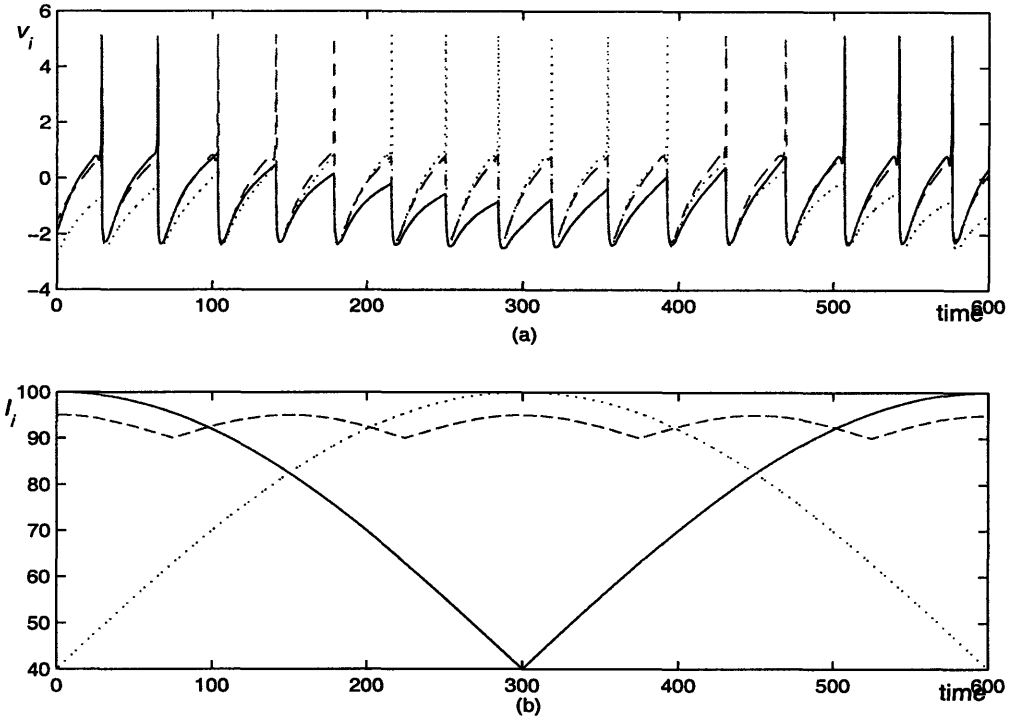

Figure 9-6: Simulation result of WTA computation with varying inputs. (a) States v_i versus time; (b) inputs I_i versus time.

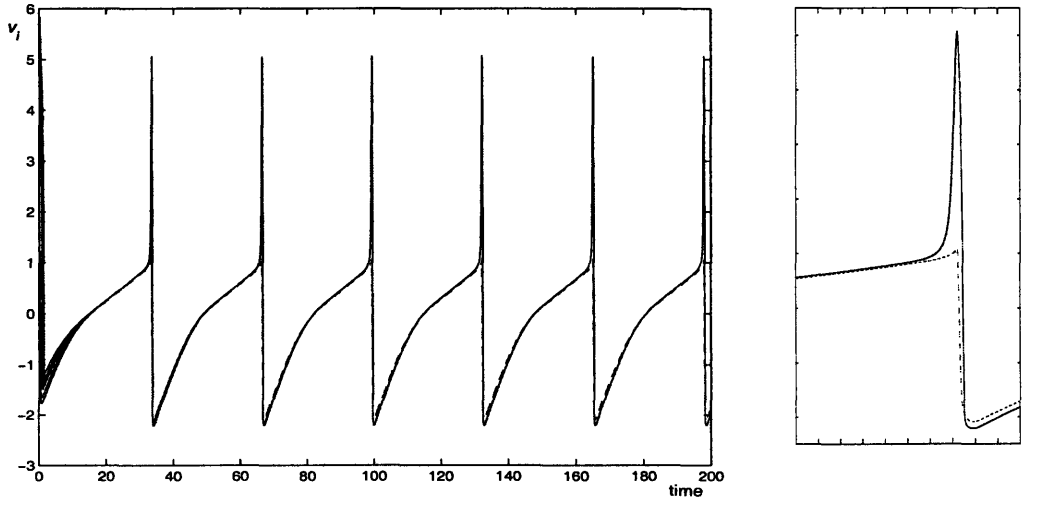

Figure 9-7: Simulation result of WTA computation with multiple winners.

v_i's. The first nine neurons converge together during the waiting time and spike simultaneously as a group of winners. The second plot, an enlarged version of the first at a spiking moment, shows that v_{10} is completely depressed by the winners even though the input difference is very small.

If its size is small, the network may be augmented with all-to-all couplings *between* FN neurons, with the coupling gain increasing with the similarity of the inputs, for instance, of the form $e^{-\alpha|I_j - I_i|}$. This lets the neurons receiving identical inputs converge together exponentially and thus provides another solution to the multiple-winner problem.

- **Computation resolution**
  Computation resolution can be improved by decreasing the global neuron's discharging rate k_d while increasing the charging rate k_c. Decreasing k_d allows the winner fully distinguished with the following neurons; increasing k_c prevents the following neurons spike after the winner. In simulation, by setting $k_c = 5$ and $k_d = 1/80$, a winner with $I_{max} = 120$ can be clearly identified while the second largest input $I = 119.5$ (Figure 9-7). The resolution here is much better than the WTA models presented previously, including [72, 154]. It can be further enhanced by decreasing the relaxation time of the FN neurons.

- **Input bounds**
  The inputs to the FN neurons should be lower-bounded by I_l (the lower threshold of the oscillation region) to guarantee that the neurons can spike before the inhibition is fully released. They should also be upper bounded to set z_0.

- **Spike-controlled coupling and slow inhibition**
  The feedforward and recurrent connections used in our WTA network are similar to those in [61], where a "universal" control system is developed based on olivocerebellar networks, and the neuron model is FitzHugh-Nagumo-like containing four variables. The couplings inside the circuit are spike-controlled. Another example is [161], where WTA is implemented to compute the object with the largest size. Biologically motivated models using slowly-discharged inhibition can be found in e.g. [80, 161, 171].

- **Computational complexity**
  The complexity of the network is $O(n)$. Since the FN neurons are independent, they can be added or removed from the network at any time.

9.3 Extensions

9.3.1 K-Winner-Take-All Network

K-WTA is a common variation of WTA computation, where the output indicates for each neuron whether its input is among the k largest [7, 37, 154, 178, 181]. Most previous k-WTA studies are based on steady-state stability analysis. Many of them

define the winners as the neurons with the largest initial states [88, 178], or require initial conditions to be set precisely [181], which makes the networks not well suited to time-varying inputs. Others adopt particular design methodologies [116, 126] but the network size or the number of winners is limited. K-WTA is also implemented in analog VLSI circuits [154], which extend the elegant WTA model in [72] but inherit its low resolution limit as well.

The neural network described in Section 9.2 can be easily extended to k-WTA computation, where an FN neuron spikes if and only if its input is among the k largest. Indeed, as the global inhibition force decreases, the FN neurons approach the oscillation region *rank-ordered* by their inputs. Thus, while for WTA computation, the global inhibition neuron is charged after the first FN neuron spike, for k-WTA computation the charging moment is simply modified to capture the k^{th} instead.

To get this effect, we augment the dynamics of each FN neuron with a self-inhibitory portion, which receives synaptic inputs both from the FN portion and the global neuron. The specific form of the self-inhibition's dynamics can be very general. Here we give an example:

$$\begin{cases} \dot{v}_i = v_i(\alpha - v_i)(v_i - 1) - w_i + I_i - u_i - z \\ \dot{w}_i = \beta v_i - \gamma w_i \\ \dot{u}_i = k_u \left(\zeta_i u_0 - u_i\right) \end{cases}$$

where u_0 is a constant saturation value and k_u the changing rate. The value of ζ_i has two possibilities, namely it switches to 0 if the global neuron spikes, else it switches to 1 if the FN neuron spikes. Thus the value of u_i varies between 0 and u_0, with the transition periods very fast by setting a large k_u.

The dynamics of the global inhibitory neuron is the same as before, except that we start its charging mode if any k FN neurons in the network spike. Such a moment can be captured by determining whether $\sum_{i=1}^{n} u_i$ approaches ku_0. Therefore, if any FN neuron spikes, it excites only the corresponding local inhibition but has no effect on the rest of the network. But if there are k local inhibitions turned on, the global inhibitory neuron spikes, which then releases all the local inhibitions and ignites a new period.

Compared to the WTA network in Section 9.2, the basic principle underlying the k-WTA network described above is the same, exploiting the simple properties of the FN model. Thus, most of the computational advantages of the WTA network are inherited by the k-WTA extension. Figure 9-8 illustrates an example which tracks time varying inputs with $n = 3$, $k = 2$. The parameters of the FN neurons are the same as those in Figure 9-3. The parameters of local inhibitions are $u_0 = 160, k_u = 100$, and those of the global neuron are $z_0 = 240, k_c = 100, k_d = 1/40$. All initial conditions are chosen arbitrarily. The inputs are not constant. Each state in plot (a) corresponds to the input in plot (b) with the same color and style. The spiking neurons always tracks the two largest inputs.

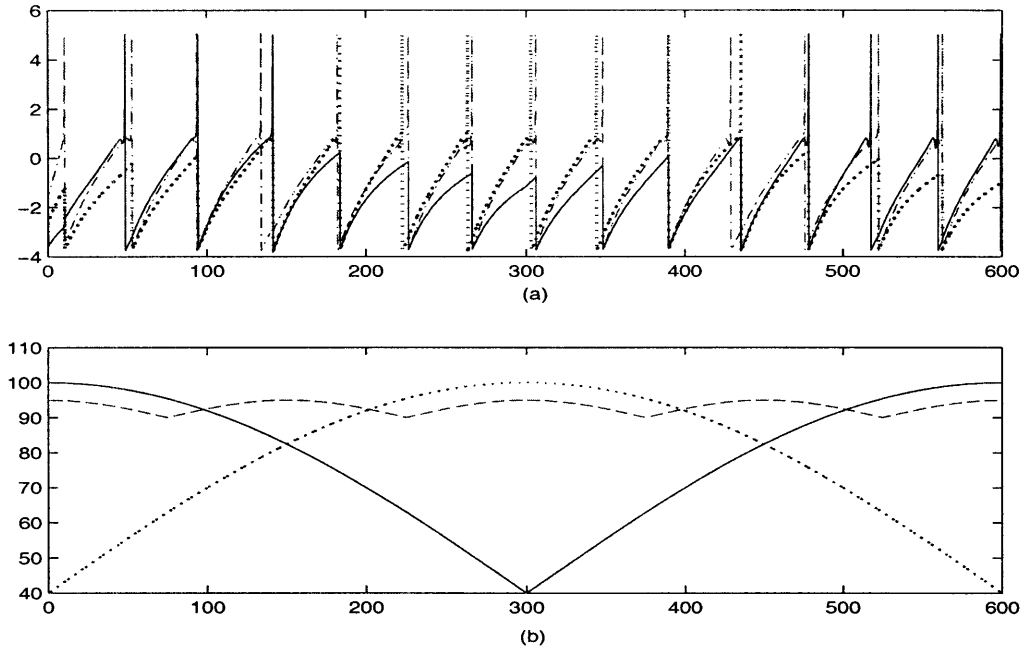

Figure 9-8: Simulation of k-WTA computation. (a) States v_i versus time; (b) inputs I_i versus time.

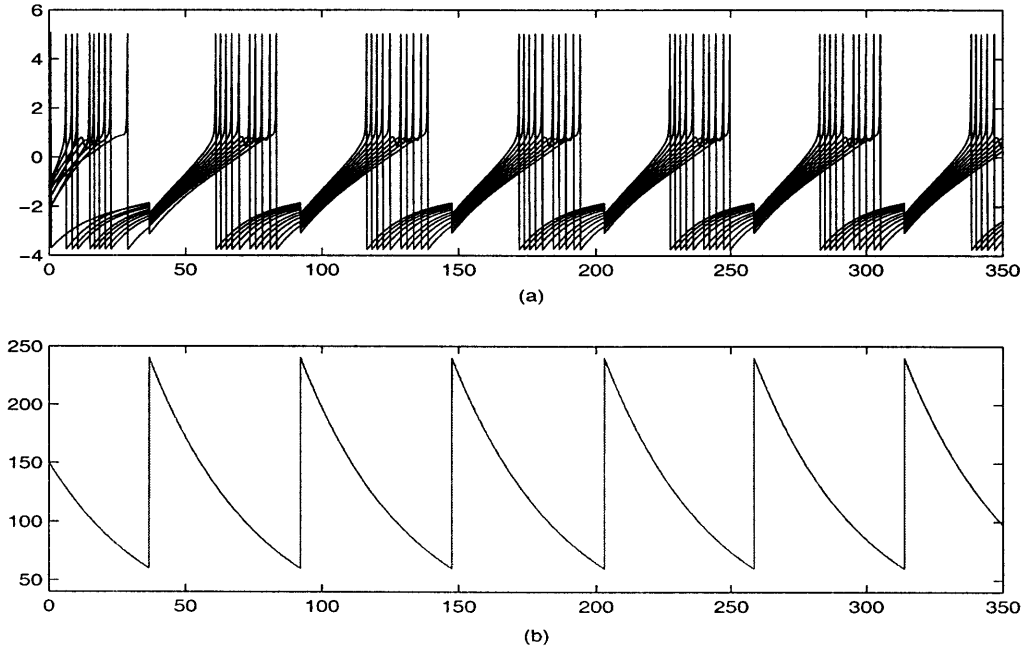

Figure 9-9: Simulation of soft-WTA computation. (a) States v_i versus time; (b) global inhibition z versus time.

9.3.2 Soft-Winner-Take-All

Soft-WTA [85] (or softmax) is another variation of WTA computation, where the outputs reflect the rank of all inputs according to their size. Although soft-WTA is a very powerful primitive [85, 86] in that it can be used to compute any continuous function, its "neural" implementation is complex. Recently, [184] studied soft-WTA as an optimization problem not based on a biologically plausible mechanism; [55] presented a hardware model of selective visual attention which lets the attention switch between the selected inputs, but whose switching order does not completely reflect the input ranks. In this section, we develop a simple soft-WTA neural network which generates spiking outputs rank-ordered by their inputs, and inherits the main computational advantages of the WTA network. Potential applications may include selective attention, associative memory and competitive learning, and desynchronization mechanisms for perceptional binding [44, 129, 160, 163].

Letting $k = n$ in the k-WTA network described in Section 9.3.1 yields a pre-ordered spiking sequence in each stable period. However, such an n^{th} spiking moment may not be measurable if the number of inputs n is unknown or time-varying. To make the solution more general, we let the global inhibitory neuron spike autonomously, for instance let it spike if the inhibition z is lower than a given bound z_{low}. Thus, the spikings of all the FN neurons in the network are guaranteed by the sufficient condition

$$z_{low} < I_{min} - I_l$$

where I_l is the lower bound of the oscillation region of the FN model and I_{min} is the minimum input value.

Figure 9-9 illustrates such an example with $n = 10$. The parameters are the same as those in Figure 9-8. The inputs I_i are distributed uniformly between 80 and 120. The inhibition lower bound is $z_{low} = 60$. Initial conditions are chosen arbitrarily. The computation is completed in the second period, during and after which the spiking times of the FN neurons are ranked by their inputs.

9.3.3 Fast Coincidence Detection

Recent neuroscience research suggests that coincidence detection plays a key role in temporal binding [78, 152]. Hopfield *et al.* [14, 50] proposed two neural network structures, both able to capture a "many-are-equal" moment, to model speech recognition and olfactory processing. A similar computation can be implemented by FN neurons, with faster and more salient response.

Consider a leader-followers network with a structure similar to Figure 9-2, except that the global neuron (the leader) is now *excitatory*, and the connections from the leader to the followers are unidirectional. For simplicity, we assume that all the neurons are FN neurons with the same parameters but different inputs. The dynamics of the leader (v_o, w_o) obeys equations (9.1) while those of the followers $(i = 1, \ldots, n)$ are

$$\begin{cases} \dot{v}_i = v_i(\alpha - v_i)(v_i - 1) - w_i + I_i + k(v_0 - v_i) \\ \dot{w}_i = \beta v_i - \gamma w_i \end{cases}$$

where $k(v_0 - v_i)$ is the coupling force from the leader to the followers. Neurons i and j synchronize only if inputs I_i and I_j are identical. We define the system output accordingly to capture the moment when this condition becomes true for a large number of inputs, as illustrated in Figure 9-10 with $n = 30$. The parameters of the FN neurons are the same as in Figure 9-3. The inputs are $I_0 = 90$ and $I_1, \ldots, I_{30}$ varying from 20 to 80, and the coupling gain is $k = 1.7$.

Note that the coupling gain k should be large enough to guarantee synchronization (an explicit threshold can be computed analytically), but not so large as to have the leader numerically dominate the dynamic differences between the followers. As in Section 9.2, the network structure can be fully distributed by replacing the single leading neuron by a group of interneurons synchronized through electrical synapses.

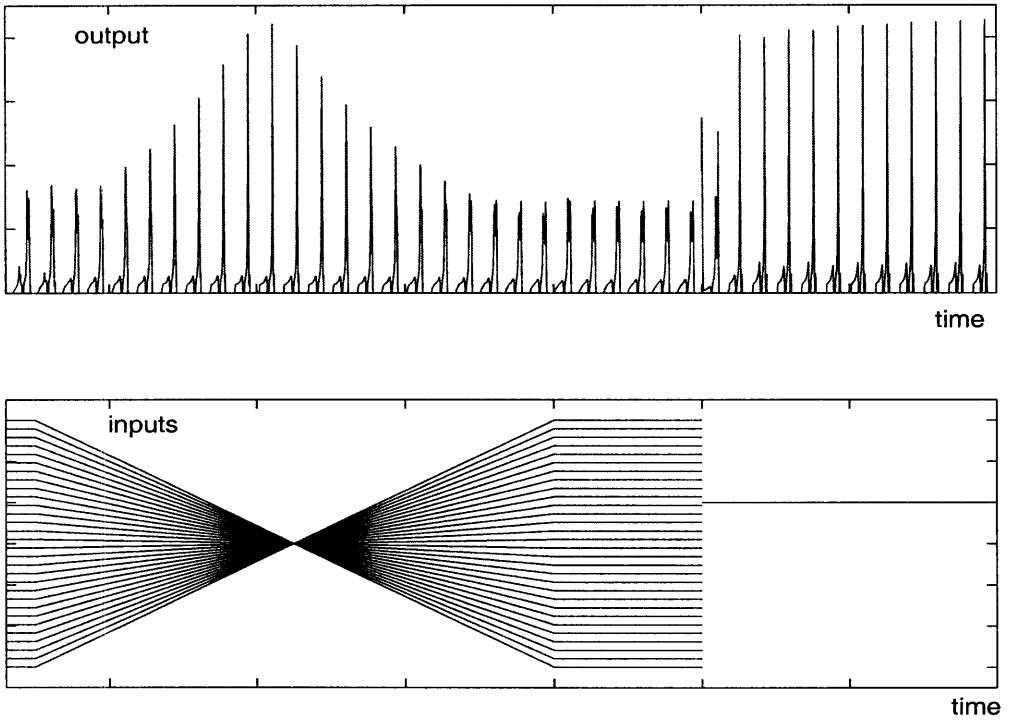

Figure 9-10: Simulation of fast coincidence detection. The upper plot shows $\sum_{i=1}^{n} \max(0, \dot{v}_i)$ versus time, and the lower $I_1, \ldots, I_n$.

Chapter 10

Concluding Remarks

The combination of contraction analysis and graph theory generates a powerful tool to study the collective behaviors of distributed nonlinear networks. In this thesis, we derive explicit conditions for synchronization, identify different leader roles in dynamic networks, investigate the effect of time-delayed communication, and propose simple models to implement neural computation tasks.

Particularly, we introduce the concept of partial contraction, which investigates stability with respect to a specific behavior or property, and therefore can be very powerful to analyze large-scale systems. Based on contraction and/or partial contraction properties, synchronization analysis is greatly simplified by isolating the desired convergence behavior from the overall system dynamics. Furthermore, because it is virtual, the auxiliary, meta-system $\mathbf{y}$ can actually be centralized. Although this thesis focuses mainly on identical properties of subsystem states, future applications of partial contraction to synchronization should investigate convergence to more general properties, such as phase locking in locomotion systems.

Partial contraction analysis could also be applied in the context of discrete-time systems, hybrid systems or switching systems. It then allows one to study, for instance, the synchronization of pulse-coupled neurons in a distributed network, a wide-used model in neuroscience which still lacks a complete theoretical explanation.

Finally, the results presented in this thesis could be extended to study systems described by nonlinear partial differential equations such as reaction-diffusion equations, and to the case when connections occur stochastically. The principle of a virtual centralized system may also have applications in quantum physics.

Bibliography

[1] Amari, S., and Arbib, M. (1977) Competition and Cooperation in Neural Nets, in *Systems Neuroscience*, J.Metzler, Ed., Academic Press (San Diego) 119-165

[2] Anderson, R., and Spong, M.W. (1989) Bilateral Control of Teleoperators, *IEEE Trans. Aut. Contr.*, **34**(5),494-501

[3] Ando, H., Oasa, Y., Suzuki, I., and Yamashita, M. (1999) Distributed Memoryless Point Convergence Algorithm for Mobile Robots with Limited Visibility, *IEEE Transactions on Robotics and Automation*, 818-828

[4] Arbib, M.A. (1995) The Handbook of Brain Theory and Neural Networks, *MIT Press*, Cambridge, MA, USA

[5] Aronson, D.G., Ermentrout, G.B., and Kopell, N. (1990) Amplitude response of coupled oscillators, *Physica D*, **41**:403-449

[6] Ashwin, P., King, G.P., and Swift, J.W. (1990) Three identical oscillators with symmetric coupling, *Nonlinearity*, **3**

[7] Badel, S., Schmid, A., and Leblebici Y. (2003) A VLSI Hamming Artificial Neural Network with k-Winner-Take-All and k-Loser-Take-All Capability, *International Joint Conference on Neural Networks*, Portland, OR, 977-982

[8] Bar-Eli, K. (1985) On the Stability of Coupled Chemical Oscillators, *Physica D*, **14**:242-252

[9] Barahona, M., and Pecora, L.M. (July 2002) Synchronization in Small-world Systems, *Physical Review Letters*

[10] Bay, John S., and Hemami, H. (April 1987) Modeling of a Neural Pattern Generator with Coupled Nonlinear Oscillators, *IEEE Transactions on Biomedical Engineering*

[11] Beierlein, M., Gibson, J.R., and Connors, B.W. (2000) A Netwrok of Electrically Coupled Interneurons Drives Synchronized Inhibition in Neocortex, *Nature Neuroscience*, **3**(9):904-910

[12] Belta, C., and Kumar, V. (2003) Abstraction and Control for Groups of Fully-Actuated Planar Robots, *IEEE International Conference on Robotics and Automation, (Taipei, Taiwan)*

[13] Bressloff, P.C., Coombes, S., Souza, B. de (October 1997) Dynamics of a Ring of Pulse-Coupled Oscillators: Group Theoretic Approach, *Physical Review Letters*

[14] Brody, C.D., and Hopfield, J.J. (2003) Simple Networks for Spike-Timing-Based Computation, with Application to Olfactory Processing, *Neuron*, **37**:843-852

[15] Bruckstein, A.M., Mallows, C.L., and Wagner, I.A. (1997) Cooperative Cleaners: a Study in Ant-Robotics, *American Mathematical Monthly*, **104**(4): 323-343

[16] Buccino G. (2001) *European J. Neuroscience*, **13**:400

[17] Chakraborty, T., Rand, R.H. (1988) The Transition from Phase Locking to Drift in a System of Two Weakly Coupled Van der Pol Oscillators, *International J. Nonlinear Mechanics*, **23**:369-376

[18] Chopra, N., Spong, M.W., Hirche, S., and Buss, M. (2003) Bilateral Teleoperation over the Internet: the Time Varying Delay Problem, *Proceedings of the American Control Conference, Denver, CO.*

[19] Chu, T., Wang, L., and Mu, S. (2004) Collective Behavior Analysis of an Anisotropic Swarm Model, The 16th International Symposium on Mathematical Theory of Networks and Systems,

Belgium

[20] Chua, L.O. (1998) CNN: a paradigm for complexity, *Singapore; Hong Kong: World Scientific*

[21] Collins, J.J., and Stewart, I.N. (1993) Coupled Nonlinear Oscillators and the Symmetries of Animal Gaits, *Nonlinear Science*, **3**:349-392

[22] Collins, J.J., and Stewart, I.N. (1993) Hexapodal Gaits and Coupled Nonlinear Oscillator Models, *Biological Cybernetics*, **68**:287-298

[23] Connors, B.W., and Long, M.A. (2004) Electrical Synapses in The Mammalian Brain, *Annual Review of Neuroscience*, **27**:393-418

[24] Coombes, S. (2001) Phase-locking in networks of pulse-coupled McKean relaxation oscillators, *Physica D*

[25] Cutts, C., and Speakman, J. (1994) Energy Savings in Formation flight of Pink-Footed Geese, *J. Exp. Biol.*, **189**:251-261

[26] D'Andrea, R., and Dullerud, G.E. (2003) Distributed Control Design for Spatially Interconnected Systems, *IEEE Transactions on Automatic Control*, **48**(9):1478-1495

[27] Deans, M., Gibson, J.R., Connors, B.W., and Paul, D.L. (2001) Synchronous Activity of Inhibitory Networks in Neocortex Requires Electrical Synapses Containing Connexin36, *Neuron*, **31**:477-485

[28] Decety, J. (2002) in Simulation and Knowldege of Action, *Benjamin, Philadelphia*

[29] Dehaene, S., Kerszberg, M., and Changeux J.P. (1998) A Neuronal Model of a Global Workspace in Effortful Cognitive Tasks, *PNAS* **95**:14529-14534

[30] Dragoi, V., and Grosu, I. (1998) Synchronization of Locally Coupled Neural Oscillators, *Neural Processing Letters*, **7**

[31] Ermentrout, B. (1992) Complex Dynamics in Winner-Take-All Neural Nets with Slow Inhibition, *Neural Networks*, **5**(3):415-431

[32] Fang, Y., Cohen, M., and Kincaid, M. (1996) Dynamics of a Winner-Take-All Neural Network, *Neural Networks*, **9**(7):1141-1154

[33] Feldman, J.A., and Ballard, D.H. (1982) Connectionist Models and Their Properties, *Cognit. Sci.*, **6**:205-254

[34] Fiedler, M., (1973) Algebraic Connectivity of Graphs, *Czechoslovak Mathematical Journal*, **23**(98):298-305

[35] Fierro, R., Song, P., Das, A., and Kumar, V. (2002) Cooperative Control of Robot Formations, in *Cooperative Control and Optimization: Series on Applied Optimization*, Kluwer Academic Press, 79-93

[36] FitzHugh, R.A. (1961) Impulses and Physiological States in Theoretical Models of Nerve Membrane, *Biophys. J.*, **1**:445-466

[37] Fukai, T., and Tanaka, S. (1997) A Simple Neural Network Exhibiting Selective Activation of Neuronal Ensembles: From Winner-Take-All to Winners-Share-All, *Neural Computation*, **9**:77-97

[38] Gerstner, W. (2001) A Framework for Spiking Neuron Models: The Spike Response Model, In *The Handbook of Biological Physics*, **4**:469-516

[39] Gibson, J.R., Beierlein, M., and Connors, B.W. (1999) Two Electrically Coupled Inhibitory Networks, *Nature* **402**(4):75-79

[40] Godsil, C., and Royle, G. (2001) Algebraic Graph Theory, *Springer*

[41] Golubitsky, M., Stewart, I., Buono, P.L., and Collins, J.J. (1998) A modular Network for Legged Locomotion, *Physica D.*, **115**:56-72

[42] Golubitsky, M., Stewart, I., Buono, P.L., and Collins, J.J. (1999) The Role of Symmetry in Locomotor Central Pattern Generators and Animal Gaits, *Nature*, **401**

[43] Golubitsky, M., and Stewart, I. (2002) Patterns of Oscillation in Coupled Cell Systems, *Geometry, Dynamics, and Mechanics: 60th Birthday Volume for J.E. Marsden*, 243-286, Springer-Verlag.,

[44] Gray, C.M. (1999) The Temporal Correlation Hypothesis of Visual Feature Integration: Still Alive and Well, *Neuron*, **24**:31-47

[45] Grossberg, S. (1973) Contour Enhancement, Short-Term Memory, and Constancies in Reverberating Neural Networks, *Studies in Applied Mathematics*, **52**:217-257

[46] Grossberg, S. (1978) Competition, Decision, and Consensus, *Journal of Mathematical Analysis and Applications*, **66**:470-493

[47] Hahnloser, R.H., Seung, H.S., and Slotine. J.J.E. (2003) Permitted And Forbidden Sets in Symmetric Threshold-Linear Networks, *Neural Computation* **15**:621-38

[48] Hirsch, M., and Smale, S. (1974) Differential Equations, Dynamical Systems, and Linear Algebra, *Academic Press, New York*

[49] Hodgkin, A.L., and Huxley, A.F. (1952) A Quantitative Description of Membrane Current and its Application to Conduction and Excitation in Nerve, *J. Physiol.*, **117**:500

[50] Hopfield, J.J., and Brody, C.D. (2001) What Is A Moment? Transient Synchrony as a Collective Mechanism for Spatiotemporal Integration, *Proc. Natl. Acad. Sci. USA*, **98**:1282-1287

[51] Horn, R.A., and Johnson, C.R. (1985) Matrix Analysis, *Cambridge University Press*

[52] Horn, R.A., and Johnson, C.R. (1989) Topics in Matrix Analysis, *Cambridge University Press*

[53] Hu, J.J. (2000) Stable Locomotion Control of Bipedal Walking Robots: Synchronization with Neural Oscillators and Switching Control, *Ph.D. Thesis, Department of Electrical Engineering and Computer Science, MIT*

[54] Ijspeert, A.J. (2001) A Connectionist Central Pattern Generator for the Aquatic and Terrestrial Gaits of a Simulated Salamander, *Biol. Cybern.*, **84**:331-348

[55] Indiveri, G. (2000) A 2D Neuromorphic VLSI Architecture for Modeling Selective Attention, *IEEE-INNS-ENNS International Joint Conference on Neural Networks*, Como, Italy

[56] Izhikevich, E.M. (2003) Which Model to Use for Cortical Spiking Neurons? *IEEE Trans. on Neural Networks*, submitted

[57] Jadbabaie, A., Lin, J., and Morse, A.S. (May 2003) Coordination of Groups of Mobile Autonomous Agents Using Nearest Neighbor Rules, *IEEE Transactions on Automatic Control*

[58] Jadbabaie, A., Motee, N., and Barahona, M. (2004) On the Stability of the Kuramoto Model of Coupled Nonlinear Oscillators, *American Control Conference*

[59] Jin, D.Z., and Seung, H.S. (2002) Fast Computation With Spikes in a Recurrent Neural Network, *Physical Review E*, **65**:051922

[60] Jouffroy, J., and Slotine, J.J.E. (2004) Methodological Remarks on Contraction Theory, *NSL Report, MIT, Cambridge, MA*, submitted

[61] Kazantsev, V.B., Nekorkin, V.I., Makarenko, V.I., and Llinás, R. (2003) Olivo-Cerebellar Cluster-Based Universal Control System, *PNAS*, **100**(22):13064-13068

[62] Ketterle, W. (2002) When atoms behave as waves: Bose-Eintein condensation and the atom laser, *Rev. Mod. Phys.*,**74**

[63] Khalil H.K. (1996) Nonlinear Systems, *Prentice-Hall*

[64] Klavins, E., and Koditschek, D.E. (March 2002) Phase Regulation of Decentralized Cyclic Robotic Systems, *International Journal of Robotics and Automation*

[65] Kopell, N., and Ermentrout, G.B. (1986) Symmetry and Phase-locking in Chains of Weakly Coupled Oscillators, *Communications on Pure and Applied Mathematics*, **39**:623-660

[66] Kopell, N., and Somers, D.C. (1995) Anti-phase Solutions in Relaxation Oscillators Coupled Through Excitatory Interactions, *Journal of Mathematical Biology*, **33**

[67] Kopell, N. (2000) We got rhythm: Dynamical Systems of the Nervous System, *published version of the 1998 Gibbs Lecture of the AMS, Notices of the AMS*, **47**:6-16

[68] Krishnaprasad, P.S., and Tsakiris, D. (2001) Oscillations, SE(2)-Snakes and Motion Control: A Study of the Roller Racer, *Dyanmics and Stability of Systems*

[69] Kuramoto, Y. (1984) Chemical Oscillations, Wave, and Turbulence, *Springer, Berlin*

[70] Langbort, C., and D'Andrea, R. (2003) Distributed Control of Spatially Reversible Interconnected Systems with Boundary Conditions, *submitted to SIAM Journal on Control and Optimization*

[71] Latham, P.E., Deneve, S., and Pouget, A. (2003) Optimal Computation With Attractor Networks, *J. Physiol. (Paris)*, **97**:683-694

[72] Lazzaro, J., Ryckebusch, S., Mahowald, M.A., and Mead, C. (1988) Winner-Take-All Networks of $O(n)$ Complexity, in *Advances in Neural Information Processing Systems 1.* San Mateo, CA:Morgan Kaufmann Publishers, 703-711

[73] Leonard, N.E., and Fiorelli, E. (2001) Virtual Leaders, Artificial Potentials and Coordinated Control of Groups, *40th IEEE Conference on Decision and Control*

[74] Leonov, G., Burkin, I., and Shepeljavyi, A. (1996) Frequency Methods in Oscillation Theory, *Kluwer*

[75] Lin, J., Morse, A., and Anderson, B. (2003) Multi-Agent Rendezvous Problem, *Proceedings of the 42nd IEEE Conference on Decision and Control*

[76] Lin, Z., Broucke, M., and Francis, B. (2003) Local Control Strategies for Groups of Mobile Autonomous Agents, *submitted to IEEE Trans. Automatic Control*

[77] Llinás, R., Ribary, U., Contreras, D., and Pedroarena, C. (1998) The Neuronal Basis for Consciousness, *Phil. Trans. R. Soc. Lond.* B **353**:1841-1849

[78] Llinás, R.R., Leznik, E., and Urbano, F.J. (2002) Temporal Binding via Cortical Coincidence Detection of Specific and Nonspecific Thalamocortical Inputs: a Voltage-Dependent Dye-Imaging Study in Mouse Brain Slices, *PNAS*, **99**(1):449-454

[79] Loewenstein, Y., and Sompolinsky, H. (2002) Oscillations by Symmetry Breaking in Homogeneous Networks with Electrical Coupling, *Physical Review E*, **65**:1-11

[80] LoFaro, T., Kopell, N., Marder, E., and Hooper, S.L. (1994) Subharmonic Coordination in Networks of Neurons with Slow Conductances, *Neural Computation*, **6**:69-84

[81] Lohmiller, W., and Slotine, J.J.E. (1998) On Contraction Analysis for Nonlinear Systems, *Automatica*, **34**(6)

[82] Lohmiller, W. (1999) Contraction Analysis of Nonlinear Systems, *Ph.D. Thesis, Department of Mechanical Engineering, MIT*

[83] Lohmiller, W., and Slotine, J.J.E. (2000) Control System Design for Mechanical Systems Using Contraction Theory, *IEEE Trans. Aut. Control*, **45**(5)

[84] Lohmiller, W., and Slotine, J.J.E. (2000) Nonlinear Process Control Using Contraction Theory *A.I.Ch.E. Journal, March 2000.*

[85] Maass, W. (2000) On the Computational Power of Winner-Take-All, *Neural Comput.*, **12**(11):2519-35

[86] Maass, W. (2000) Neural Computation with Winner-Take-All as The Only Nonlinear Operation, in *Advances in Information Processing Systems*, **12**:293-299, MIT Press

[87] Maass, W., Natschläger, T., and Markram, H. (2003) On the Computational Power of Circuits of Spiking Neurons, submitted

[88] Majani, E., Erlanson, R., and Abu-Mostafa, Y. (1989) On the k-Winners-Take-All Network, in *Advances in Neural Information Processing Systems I*, D.S. Touretzky, Ed. 634-642

[89] Manor, Y., Nadim, F., Ritt, J., Epstein, S., Marder, E., Kopell, N. (1999) Network Oscillations Generated by Balancing Asymmetric Inhibition in Passive Neurons, *Journal of Neuroscience.*, **19**

[90] Matsuoka, K. (1985) Sustained Oscillations Generated by Mutually Inhibiting Neurons with Adaption, *Biol. Cybern.*, **52**:367-376

[91] Matsuoka, K. (1987) Mechanisms of Frequency and Pattern Control in the Neural Rhythm Generators, *Biol. Cybern.*, **56**:345-353

[92] May, R.M., Gupta, S., and McLean, A.R. (2001) Infectious Disease Dynamics: What Characterizes a Successful Invader? *Phil. Trans. R. Soc. Lond. B*, **356**:901-910

[93] Micchelli, C.A. (1986) Interpolation of Scattered Data, *Constructive Approximation*, **2**:11-22.

[94] Milner, P.M. (1974) A Model for Visual Shape Recognition, *Psychological Review*, **81**(6):521-535

[95] Milo, R. (2002) Network Motifs, *Science* **298**

[96] Mirollo, R.E., Strogatz, S.H. (December 1990) Synchronization of Pulse-Coupled Biological Oscillators, *SIAM J. Appl. Math.*, **50**:1645-1662

[97] Mohar, B. (1991) Eigenvalues, Diameter, and Mean Distance in Graphs, *Graphs and Combinatorics* **7**:53-64

[98] Moreau, L (2004) Stability of Continuous-Time Distributed Consensus Algorithms, *submitted*

[99] Murray, J.D. (1993) Mathematical Biology, *Berlin;New York: Springer-Verlag*

[100] Nagumo, J., Arimoto, S., and Yoshizawa, S. (1962) An Active Pulse Transmission Line Simulating Nerve Axon, *Proc. Inst. Radio Engineers*, **50**:2061-2070

[101] Neuenschwander, S., Castelo-Branco, M., Baron, J., and Singer, W. (2002) Feed-forward Synchronization: Propagation of Temporal Patterns along the Retinothalamocortical Pathway, *Philosophical Transactions: Biological Sciences*, **357**(1428): 1869-1876

[102] Niemeyer, G., and Slotine, J.J.E. (1991), Stable Adaptive Teleoperation, *IEEE J. of Oceanic Engineering*, **16**(1)

[103] Niemeyer, G., and Slotine, J.J.E. (1998) Towards Force-Reflecting Teleoperation Over the Internet, *IEEE Conf. on Robotics and Automation, Leuven, Belgium*

[104] Niemeyer, G., and Slotine, J.J.E. (2001) Towards Bilateral Internet Teleoperation, in *Beyond Webcams: An Introduction to Internet Telerobotics*, eds. K. Goldberg and R. Siegwart, The MIT Press, Cambridge, MA.

[105] Nowak, M.A., and Sigmund, K. (2004) Evolutionary Dynamics of Biological Games, *Science*, **303**:793-799

[106] Olfati-Saber, R., and Murray, R.M. (2003) Consensus Protocols for Networks of Dynamic Agents, *American Control Conference, Denver, Colorado*

[107] Olfati-Saber, R., and Murray, R.M. (2003) Agreement Problems in Networks with Directed Graphs and Switching Topology, *IEEE Conference on Decision and Control*

[108] Olfati-Saber, R., and Murray, R.M. (2003) Flocking with Obstacle Avoidance: Cooperation with Limited Communication in Mobile Networks, *IEEE Conference on Decision and Control*

[109] Olfati-Saber, R., and Murray, R.M. (2004) Consensus Problems in Networks of Agents with Switching Topology and Time-Delays, to appear in the special issue of the *IEEE Transactions On Automatic Control on Networked Control Systems*

[110] Ögren, P., Fiorelli, E., and Leonard, N.E. (2002) Formations with a Mission: Stable Coordination of Vehicle Group Maneuvers, *SIAM Symposium on Mathematical Theory of Networks and Systems*

[111] Page, K.M., and Nowak, M.A. (2002) Unifying Evolutionary Dynamics, *J. theor. Biol.*, **219**:93-98

[112] Parlett, B.N. (1980) The Symmetric Eigenvalue Problem, *Prentice-Hall*

[113] Pecora, L.M., and Carroll, T.L. (1990) Synchronization in Chaotic Systems, *Phys. Rev. Lett.*, **64**:821-824

[114] Pecora, L.M., and Carroll, T.L. (March 1998) Master Stability Functions for Synchronized Coupled Systems, *Physical Review Letters* (March 1998).

[115] Pecora, L.M. (July 1998) Synchronization Conditions and Desynchronizing Patterns in Coupled Limit-cycle and Chaotic Systems, *Physical Review E*

[116] Perfetti, R. (1995) On the Robust Design of k-Winners-Take-All Networks, *IEEE Transactions on Circuits and Systems-II*, **42**(1):55-58

[117] Pikovsky, A., Rosenblum, M., and Kurths, J. (2003) Synchronization: A Universal Concept in Nonlinear Sciences, *Cambridge University Press*

[118] Pogromsky, A., Santoboni, G., and Nijmeijer, H. (2002) Partial Synchronization: From Sym-

metry Towards Stability, *Physica D*, **172**:65-87

[119] Rand, R.H., Holmes, P.J. (1980) Bifurcation of Periodic Motions in Two Weakly Coupled Van der Pol Oscillators, *Int. J. Nonlinear Mechanics*, **15**:387-399

[120] Ravasz, Z.N.E., Vicsek, T., Brechet, T., Barabási, A.L. (June 2000) Physics of The Rhythmic Applause, *Physical Review E*

[121] Reddy, D.V.R., Sen, A., Johnston, G.L. (June 1998) Time Delay Induced Death in Coupled Limit Cycle Oscillators, *Physical Review Letters*

[122] Reynolds, C. (1987) Flocks, Birds, and Schools: a Distributed Behavioral Model, *Computer Graphics*, **21**:25-34

[123] Rizzolati, G. (1996) *Cognitive Brain Research* **3**:131

[124] Rock, I., and Palmer, S. (1990) The Legacy of Gestalt Psychology, *Scientific American*, **263**:84-90

[125] Seiler, G., and Nossek, J.A. (1993) Winner-Take-All Cellular Neural Networks, *IEEE Trans. Circuits Syst.-II*, 40(3):184-190

[126] Seiler, P., Pant, A., and Hedrick J.K. (2003) A Systems Interpretation for Observations of Bird V-formations, *Journal of Theoretical Biology*, **221**:279-287

[127] Seung, H.S. (1998) Continuous Attractors and Oculomotor Control, *Neural Networks*, **11**:1253-1258

[128] Shorten, R.N., and Narendra, K.S. (1998) On the Stability and Existence of Common Lyapunov Functions for Stable Linear Switching Systems, *Proceedings of the 37th IEEE Conference on Decision and Control*

[129] Singer, W., and Gray, C.M. (1995) Visual Feature Integration and The Temporal Correlation Hypothesis, *Annu. Rev. Neurosci.*, **18**:555-586

[130] Singer, W. (1999) Neuronal Synchrony: a Versatile Code for the Definition of Relations, *Neuron*, **24**:49-65

[131] Slotine, J.J.E., and Li, W. (1991) Applied Nonlinear Control, *Prentice-Hall*

[132] Slotine, J.J.E., and Lohmiller, W. (2001) Modularity, Evolution, and the Binding Problem: A View from Stability Theory, *Neural Networks*, **14**(2)

[133] Slotine, J.J.E. (2003) Modular Stability Tools for Distributed Computation and Control, *Int. J. Adaptive Control and Signal Processing*, **17**(6).

[134] Slotine, J.J.E., and Wang, W. (2004) A Study of Synchronization and Group Cooperation Using Partial Contraction Theory, in S. Morse, N. Leonard, V. Kumar (Editors), *Proceedings of Block Island Workshop on Cooperative Control, Springer Lecture Notes in Control and Information Science*

[135] Slotine, J.J.E., Wang, W., and El-Rifai, K. (2004) Contraction Analysis of Synchronization in Networks of Nonlinearly Coupled Oscillators, *Sixteenth International Symposium on Mathematical Theory of Networks and Systems*, Belgium

[136] Smale, S. (1976) A mathematical model of two cells via Turing's equation, in *The Hopf Bifurcation and Its Applications*, 354-367, *Spinger-Verlag, NY*

[137] Somers, D.C., and Kopell, N. (1993) Rapid Synchronization Through Fast Threshold Modulation, *Biological Cybernetics*, **68**

[138] Somers, D.C., and Kopell, N. (1995) Waves and Synchrony in Networks of Oscillators of Relaxation and Non-Relaxation Type, *Physica D*

[139] Storti, D.W., Rand, R.H. (1982) Dynamics of Two Strongly Coupled Van der Pol Oscillators, *Int. J. Nonlinear Mechanics*, **17**:143-152

[140] Strogatz, S.H., and Stewart, I. (December 1993) Coupled Oscillators and Biological Synchronization, *Scientific American*

[141] Strogatz, S.H. (1994) Nonlinear Dynamics and Chaos: with applications to physics, biology, chemistry, and engineering, *Addison-Wesley Pub., Reading, MA*

[142] Strogatz, S.H. (2000) From Kuramoto to Crawford: exploring the onset of synchronization in

populations of coupled oscillators, *Physica D: Nonlinear Phenomena*, **143**(1-4)

[143] Strogatz, S.H. (2001) Exploring Complex Networks, *Nature*, **410**:268-276

[144] Strogatz, S. (2003) Sync: The Emerging Science of Spontaneous Order, *New York: Hyperion*

[145] Tanner, H., Jadbabaie, A., and Pappas, G.J. (2003) Stable Flocking of Mobile Agents, Part I: Fixed Topology; Part II: Dynamic Topology, *IEEE Conference on Decision and Control, Maui, HI*

[146] Tanner, H., Jadbabaie, A., and Pappas, G.J. (2003) Coordination of Multiple Autonomous Vehicles, *IEEE Mediterranian Conference on Control and Automation, Rhodes, Greece*

[147] Terman, D., and Wang, D.L. (1995) Global Competition and Local Cooperation in a Network of Neural Oscillators, *Physica D*, **81**:148-176

[148] Thorpe, S., Fize, D., and Marlot, C. (1996) Speed of Processing in the Human Visual System, *Nature*, **381**(6582):520-522

[149] Thorpe, S., Delorme, A., and Rullen, R.V. (2001) Spike-Based Strategies for Rapid Processing, *Neural Networks*, **14**:715-725

[150] Toner, J., and Tu Y. (1995) Long Range Order in a Two Dimensional xy Model: How birds Fly Together, *Phys. Rev. Lett.*, **75**:4326-4329

[151] Toner, J., and Tu Y. (1998) Flocks, Herds, and Schools: A Quantitative Theory of Flocking, *Phys. Rev. E.*, **58**:4828-4858

[152] Tononi, G., Srinivasan, R., Russell, D.P., and Edelman G.M. (1998) Investigating Neural Correlates of Conscious Perception by Frequency-Tagged Neuromagnetic Responses, *PNAS* **95**:3198-3203

[153] Turing, A. (1952) The Chemical Basis of Morphogenesis, *Philos. Trans. Roy. Soc.*, **B 237**

[154] Urahama, K., and Nagao, T. (1995) K-Winner-Take-All Circuit with $O(N)$ Complexity, *IEEE Trans. on Neural Networks*, **6**:776-778

[155] Varela, F., Lachaux, J.P., Rodriguez, E., and Martinerie, J. (2001) The Brainweb: Phase Synchronization and Large-Scale Integration, *Nature Reviews Neuroscience*, **2**:229-239

[156] Vicsek, T., Czirok, A., Jacob, E.B., Cohen, I., and Schochet, O. (1995) Novel type of phase transitions in a system of self-driven particles, *Physical Review Letters*, **75**:1226-1229

[157] Vicsek, T. (2001) A Question of Scale, *Nature*, **411**:421

[158] Vicsek, T. (2002) The Bigger Picture, *Nature*, **418**:131

[159] von der Malsburg, C. (1981) The Correlation Theory of Brain Function, *Max-Planck-Institut Biophys. Chem., Internal Rep. 81-2, Gttingen FRG*

[160] von der Malsburg, C. (1995) Binding in Models of Perception and Brain Function, *Current Opinion in Neurobiology*, **5**:520-526

[161] Wang, D.L. (1999) Object Selection Based on Oscillatory Correlation, *Neural Networks*, **12**:579-592

[162] Wang, D.L., and Brown, G.J. (1999) Separation of Speech From Interfering Sounds Based on Oscillatory Correlation, *IEEE Transactions on Neural Networks*, **10**:684-697

[163] Wang, D.L. (2002) The Time Dimension for Neural Computation, *Technical Report, Dept. of Computer and Information Science, Ohio State University*

[164] Wang, W., and Slotine, J.J.E. (2004) On Partial Contraction Analysis for Coupled Nonlinear Oscillators, *Biological Cybernetics*, to appear

[165] Wang, W., and Slotine, J.J.E. (2003) Fast Computation with Neural Oscillators, *NSL Report, MIT, Cambridge, MA*, submitted

[166] Wang, W., and Slotine, J.J.E. (2004) Adaptive Synchronization in Coupled Dynamic Networks, *NSL Report, MIT, Cambridge, MA*

[167] Wang, W., and Slotine, J.J.E. (2004) A Theoretical Study of Different Leader Roles in Networks, *NSL Report, MIT, Cambridge, MA*, submitted

[168] Wang, W., and Slotine, J.J.E. (2004) Contraction Analysis of Time-Delayed Communications

using Simplified Wave Variables, *NSL Report, MIT, Cambridge, MA*, submitted

[169] Wang, W., and Slotine, J.J.E. (2004) Contraction Analysis of Time-Delayed Nonlinear Systems, *NSL Report, MIT, Cambridge, MA*, submitted

[170] Wang, W., and Slotine, J.J.E. (2004) A Study of Continuous Attractors and Singularly Perturbed Systems using Contraction Theory, *NSL Report, MIT, Cambridge, MA*

[171] Wang, X.J., and Rinzel, J. (1992) Alternating and Synchronous Rhythms in Reciprocally Inhibitory Model Neurons, *Neural Computation*, **4**:84-97

[172] Watts, D.J., and Strogatz, S.H. (1998) Collective Dynamics of 'Small-World' Networks, *Nature*, **393**:440-442

[173] Watts, D.J. (1999) Small Worlds, *Princeton University Press*

[174] Williamson, M.W. (1998) Neural Control of Rhythmic Arm Movements, *Neural Networks*, **11**

[175] Winfree, A.T. (1967) Biological rhythms and the behavior of populations of coupled oscillators, *J. Theor. Biol.*, **16**:15-42

[176] Winfree, A.T. (2000) The Geometry of Biological Time, *Springer*

[177] Wolf, J.A., Schroeder, L.F., and Finkel, L.H. (July 2001) Computational Modeling of Medium Spiny Projection Neurons in Nucleus Accumbens: Toward the Cellular Mechanisms of Afferent Stream Integration *Proceedings of the IEEE* **89**(7):1083-1092

[178] Wolfe, W.J., *et al.* (1991) K-Winner Networks, *IEEE Transactions on Neural Networks*, **2**(2):310-315

[179] Xie G., Wang L. (2004) Stability and Stabilization of Switched Linear Systems with State Delay: Continuous-Time Case, *The 16th International Symposium on Mathematical Theory of Networks and Systems, Belgium*

[180] Xie G., Wang L. (2004) Stability and Stabilization of Switched Linear Systems with State Delay: Discrete-Time Case, *The 16th International Symposium on Mathematical Theory of Networks and Systems, Belgium*

[181] Yen, J.C., Guo, J.I., and Chen, H.C. (1998) A New k-Winners-Take-All Neural Network and Its Array Architecture, *IEEE Transactions on Neural Networks*, **9**(5):901-912

[182] Yen, S.C., Menschik E.D., and Finkel, L.H. (June 1999) Perceptual Grouping in Striate Cortical Networks Mediated by Synchronization and Desynchronization, *Neurocomputing*, **26**(7):609-616

[183] Yuille, A.L., and Grzywacz, N.M. (1989) A Winner-Take-All Mechanism Based on Presynaptic Inhibition, *Neural Computation*, **1**:334-347

[184] Yuille, A.L., and Geiger, D. (2002) Winner-Take-All Networks, in *The Handbook of Brain Theory and Neural Networks*, 2nd ed., Michael A. Arbib, Editor, The MIT Press, 1228-1231